EFFICIENCY OF CROSS-FLOW VS STACK-ASSISTED NATURAL VENTILATION FOR EXHAUSTING COOKING FUMES AND ODOURS IN APARTMENT KITCHENS

A THESIS SUBMITTED TO
THE GRADUATE SCHOOL OF NATURAL AND APPLIED SCIENCES
OF
MIDDLE EAST TECHNICAL UNIVERSITY

BY

CEREN GÜL SUNGUN

IN PARTIAL FULFILLMENT OF THE REQUIREMENTS
FOR
THE DEGREE OF MASTER OF SCIENCE
IN
BUILDING SCIENCE IN ARCHITECTURE

APRIL 2025

Approval of the thesis:

EFFICIENCY OF CROSS-FLOW VS STACK-ASSISTED NATURAL VENTILATION FOR EXHAUSTING COOKING FUMES AND ODOURS IN APARTMENT KITCHENS

submitted by **CEREN GÜL SUNGUN** in partial fulfillment of the requirements for the degree of **Master of Science** i**n Building Science in Architecture, Middle East Technical University** by,

Prof. Dr. Naci Emre Altun
Dean, **Graduate School of Natural and Applied Sciences** _____

Assoc. Prof. Dr. Ayşem Berrin Çakmaklı,
Head of the Department, **Architecture** _____

Prof. Dr. Soofia Tahira Elias Ozkan
Supervisor, **Architecture, METU** _____

Examining Committee Members:

Assoc. Prof. Dr. Ayşem Berrin Çakmaklı
Architecture, METU _____

Prof. Dr. Soofia Tahira Elias Ozkan
Architecture, METU _____

Assoc. Prof. Dr. Ayşegül Tereci
Architecture, Necmettin Erbakan University _____

Date: 08.04.2025

I hereby declare that all information in this document has been obtained and presented in accordance with academic rules and ethical conduct. I also declare that, as required by these rules and conduct, I have fully cited and referenced all material and results that are not original to this work.

Name Last name : Ceren Gül Sungun

Signature :

ABSTRACT

EFFICIENCY OF CROSS-FLOW VS STACK-ASSISTED NATURAL VENTILATION FOR EXHAUSTING COOKING FUMES AND ODOURS IN APARTMENT KITCHENS

Sungun, Ceren Gül
Master of Science, Building Science in Architecture
Supervisor: Prof. Dr. Soofia Tahira Elias Ozkan

April 2025, 140 pages

Ventilation shunt flues in apartment kitchens utilise the principle of natural convection, with rising warm air playing a critical role. Apartment kitchens are designed for mechanical ventilation during cooking using a kitchen hood connected to a shunt flue. However, in apartments, air pressure variations caused by the stack effect or reverse stack effect lead to airflow between the shunt flue and the connected spaces. The heat load generated by cooking induces airflow between the kitchen and the shunt flue, affecting even the kitchens on floors where cooking is not taking place. In this study, without operating the kitchen hood, a 10-story apartment building—with natural gas stoves used for cooking on all floors—was analysed. The airflow between the shunt flue and the kitchen was examined for each floor, taking into account that a horizontal flue system was designed for every floor. The buildings were oriented toward both leeward and windward directions. The performance of cross-flow natural ventilation on horizontal flue, as well as stack-assisted natural ventilation through the shunt flue, was investigated in these apartment kitchens—particularly regarding the exhaust of cooking fumes and odors. The analysis was

conducted using the Apache Dynamic Simulation tool and MicroFlo CFD within the IES VE (Integrated Environmental Solutions Virtual Environment) program, incorporating climate data from Ankara. CO_2 emissions from cooking were employed as an indicator to evaluate indoor air quality, and the analysis indicated no significant difference between kitchens with vertical or horizontal flue configurations. Ventilation effectiveness was assessed using the Local Mean Age of Air, revealing that air in kitchens with a horizontal flue was refreshed more rapidly than in those with a vertical flue.

Keywords: Apartment kitchen, Cross-flow ventilation, Stack effect, Cooking fumes, IES VE

ÖZ

APARTMAN MUTFAKLARINDA YEMEK DUMANI VE KOKULARININ GİDERİLMESİNDE ÇAPRAZ AKIŞ HAVALANDIRMAYA KARŞI BACA ETKİSİ İLE DOĞAL HAVALANDIRMANIN VERİMLİLİĞİ

Sungun, Ceren Gül
Yüksek Lisans, Yapı Bilimleri, Mimarlık
Tez Yöneticisi: Prof. Dr. Soofia Tahira Elias Ozkan

Nisan 2025, 140 sayfa

Apartman mutfaklarının şönt bacalı havalandırma sistemleri, akışkanların doğal konveksiyon prensibinden yararlanır; bu süreçte yükselen sıcak hava akışı belirleyici bir rol üstlenmektedir. Apartman mutfakları, yemek pişirme sırasında bir şönt bacaya bağlı davlumbaz ile mekanik olarak havalandırılacak şekilde tasarlanmıştır. Öte yandan, yüksek katlı apartman binalarında baca etkisiyle oluşan hava basıncındaki değişim, havalandırma bacası ile bu bacaya bağlı mekan arasında içeri veya dışarı yönlü hava akışına yol açmaktadır. Yemek pişirme sırasında ortaya çıkan ısı yükü, mutfak ile şönt baca arasındaki hava akışını etkileyerek, yemek pişirilmeyen katlardaki mutfakları da etkilemektedir. Bu çalışmada, yemek pişirme sırasında doğal gazlı ocakların kullanıldığı ve mutfak aspiratörünün kullanımda olmadığı, 10 katlı bir apartman simulasyon kullanılarak incelenmiştir. Şönt bacalı sistem ve ona alternatif olarak tasarlanan her katta yatay baca sistemi ile doğal havlandırmanın baca etkisi ve çapraz havalandırma incelenmiştir. Binalar, hakim rüzgar yönüne ve hakim olayan rüzgar yönüne göre konumlandırılmıştır. Yatay baca üzerindeki çapraz

doğal havalandırmasının yanı sıra, şönt baca aracılığıyla gerçekleşen baca etkisindeki doğal havalandırmanın performansı, özellikle yemek kokularının ve pişirme dumanının tahliyesi açısından değerlendirilmiştir. Analiz, Ankara iklim verilerinin de dahil edildiği IES VE (Integrated Environmental Solutions Virtual Environment) programı kapsamında Apache Dynamic Simulation aracı ve MicroFlo CFD kullanılarak gerçekleştirilmiştir.

Anahtar Kelimeler: Apartman mutfağı, Çapraz havalandırma, Baca etkisi, Yemek kokusu, IES VE

TABLE OF CONTENTS

LIST OF TABLES

TABLES

LIST OF FIGURES

FIGURES

ACKNOWLEDGMENTS

I feel fortunate to have been a student under the supervision of Prof. Dr. Soofia Tahira Elias Ozkan. Her knowledge, motivation, and perspective, along with her sincerity and insightful guidance, played a significant role in shaping the direction and development of this research throughout my graduate studies. From the very beginning of this research process—when I was filled with questions and unsure of which path to take—she was like a guiding lighthouse, helping me find the right direction. I am sincerely grateful for her knowledge, experience, and patience, and for her support at every detail and stage of this thesis.

I would like to express my heartfelt gratitude to my family, who have supported me not only throughout this thesis process but also at every stage of my academic and personal journey with their love and encouragement. Their invaluable support is far too great to be expressed in just a few lines and has played a fundamental role in the completion of this work.

I am thankful to Hatice Hilal Topuz for her support. Following our shared academic journey at AGU, she became the first AGU graduate to begin graduate studies at METU. Her early steps and efforts helped clear the way—like an icebreaker—for those who came after, including myself. This allowed me to follow in her footsteps and navigate the challenges she had already faced with greater ease. Her trust, and support enabled me to progress, and I remain sincerely grateful for all her contributions.

CHAPTER 1

INTRODUCTION

The research problem, aims, objectives and research questions have been outlined based on this background information, forming the foundational framework of the topic.

1.1 Argument

The roots of Turkish cuisine extend to Central Asia, while the post-Republican era (after the 1920s) is described as having a dual culinary culture, consisting of traditional cuisine and modern cuisine (Samancı, 2016). During this period, with the development of industry, the use of sunflower oil, margarine, and olive oil in meals started to be used alongside solid animal fats (Kizildemir, Öztürk, and Sarıışık, 2014). If its general characteristics are considered, according to research by Maviş (2003) and Aktaş & Özdemir (2007), it is common to cook vegetables with meat, onions, tomato paste, and tomatoes, besides, a wide variety of spices are used in dishes, and food is generally lightly fried in oil before water is added during cooking.

The most significant element in the historical development of the kitchen space is the stove and its transformation through time. Cooking directly over fire was gradually replaced by the use of stoves and ovens, and later, with the introduction of electricity, electric stoves and ovens (Erçin and Karaderi-Özsoy, 2013). The kitchen changed with the shift in the heat source, actually the stove,(Figure 1) and gained social symbolic dimensions as society accepted new technologies **(**Dönmez-Karagözler, 2022).

Figure 1. Photograph from Hacı Hulusi Efendi Mansion in Silifke, showing the location of the coal stove in the kitchen (Özözlü, 1999).

In traditional Turkish homes, the kitchen was typically located in a separate space in the yard, or on the service floor at the entrance (Pak, 1993). In the example of Gaziantep as seen in Figure 2, preparing many traditional dishes is labour-intensive; therefore, family members often work together with neighbours to make food preparations, both in the indoor kitchen and the outdoor courtyard of traditional homes, besides, in the social aspect, preparing and eating meals together fosters interaction (Yazgan-Serinkaya, 2017).

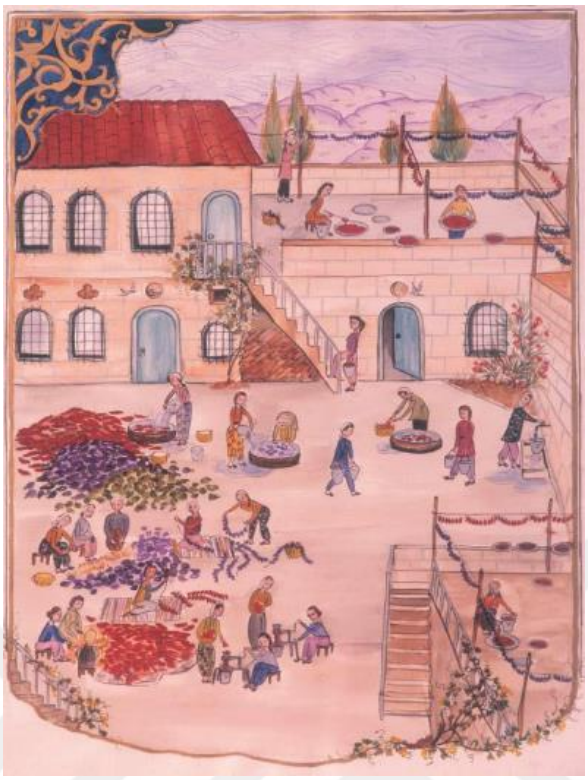

Figure 2. Illustration of Traditional Gaziantep House and Food Preparation (Painting by D. Coşkun (2014), sourced from Yazgan-Serinkaya (2017))

In Turkey, stoves that burn natural gas or LPG are used in kitchens, and the gases and moisture produced by these fuels (Ural, Akgün, and Ertürk, 2020), as well as those released from food during cooking, are attempted to be removed through shunt chimneys. According to a provision in the Ministry of Environment and Urbanisation (2017), a separate chimney must be constructed for each appliance operating on natural gas in kitchens. The implementation of this rule is detailed in the regulation TS 7363: Natural Gas Building Interior Installation Design and Application Rules (2008), which states that it is compulsory to install fixed-channel natural ventilation systems, such as window vents with an opening of 150 cm^2 or ventilation systems, in apartments where natural gas is used. This regulation means that kitchens with a

combi boiler and a gas stove must have a 150 cm² opening on their windows as seen in Figure 3.

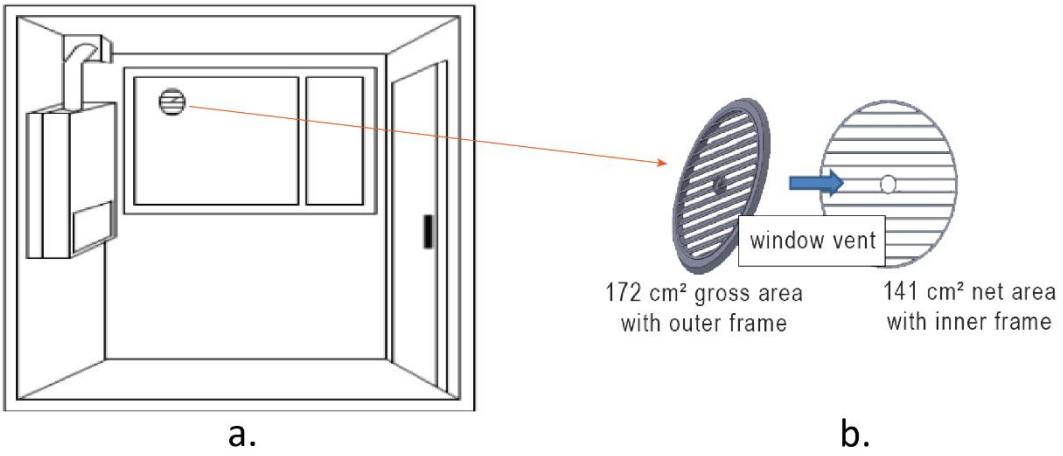

Figure 3. (a) Representation of a natural gas combi boiler with window vent positioning (AKSA Natural Gas Distribution Inc., 2014), and (b) a 3d-modelled window vent (Ural, Akgün, and Ertürk, 2020)

According to Ural, Akgün, and Ertürk (2020), the cooking stove consumes the fresh air in the environment during combustion, reducing oxygen levels. Simultaneously, it releases CO2 generated from combustion back into the same space, increasing the CO2 concentration in the environment. On the other hand, the amount of oxygen and fresh air required during the combustion of LPG and natural gas is equal; however, the amount of CO2 released into the environment is 22% higher with LPG than with natural gas (Akgün, 2019). Although LPG stoves pollute the indoor air more, window vents are required for natural gas stoves, regardless of whether the combi boiler uses oxygen from the indoor environment (Type A combi-boiler) or from outside (Type C combi-boiler), as the requirement applies to natural gas systems (Ural, Akgün, and Ertürk, 2020). As outlined above, while regulations regarding window vents are in place, users, particularly in cold climate regions, often close these openings to minimise indoor heat loss as seen in Figure 4 (Ural, Akgün, and Ertürk, 2020).

Figure 4. The combi boiler installed on the interior wall of the kitchen, with a window vent covered with paper (Akgün, 2019).

Covers specifically designed to seal these vents, promoted for their wind-blocking and cold-insulating properties, are available on the market (Figure 5).

Figure 5. Window vent covers available on the market (URL - 2).

One of the significant pollutant activities in the building is cooking (Sun and Wallace, 2021), and the cooking fumes emitted during the cooking of foods have been investigated through a literature review, as presented in Section 2.3.1.

To prevent kitchen fumes and odours from frying, from spreading to other living areas of the house, a separate frying area within the kitchen or a frying space located on an enclosed balcony has emerged as an alternative solution, representing a distinct

kitchen typology This dedicated area for frying within the kitchen is locally referred to as a "frying kitchen" or "dirty kitchen" as seen in Figure 6.

Figure 6. (a)The kitchen and its attached balcony, and (b) balcony being used as a kitchenette for frying (URL-1).

1.2 Problem Statement

In Turkey's apartment buildings, the kitchen ventilation system relies on the combined operation of the shunt flue and the kitchen hood to exhaust cooking smoke and odours. There are studies on occupant usage habits regarding the kitchen hood; however, when the kitchen hood is not in use, the literature indicates that further development is needed on ventilation efficiency. Despite these concerns, the existing literature on kitchen ventilation primarily focuses on kitchen hood efficiency to improve indoor air quality, either by measuring PM2.5 levels or by simulating the kitchen environment using Computational Fluid Dynamics (CFD). The study most directly related to the problem addressed in this thesis examined the positioning of gaseous pollutant sources relative to the neutral level, investigating pollutant transport to other floors under winter and summer conditions. Although this study offers preliminary insights into the mechanisms by which cooking odours and fumes may be transferred via the stack effect, they do not adequately describe the airflow movements within the shunt flue (double flue) system. Moreover, these investigations are limited to only one or two temperature scenarios and are not

sufficient to address how the intensity and direction of this airflow behave throughout the entire year during cooking hours.

The flue opening (an interior opening) in existing apartment buildings is specifically designed to exhaust cooking fumes and odours from the kitchen via kitchen hoods (mechanical ventilation systems). During cooking, when the kitchen hood is not operated by the occupant, the flue opening functions as a natural ventilation opening. In apartment buildings with vertical flues, cooking in one apartment flat affects the flue openings of other flats due to the stack effect. In addition to the cooking activity within the kitchen, there are internal and external factors that influence the airflow through the flue opening. Seasonal heating impacts the airflow over extended periods, acting as a constant and periodic factor, whereas wind, as an external environmental factor, affects the airflow through the flue opening with shorter-term variations in direction and intensity.

1.3 Aim and Objectives

The research aims to investigate the performance of apartment kitchen ventilation by comparing the efficiency of cross-flow and stack-assisted natural ventilation in exhausting cooking fumes and odours. There are several objectives;

1. To reduce inter-floor kitchen polluted air transmission due to the stack effect in winter in apartment buildings
2. To investigate the indoor air quality while cooking in apartment kitchens
3. To explore the potential of cross-flow ventilation while cooking
4. To propose an alternative strategy to reduce dependence on mechanical ventilation

1.4 Research Questions

- In the context of natural ventilation in apartment building kitchens, which is more effective in terms of airflow volume per unit time: stack-assisted ventilation or cross-flow ventilation?
- Which one is more effective in terms of indoor air quality in apartment kitchens, stack-assisted ventilation or cross-flow ventilation?
- How are the ventilation performances of both vertical and horizontal flue systems affected when an apartment building is oriented with its windward or leeward side?
- In apartments with a natural gas vent on the kitchen window, how does the vent behave—as a supply or an extract opening—in buildings with vertical flues compared to those with horizontal flues?
- How does the kitchen's floor level influence whether the natural gas vent functions as a supply or extract opening in apartment buildings with either vertical or horizontal flue systems?

1.5 Research Methodology

To examine the exhaust of cooking fumes and odours from a nuclear family kitchen during cooking, stack-assisted and cross-flow natural ventilation strategies are compared. The Integrated Environmental Solutions Virtual Environment (IES VE) is employed for modelling, visualisation, and simulation in apartment buildings. To investigate the natural ventilation performance, the apartment building is oriented either towards or against the prevailing wind direction (Scenario I-II). This research first determines the natural ventilation performance of apartment buildings with either vertical or horizontal flue systems using the IES-VE Apache Dynamic Simulation Modelling (DSM). Following this, the flow-out rate and the mode value of the airflow volume representing the overall performance of both systems are used to compare the scenarios(Figure 7). Based on this comparison, apartment floors are

selected for kitchens with vertical and horizontal flue configurations for further CFD analysis. The specific day on which each selected kitchen achieves its mode airflow value is identified as the "design date." CFD simulations are run for the selected kitchens under the environmental conditions of the designated design date. To represent cooking fumes and odours, the CO_2 and moisture profiles of the kitchens are evaluated together with airflow velocity, temperature, and the local mean age of air. The results are then compared and analysed.

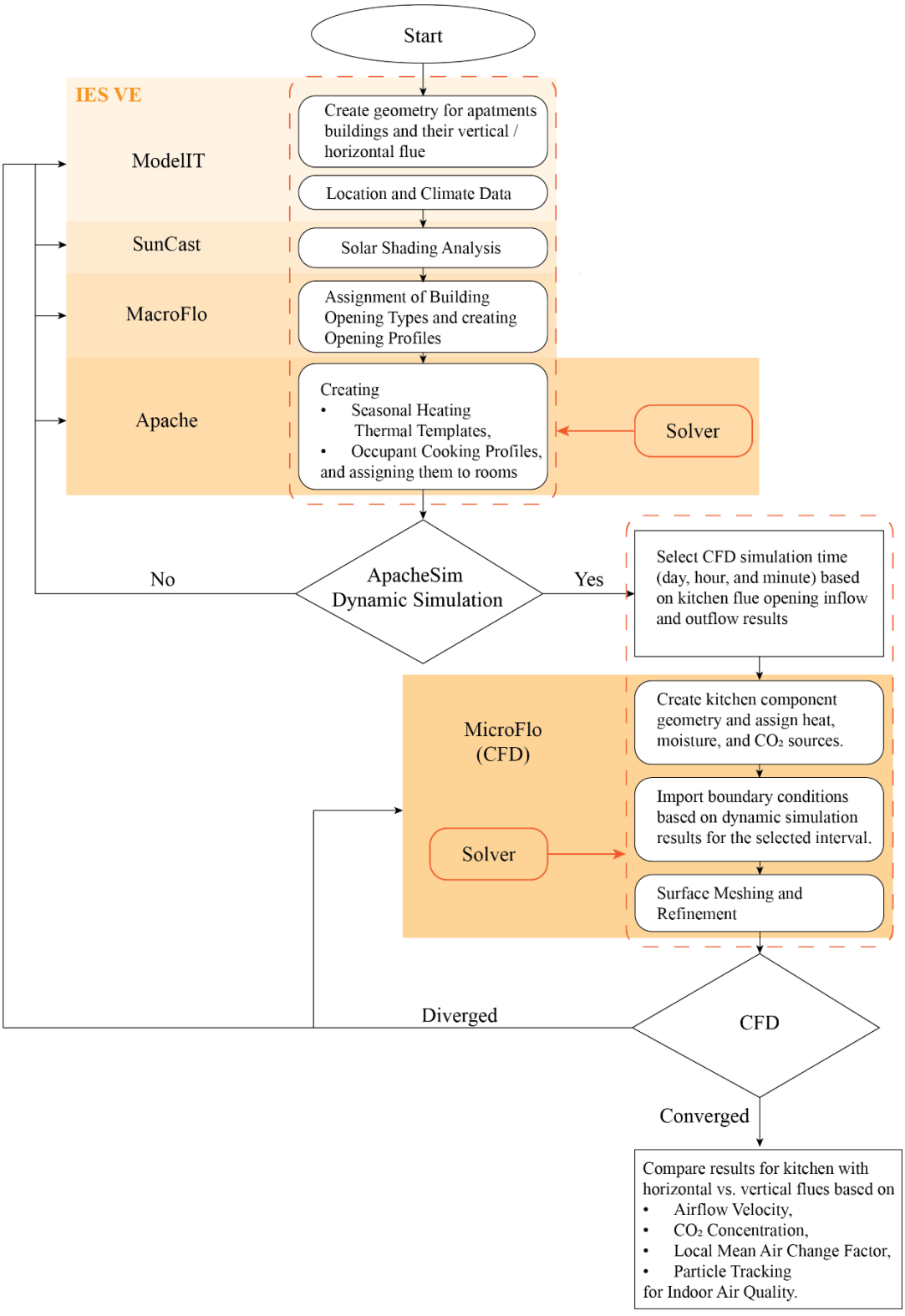

Figure 7. Methodology flowchart to investigate indoor air quality through stack-assisted vs cross-flow ventilation using (IES VE)

1.6 Disposition

In this research, the first chapter examines the typical foods prepared in apartment kitchens in Turkey, the methods used to ventilate cooking fumes and odours, the challenges encountered, and the implications of these challenges. Subsequently, the research problem is identified, and the aims, objectives, research questions, and research methodology are discussed.

The second chapter is dedicated to the literature, providing background information on Turkish regulations regarding apartment building planning, kitchen ventilation, and flue systems. It discusses both natural and mechanical ventilation systems, as well as indoor air quality measurements.

In the next chapter, the primary research materials, specifically apartment buildings, and the secondary materials, including climate data and software, are discussed, along with the methodology used to analyse these materials.

In the fourth chapter, based on the results of the natural ventilation analysis from the previous chapter, the design date for the CFD simulation was determined, and the apartment building kitchens were selected along with their respective scenarios. CFD simulations were conducted for kitchens with both vertical and horizontal flue systems, and the results are presented, compared, and explained.

In the final chapter, the research aims and objectives, along with the results of the natural ventilation analysis and CFD simulations, are evaluated and discussed. The similarities and differences between these findings and the studies examined in the literature review are compared, and the various methodological approaches are assessed.

CHAPTER 2

LITERATURE REVIEW

The literature review progresses through the main topics of ventilation types, indoor air quality, and indoor thermal comfort. The research on kitchen ventilation has been evaluated from various perspectives within the subheadings. The knowledge of the literature aims to provide a foundation for further investigation into this field.

2.1 Background Information

The background information includes an evaluation of apartment buildings, their kitchens, and the associated cultural aspects in Turkey, as well as the regulations governing kitchen ventilation systems.

2.1.1 The Transformation of Apartment Buildings from Low Rise to High Rise

This section explores various aspects of apartment housing in Turkey. It highlights the shift in housing stock from individual buildings to apartment blocks and mass housing developments (Cengizkan, 2000; Çiftçi, 2020). Changes in household types are also examined, including a decrease in multi-family structures and an increase in single-person households (Turkish Statistical Institute, 2021). Additionally, regulatory standards for apartment design are discussed, with a focus on setback rules based on building height (Ministry of Environment and Urbanization, 2017). The spatial integration of kitchens and the redefinition of public and private spaces are linked to evolving family structures (Guney & Wineman, 2008; Avcı Hosanlı,

2021). Lastly, the transformation of TBMM Members' housing into Park Oran housing is analysed, along with insights into apartment layout designs and kitchen configurations from that period (Kale, 2008).

According to Cengizkan (2000), in 1950, more than 60% of the housing stock was two-storey buildings, and more than 30% of the buildings were one-storey. During 1955 -1962, there was an increase in apartment block stock among all other types of residential buildings. As seen in Figure 8, there is a shift in the residential building stock towards apartment-type buildings.

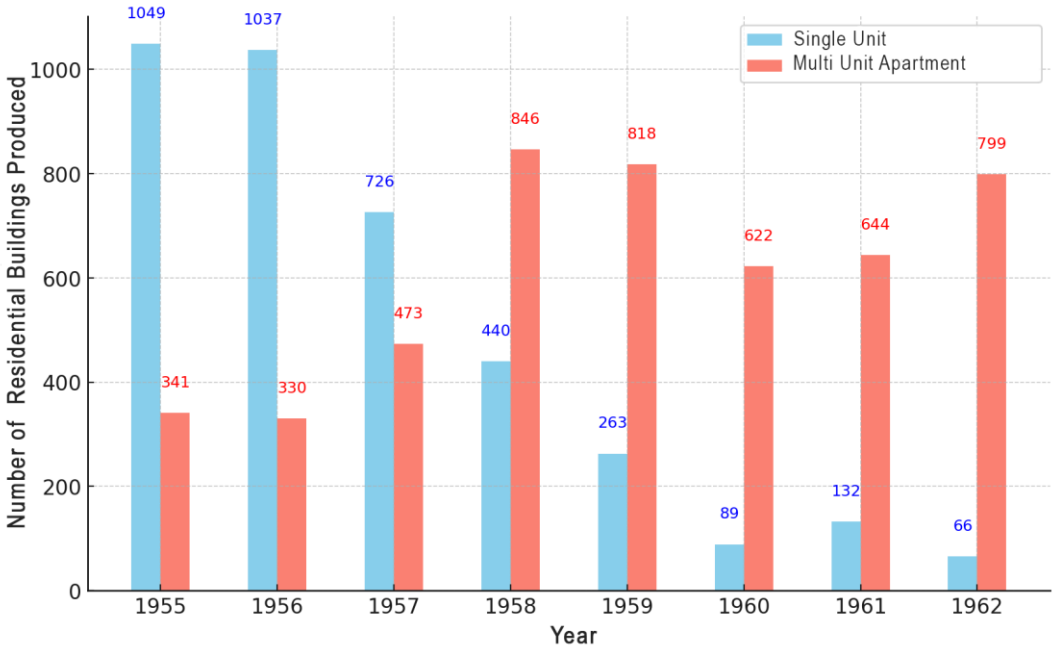

Figure 8. Relationship between the years and the number of single-unit residential buildings and multi-unit apartment buildings constructed in Turkey (between 1955 and 1962) (Created by the author based on Yörükhan & Çulhacı (1974), as cited in Cengizkan, 2000).

The long-term development of apartment building production reveals that approximately 2.5 million apartment units were built over the 56 years from 1964 to 2019. From 1964 to 1979, 250,000 new residential apartments were built. This number increased to 1,065,000 between 1980 and 2002, and an additional 1,172,000 apartment-type residential units were constructed from 2003 to 2009 (Çiftçi, M., 2020). According to a survey conducted by the Turkish Statistical Institute (2021),

It is observed that 34.4% of residential units exist in buildings with 5 floors, while 9.5% of the residential units are located in buildings with 10 or more (Figure 9).

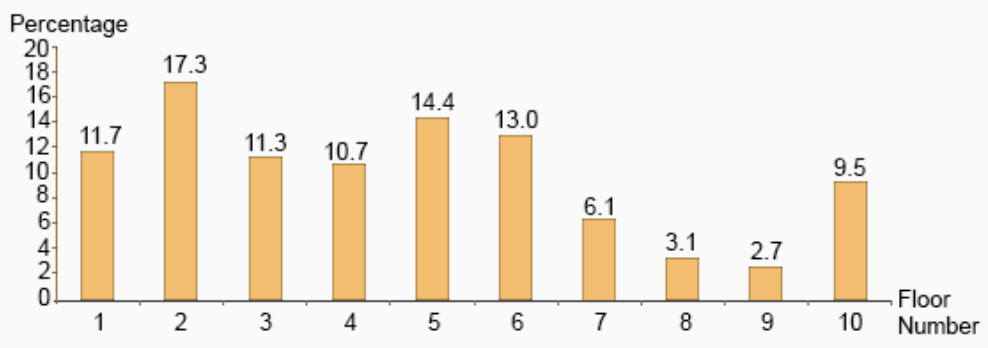

Figure 9. Distribution of households by the number of building floors (Turkish Statistical Institute, Building and Housing Characteristics Survey 2021, (2022))

The shift of the building stock towards apartments has also altered the pattern of the city plan in a transformative way. Çalışkan, Parlak Temizel, Akay, and Mashhoodi (2023) examined the residential fabric through four basic form types: linear blocks, point blocks (tower), podium blocks (tower with a podium), as seen in Table 1, and single houses (detached, semi-detached, or row houses). It analyses how these apartment typologies integrate within the urban fabric, considering typological variation and morphological continuation. This study is particularly relevant, as factors such as the position of the apartment within the urban fabric, its integration with similar or diverse types, and its orientation are essential environmental design parameters to consider when evaluating the environmental aspects of planned natural ventilation for apartments. For example, whether in linear blocks or point blocks, and whether part of mass housing or cooperatives, efforts have been made to leave certain spaces between apartment buildings. However, it has been observed that individual apartments, especially those built by independent contractors, contribute to a dense texture within the urban fabric.

Table 1.The apartment as a basic unit of the linear block, point block and podium block, in the urban fabric (Adapted from Çalışkan et al., 2023)

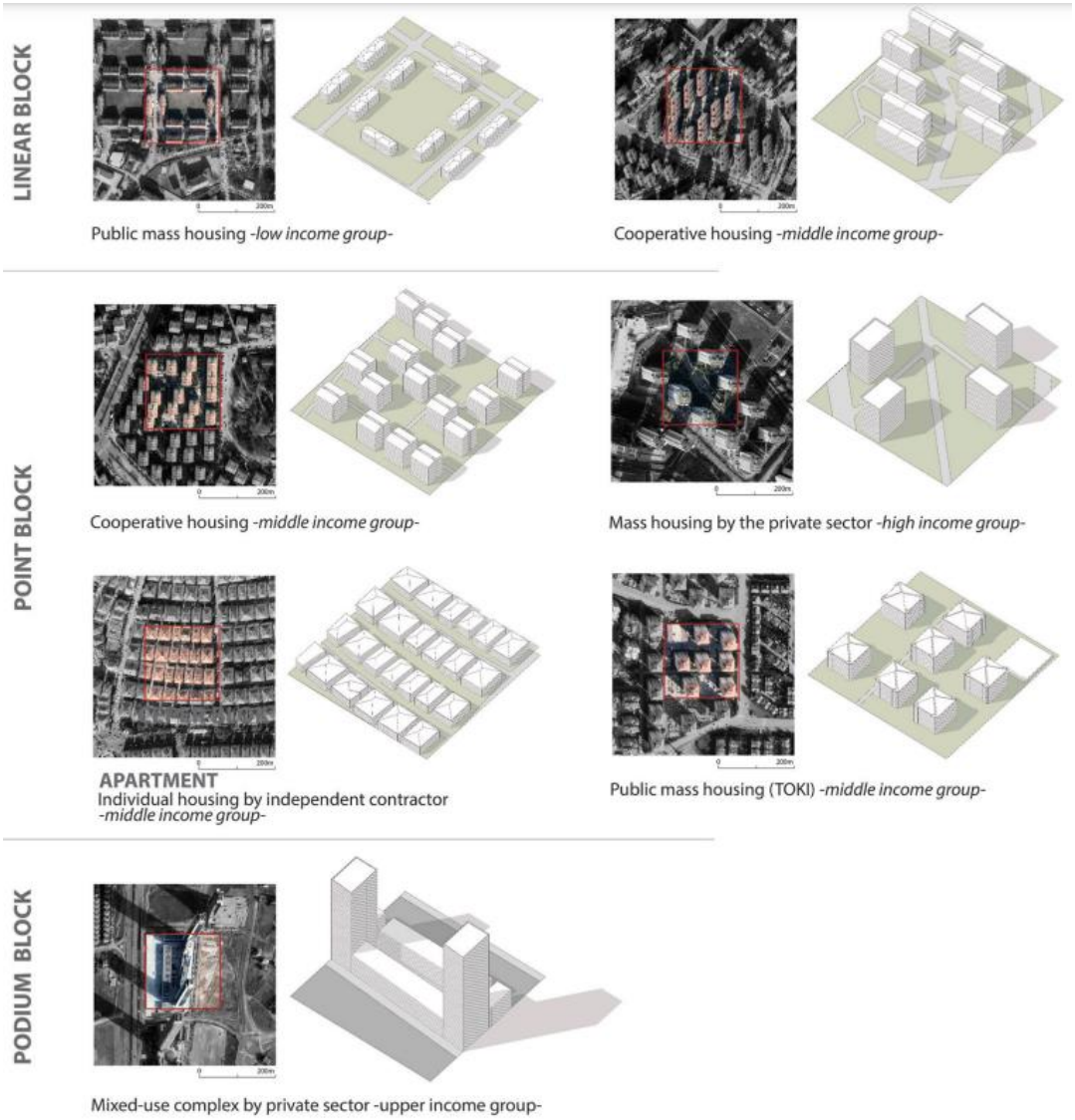

The building's setback distances are calculated through a detailed evaluation of various parameters, including the building's placement on the parcel, its distance from the road, its distance from the parcel's side and rear boundaries, the width of the adjacent road, whether structures are planned on the same or separate parcels and the building's form. According to the Ministry of Environment and Urbanisation. (2017), the setback distance increases according to specific rules as the building height rises, illustrated in Figure 10. For residential buildings shorter than 12.5

meters, the setback distance is set at 3 meters, whereas for taller buildings, the setback distance increases by 0.5 meters with each additional floor. A height of 60.5 meters has been designated as another threshold. For residential buildings shorter than 60.5 meters, the previous setback calculation is applied. However, for buildings reaching 60.5 meters, a setback distance of 15 meters is required. For taller buildings, an additional 0.5 meters is added to the setback distance for every additional 3 meters in height.

According to the Ministry of Environment and Urbanisation (2017), these residential

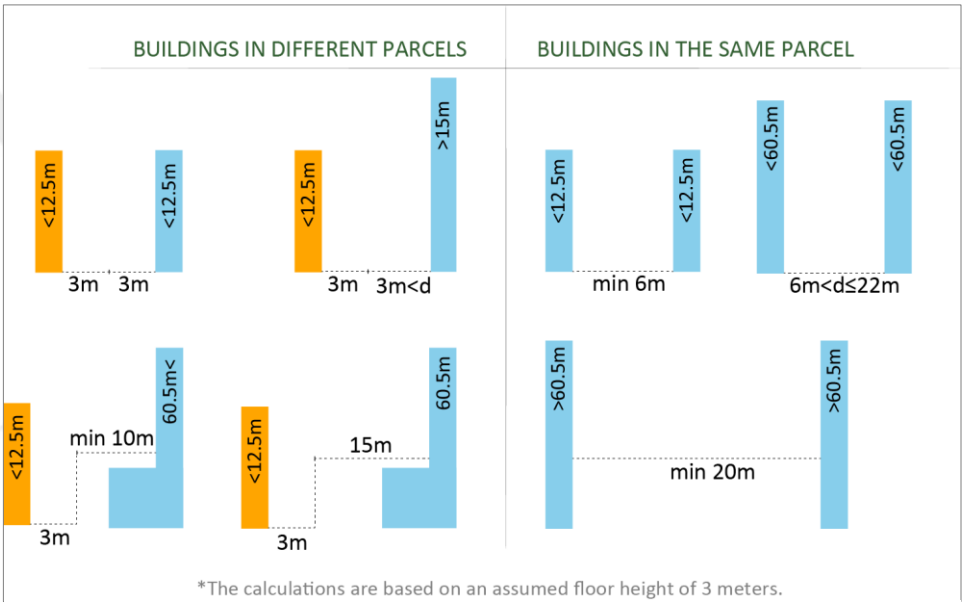

Figure 10. Diagrammatic Representations of Setback Regulations for Residential Buildings the Ministry of Environment and Urbanization, 2017

buildings must include a minimum of a 12 m² living room, a 9 m² bedroom, a 3.3 m² kitchen or cooking area, a 3 m² bathroom or wash area, and a 1.2 m² toilet.

Guney and Wineman (2008) discuss the design of 20th-century apartments in Ankara through their plan layouts, examining how spaces such as the entry(crossed circle); distribution spaces(black-colored circle) like halls, corridors, or sofas; rooms(hollow circle) like the living room, guest room, and bedrooms; and service spaces like the

kitchen(pink-colored circle), bathroom(hollow circle), and toilets(hollow circle) come together, based on an evaluation of 108 apartment buildings (Table 2).

Table 2.Stages of visualising and analysing apartment plan layouts (The table was generated by the author based on drawings by Guney and Wineman (2008))

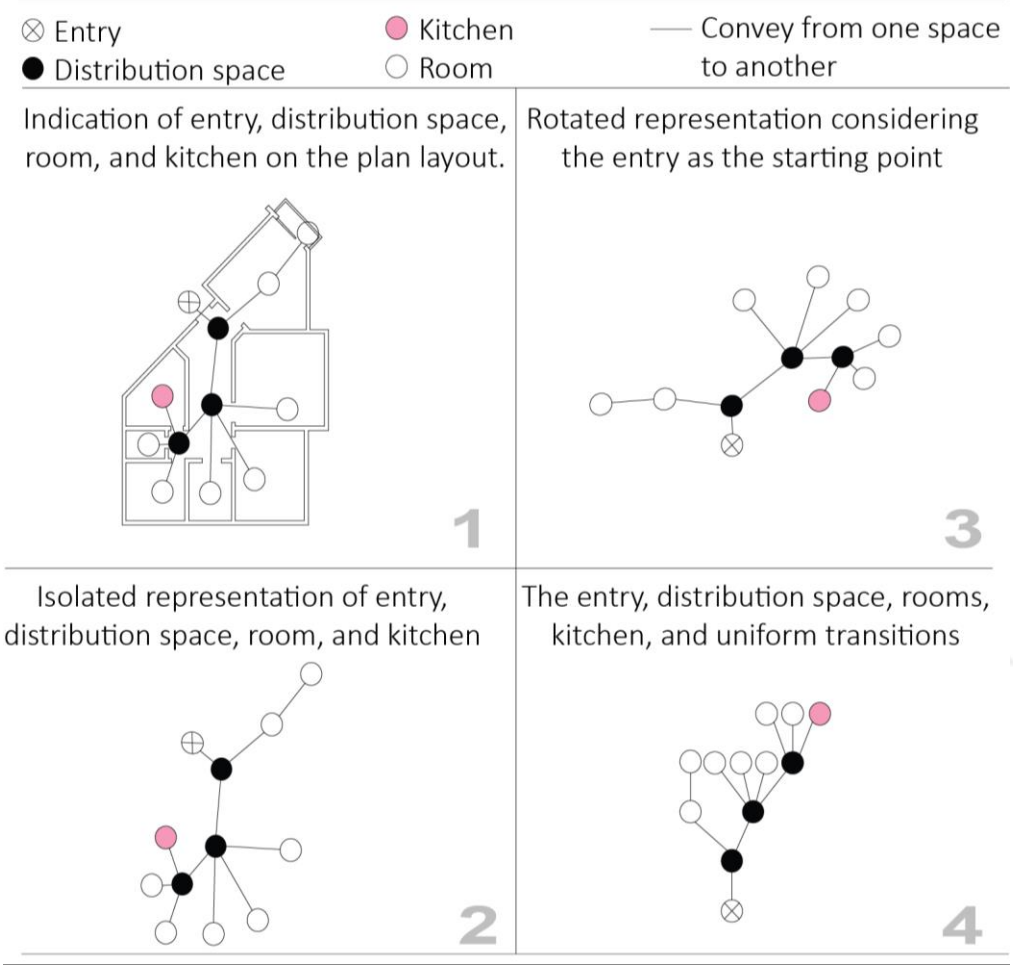

From 1920 to 1990, the most remarkable and consistent changes were observed in the kitchen: increased integration levels and enhanced functionality. The integration of the kitchen has evolved from being connected to narrow corridors or central halls to a larger space called a sofa. Later on, it became connected to smaller entrance halls; however, the dining area and living room eventually became more integrated with the kitchen, as seen in Table 3 (Guney and Wineman, 2008).

Table 3.The access graph of selected apartment plans in Ankara (1920–1990): Two sample apartment layouts selected per decade from 108 buildings (Adapted from Guney & Wineman, 2008 and pink remarked kitchen area by author).

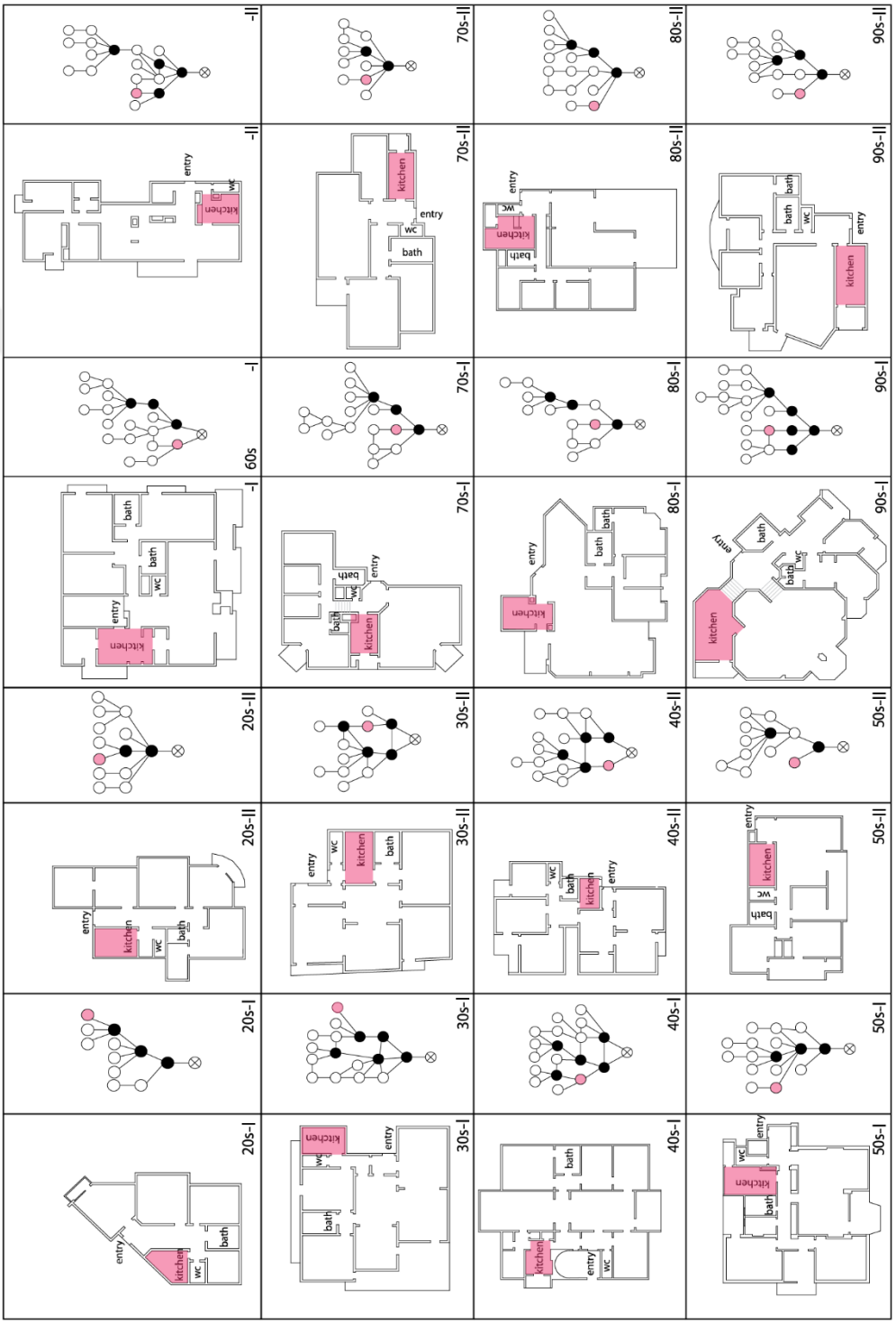

During this transition, the dining table and chairs, or a dining corner, and in some cases a TV, became elements of the kitchen space (Guney & Wineman, 2008). According to Schütte (1944), as given in Cengizkan, 2000, in the post-war (Second World War) era, the kitchen and living room were connected by a service window, and the dining area was placed as a niche within the living room. Avcı-Hosanlı (2021) considers the shift from extended family structures to nuclear family structures as one of the main reasons for changes in spatial configuration. He states that the shared space for guests, the shared space for family members, and the private spaces for individual family members have redefined the boundaries between shared and private areas within the house.

At the beginning of the 2000s, the transformation from TBMM Members' residents—a community of detached, triplex-style buildings(Figure 11-2004)—to Park Oran residents(Figure 8-2024), which consists of 12 apartment blocks with 31 floors and 5 apartment blocks with 7 floors (Figure 11-2024), was examined by Kale (2008) in terms of social, political, economic, spatial, and scale aspects.

In the site plan view, it is observed that in 2024, the area is spatially diversified into apartment blocks and linear blocks, and in terms of scale, building heights have increased from 3 stories to 7 and 31 stories.

Figure 11. The aerial view of TBMM Members' Residential complex (2004) and Park Oran Housing blocks (2024), (Google Earth, 2023).

Furthermore, this study provides insights into the spatial integration of apartments of various sizes in the early 2000s, highlighting the new layout types of 1+1 and 2+1, as well as the altered layout types of 3+1, 4+1, 5+1, and 6+1, which reflect the evolving spatial and functional demands of the period. For instance, open kitchens were planned in the designs of 1+1 and 2+1 apartments, while in 3+1 and 4+1 layouts, wide, doorless transitions were planned between the kitchen and living room. In contrast, closed kitchens were preferred in the designs of 5+1 and 6+1 (duplex) apartments as seen in Figure 12.

Figure 12. Floor plans of apartment flat types in Park-Oran Housing (Adapted from Kale, 2008)

According to the Turkish Statistical Institute (n.d), average household size data, the national average was 4 people in 2008, while it was 3.6 people for Ankara. By 2023, the national average had decreased to 3.1 people, and for Ankara, it had dropped to 2.9 people. Over these 15 years, household size has shown a decreasing trend both at the national level and in the capital, Ankara. On the other hand, the Turkish Statistical Institute (n.d) examines household types under four main categories:

Single-occupant household, a single nuclear family consisting of a couple or a parent and a child, one nuclear family and other individuals who are not a member of the nuclear family, multiple occupants without a nuclear family. When examining household types in Ankara in Figure 13, a decrease is observed only in the "one nuclear family and multiple occupants without family ties type, while an increase is seen in the other three types. The most dramatic increase, however, has occurred in the "single-occupant household" type. According to Ulusoy & Özkaynak (2016) students, individuals living alone, and newly married couples who are living separately from their families are increasingly seeking studio-type residences.

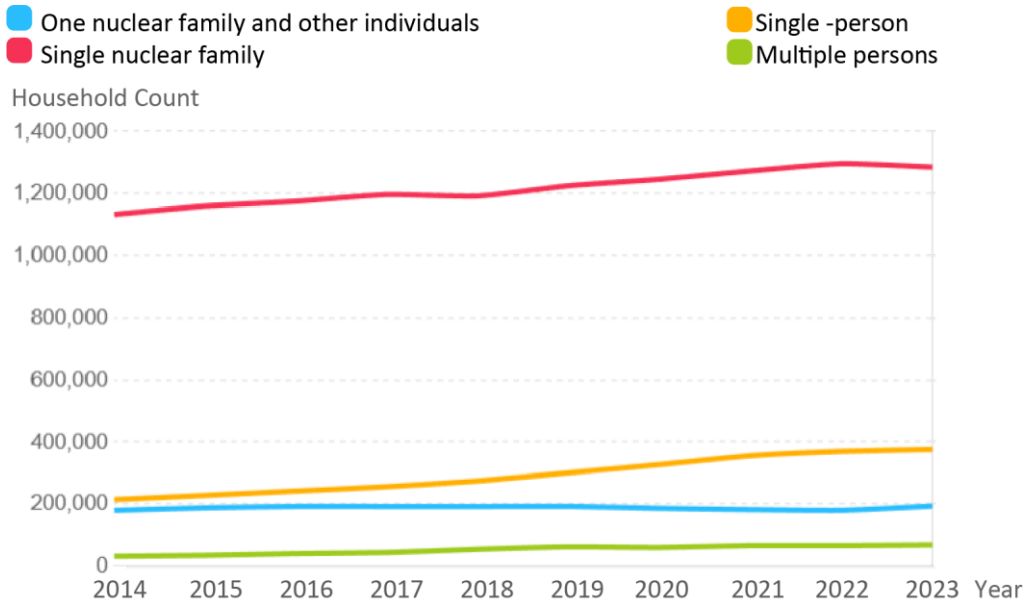

Figure 13. Relationship between the number of household types and the years from 2014 to 2023 in Ankara (Turkish Statistical Institute, n.d.)

2.1.2 The Evolution of the Cooking Space Towards Apartment Kitchen Design

Avcı-Hosanlı (2021) examines the transition from traditional houses to modern apartments through an analysis of five apartment cases in Ankara in the 1920s. While water supply, drainage, and electricity were provided in all five examples, city gas was available in only two of them. The introduction of water and gas into homes

separated the functions of cooking and heating, leading to the independent planning of kitchen and living areas **(**Dönmez-Karagözler, 2022). The service spaces are planned together due to the installation of new infrastructure and are distanced from the living areas due to ventilation needs provided by shafts. One of these apartments, the Çocuk Sarayı Apartment is seen in Figure 14. Ventilation for the service area is provided through the central courtyard, which functions exclusively for ventilation purposes (Yavuz, 2000).

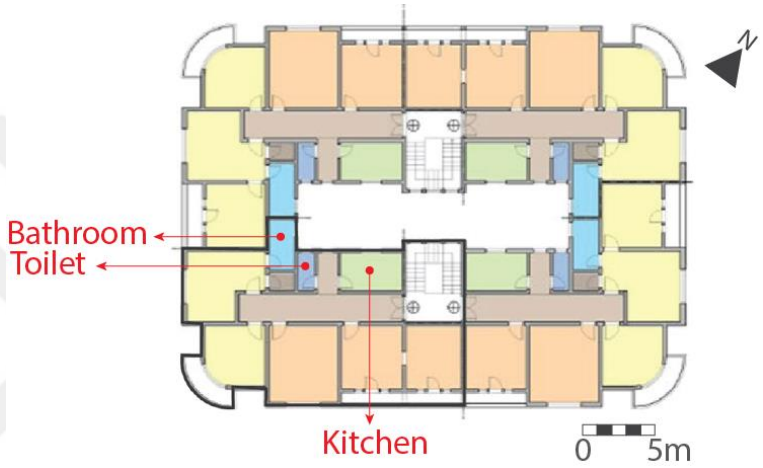

Figure 14. The upper floor plan of the Çocuk Sarayı Apartment and the ventilation of the bathroom, toilet, and kitchen through the central courtyard. (Adapted and annotated image based on Avcı-Hosanlı, 2021).

According to a more recent study, Dönmez-Karagözler (2022) states that another reason for planning the kitchen area separately from the living areas is the risk of improper gas use or gas leaks. Detailed information on kitchen applications—including gas stoves, combi-boilers, and natural-gas venting systems—is provided in Section 1.1. The design principles of today's kitchens are based on the industrialisation era of the 20th century, with Ernst May and Grete Schütte-Lihotzky's "Frankfurt Kitchen" (Yazgan-Serinkaya, 2022). Three important themes emerged in the design of the Frankfurt Kitchen: efficiency, health, and hygiene. This kitchen was a product of a design concept of "the kitchen as a machine," using shiny surfaces like glass, metal, and tiles, with simple and strong colours, modular unity, and components that seamlessly fit together, along with various technical equipment,

as seen in Figure 15 **(**Dönmez-Karagözler, 2022). The Frankfurt Kitchen is a 6.5 square meter work kitchen, initially designed for the social housing program in Weimar. In this design approach, the role of the housewife was considered similar to that of an industrial worker (Özkocak, 2015).

Figure 15. Replica of Margarete Schütte-Lihotzky's 1926 design, The Frankfurt Kitchen, (Zugmann, n.d)

Due to women's participation in public life and their limited time, the kitchen began to be designed more functionally and started to evolve into a living space (Erdaş & Özmen, 2019) This change also contributed to the emergence of different kitchen types. The size of the apartment, the family type (nuclear or extended family), traditions, the orientation of the kitchen in the floor plan and its relationship to other spaces, and financial resources all affect the kitchen layout type (Pak, 1993) The enclosed kitchen layout type, which does not have a direct connection with the dining room or living room, is classified as I, L, H, U, and G based on the shape of the kitchen countertops in the plan (as seen in Figure 16).

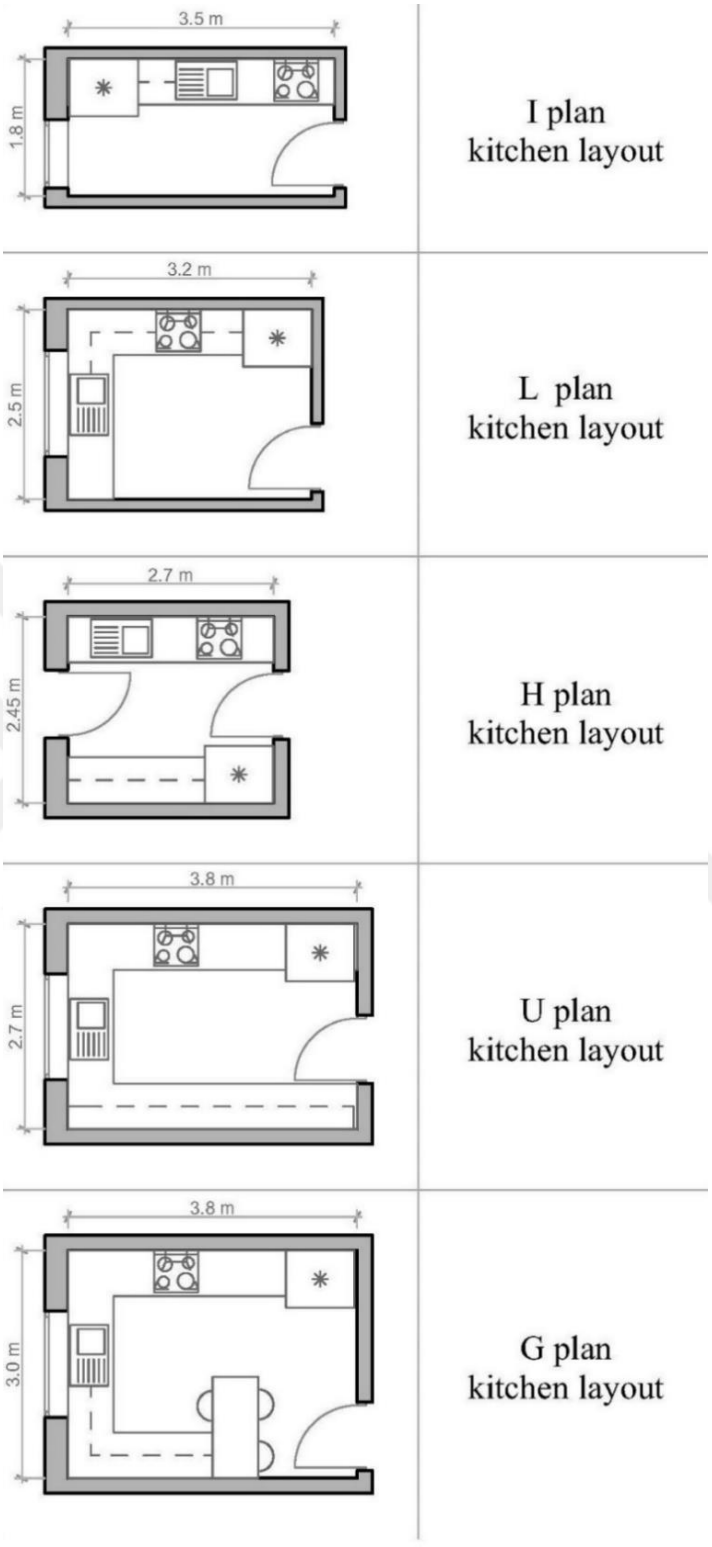

Figure 16. The enclosed kitchen layout types (Redrawn by the author, adapted from Pak, 1993).

In contrast, open kitchen layout types, which are planned within the same space as the living room or dining room, are shown in Figure 17 (Beamish et al., 2013).

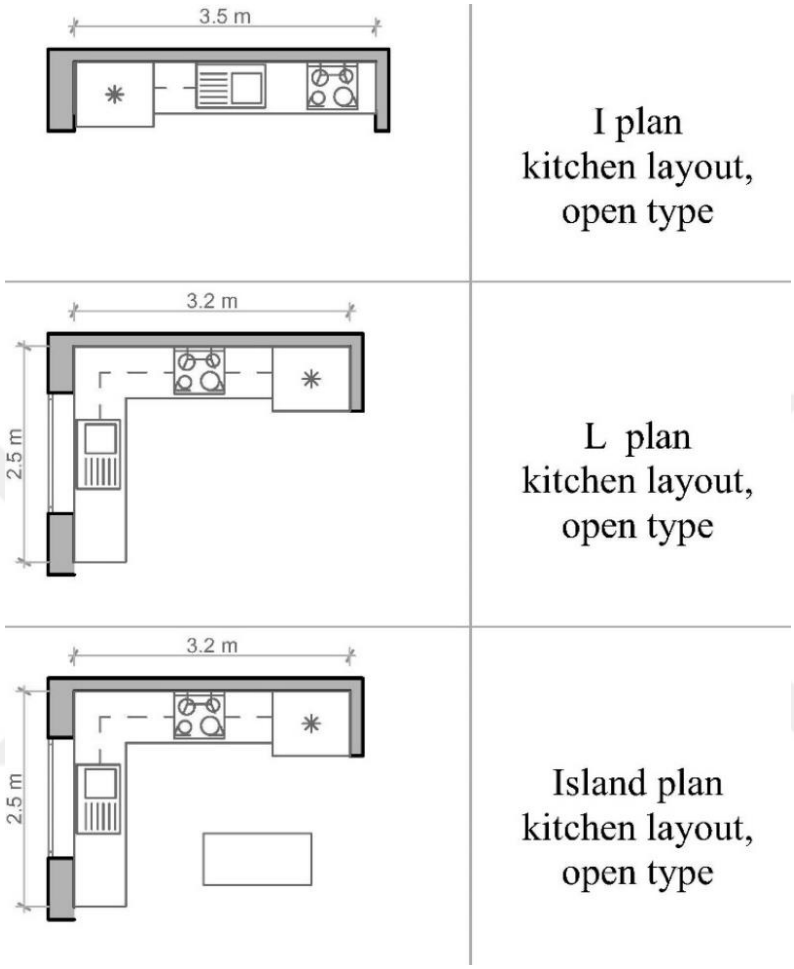

Figure 17. The open kitchen layout types (Redrawn by the author, adapted and annotated image from Beamish, et al., 2013, p.195)

According to a study by Uyar (2014), 51 mass housing projects in Istanbul were examined, and the relationship between kitchen layout types and apartment flat size was analysed through a survey. The findings revealed that L-type kitchens were the most commonly planned, followed by I-type, U-type, H-type, and island kitchens (Table 4).

Table 4.Relationship between kitchen layout types and apartment size in Istanbul (1950–2005): Analysis of 51 mass housing projects (Yıldırım, Çağatay, and Özkan,2009).

Kitchen Layout Type	1+0	1+1	2+1	3+1
I - Type	2		4	6
U -Type		6	4	1
L - Type	1	3	7	5
H - Type			2	5
Island Type				5

2.1.3 Turkish Kitchens: Cooking Practices, Ventilation Requirements, and Implementation Challenges

According to CIBSE Guide B (2005), a kitchen is an area where occupants engage in tasks such as walking, dining, meal preparation and cooking, all of which are intense. Foods without packaging that are stored and prepared for cooking contribute to elevated concentrations of indoor contaminants and the kitchen has been classified as Air Class 2 out of the three air quality levels.

According to the Ministry of Environment and Urbanization (2017), there are specific rules regarding the lightwell, ventilation chimney, and exhaust chimneys of residential kitchens. Kitchens can be designed without being adjacent to a facade that receives natural light and fresh air. In such cases, a ventilation chimney or light well must be planned to ensure proper ventilation. For buildings with 1 to 6 floors, the narrow side of the lightwell must be at least 1.50 meters, and the area must not be less than 4.5 m². For buildings with 7 or more floors, the narrow side must be at least 2.0 meters, and the area must not be less than 9.00 m². The minimum dimensions for ventilation shafts are 0.60 x 0.60 meters. On a single floor, a lightwell or ventilation shaft can serve up to four units; if there are more than four, an additional lightwell of the same dimensions must be planned. Additionally, ventilation chimneys and light wells should not be designed as shunt shafts. On the other hand, for kitchens with a facade that receives sunlight and natural air, lightwell and ventilation chimney

requirements are not necessary. No restrictions have been imposed on these kitchens regarding minimum window or door dimensions.

For both types of kitchens, whether they are open to sunlight and fresh air or not, at least one exhaust chimney must be installed, for the stove or range hood in individual units that should be designed as shunt chimneys in compliance with standards. However, in buildings with more than 10 floors, the same chimney system is used, but hermetic devices are required (Ministry of Environment and Urbanization, 2017) which are used in special systems such as combination boilers, that provide both space heating and hot water (Figure 18).

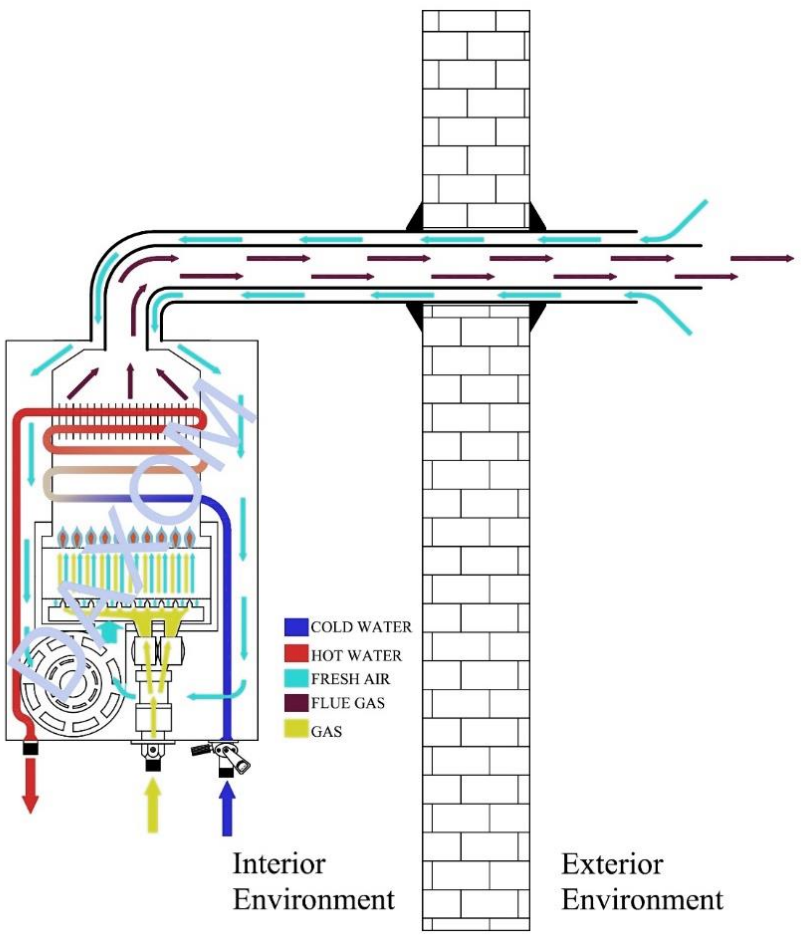

Figure 18. The working principle of the sealed combustion system with fresh air intake and flue gas exhaust, where no indoor air is used (Daxom, n.d.).

In the shunt chimney system, the use of special bricks allows for the solution of the flue with the same cross-sectional area for each floor, even as the floor height increases. Each floor's particular flue is connected to a central flue near the ceiling level of the floor, as shown in Figure 19. Chimney brick-I draws kitchen fumes and odours, filtered through the kitchen hood, into the chimney through a hole on its side surface. Chimney brick-II conveys the air from one kitchen on one side and the air from kitchens on other floors along the central flue. Chimney brick-III transfers the air taken from a floor's kitchen into the central flue, without mixing with the air at the point where other floors' kitchens are connected to the flue (Arıoğlu & Hatipoğlu, 2005).

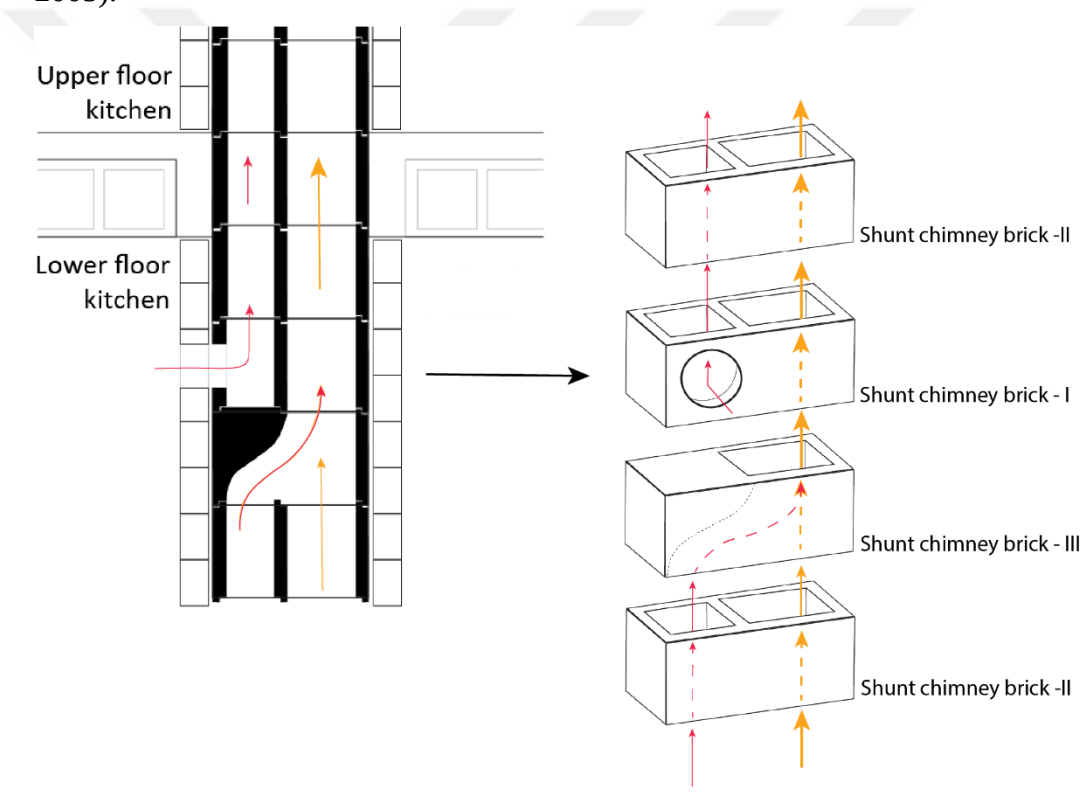

Figure 19. The shunt chimney section (left), is constructed using shunt chimney bricks (right). (Redrawn by the author, adapted and annotated image based on Arıoğlu & Hatipoğlu, 2005.).

According to Ural, Akgün, and Ertürk (2020), in Turkey, individual natural gas subscriptions constitute the majority, which includes Type C gas-burning devices such as combi boilers and Type A gas-burning devices such as kitchen stoves. Type C combi boilers do not use indoor air because they have their separate chimney to draw oxygen from and release carbon dioxide outside; therefore, they do not degrade indoor air quality.

2.2 Types of Ventilation Systems

The process where levels of hazardous contaminants are reduced and extracted from an area while clean air is supplied to residents is called ventilation, which also serves to facilitate the natural cooling of the interior (CIBSE, 2015). Ventilation describes the process of exchanging indoor air with outdoor air to maintain air quality, regulate temperature, and remove pollutants or excess moisture within a space over a specified period. The airflow occurs depending on the pressure differences, which move from high-pressured to low-pressured areas. The daily and yearly movement of the Earth creates temperature differences, which in turn lead to pressure differences, eventually generating airflow—wind. (Stevens, 2010). Designing a natural ventilation system, the earliest form of ventilation involves managing wind direction and density to facilitate clean air intake and ensure thermal comfort within a defined space. On the other hand, generating and regulating airflow, increasing airflow concentration, and filtering air through the use of mechanical components are known as mechanical ventilation systems. (Brager, Alspach, and Nall, 2011). According to the Ministry of Housing, Communities & Local Government and Department for Levelling Up, Housing and Communities (2021), ventilation can be achieved through natural, mechanical or a hybrid approach that combines both methods.

2.2.1 Natural Ventilation

Natural ventilation is governed by two primary natural effects: temperature differences, which cause the stack effect, and/or the force of wind (CIBSE, 2015). Heiselberg (2004) defined natural ventilation as comprising single-sided, cross, and stack ventilation, as illustrated in Figure 20.

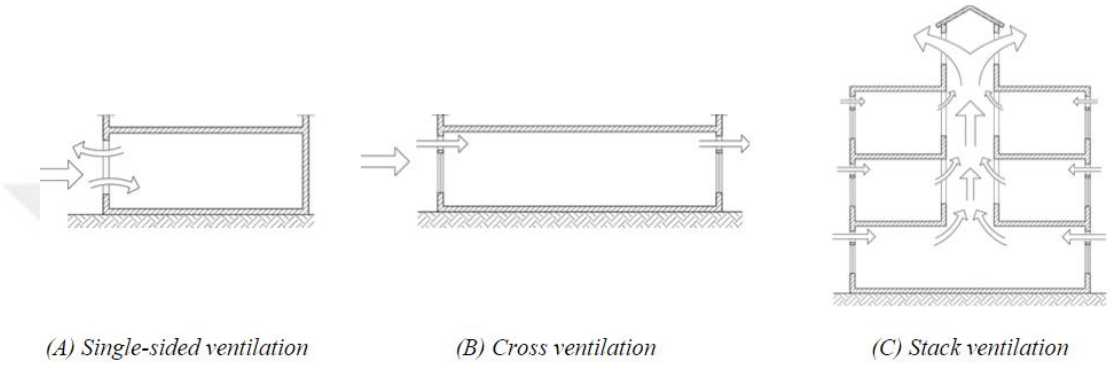

Figure 20. Natural ventilation types: (A) single-sided ventilation, (B) cross ventilation, and (C) stack ventilation (Heiselberg, 2004).

Early examples of natural ventilation in traditional buildings benefit as cooling strategies for indoor thermal comfort (Izadpanahi, Farahani, and Nikpey, 2021). For instance, wind catchers and solar chimneys in Iranian houses utilise cross-ventilation and stack ventilation to enhance natural ventilation. (Izadpanahi et al., 2021). Single-sided and cross-ventilation conditions are relatively constrained by distance; however, stack ventilation remains effective even with a longer airflow pathway. (Heiselberg, 2004).

2.2.1.1 Natural Ventilation by Wind

The wind pushes air into the building, and the side facing the wind is referred to as the windward side, where the wind pressure is higher. Air enters through the openings on the windward side of the building and moves towards the openings on the leeward side, where the wind is moving away and the pressure is lower. Wind speed has a positive relationship with the level of natural ventilation and air

infiltration (CIBSE, 2015). Natural ventilation and air infiltration exhibit variability based on the size of the opening, whether small or large, with corresponding differences in airflow energy within the interior. The kinetic energy loss of the air entering through a large opening is less than that of the airflow entering through a small opening. The kinetic energy loss of the air entering through a large opening is less than that of the airflow entering through a small opening. Therefore, in natural ventilation through a small opening, the pressure inside is almost uniform (Figure 21-a), whereas in natural ventilation through a large opening, the pressure distribution is more irregular (Figure 21-b).

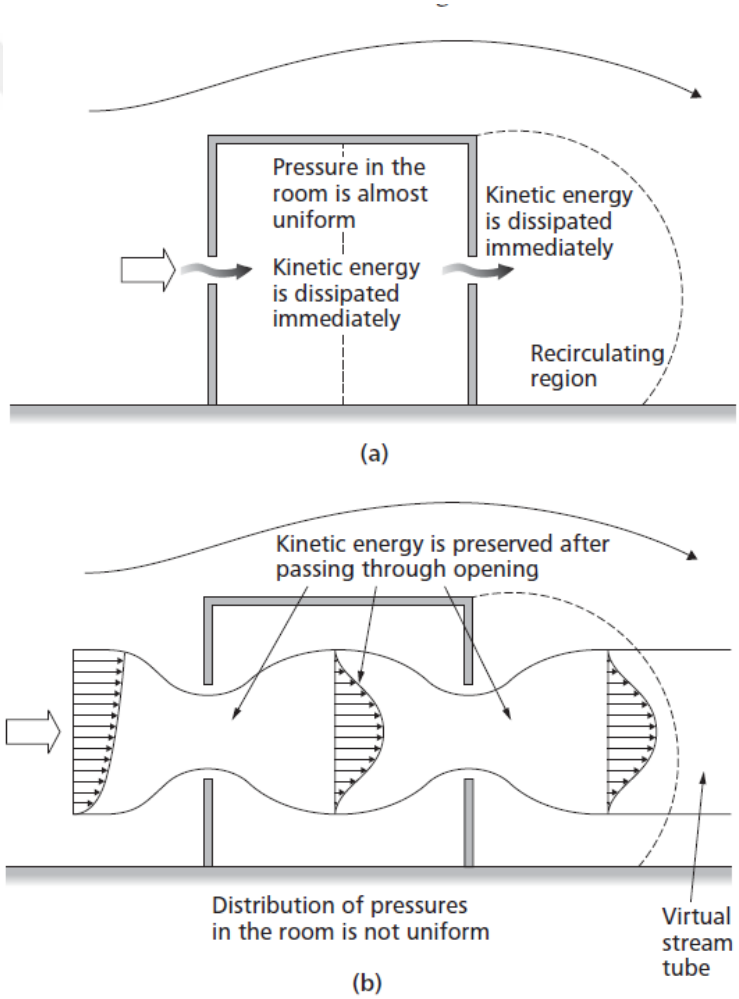

Figure 21. Airflow and its kinetic energy behaviour through (a) a small opening and (b) a large opening (Adapted from Kato, 2004, as cited in CIBSE, 2015).

On the other hand, according to Park, Choi, and Rhee (2016), the presence of an overhang, such as a balcony slab, results in an increase in the single-sided ventilation rate in the windward direction while causing a decrease in the leeward direction. According to the research conducted by Zhang, Weerasuriya, Wang, Li, Chen, Tse, and Hang (2022) using CFD, increasing the number of openings from 1 to 2 significantly enhanced the ventilation rate, whereas the subsequent increases from 2 to 3 and then to 4 resulted in progressively smaller improvements in the ventilation rate (Figure 22).

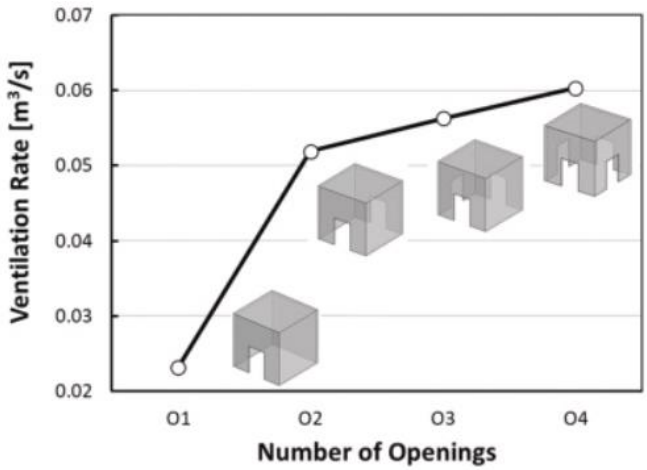

Figure 22. Relationship between the number of external openings and the change in ventilation rate (Zhang et al., 2022)

2.2.1.2 Natural Ventilation by Stack Effect

The stack effect is driven by temperature differences between the interior and exterior of the building, as well as variations in air density. This situation causes instability between the inside and outside air pressure, resulting in vertical pressure disparity (CIBSE 2015).

Warmer air rises while cooler air flows downward, a movement resulting from the density differences caused by temperature variations (Khan, Su, and Riffat, 2008). When the indoor temperature exceeds the outdoor temperature, air enters the building through openings near the ground floor and exits through openings close to the roof (stack effect, Figure 23-a). Conversely, when the outdoor temperature is

higher than the indoor temperature, the airflow occurs in the reverse direction (reverse stack effect, Figure 23-b) (CIBSE 2015).

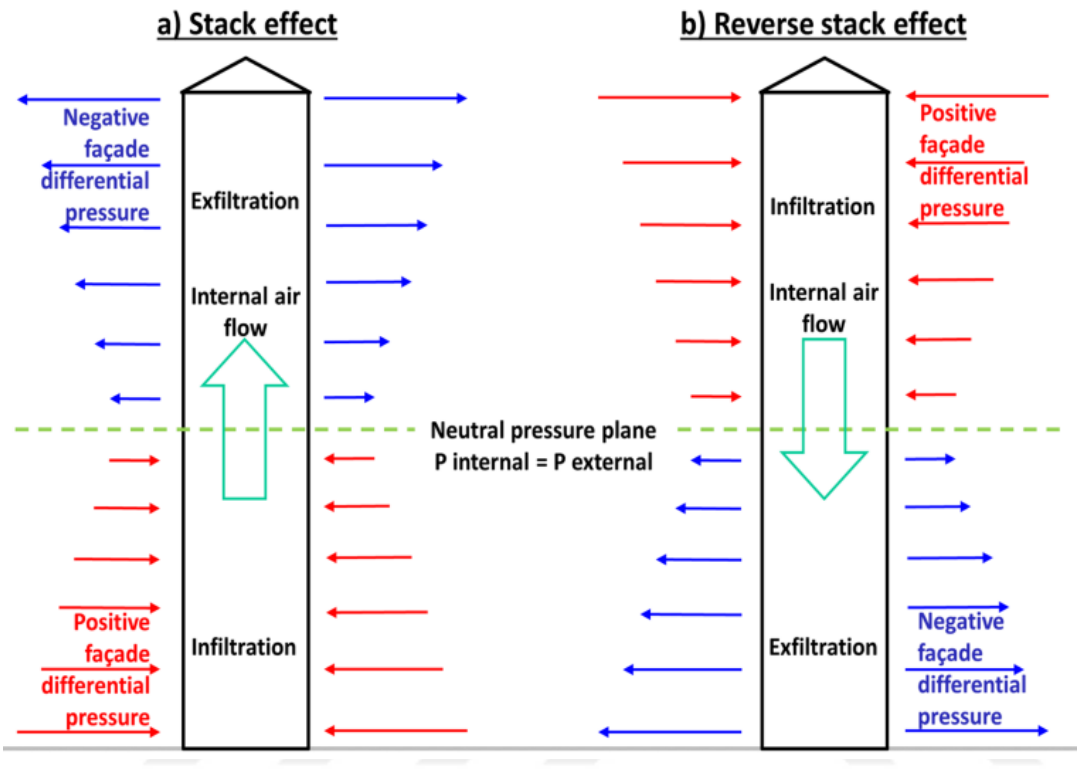

Figure 23. Representation of (a) the stack effect and (b) the reverse stack effect in buildings (Mijorski and Cammelli, 2016)

Song, Yoon, Jeong, Kim, and Lim (2019) conducted a study on the effects of the stack effect and reverse stack effect on heat, vapour, and CO2 in the elevator hall of a 29-story residential apartment. The study was carried out over two months during the winter, focusing on morning hours to reduce airflow variations due to occupants and wind. The data was recorded using sensors. In this study, indoor temperature, CO2 concentration, and vapour levels obtained from the 7th, 13th, and 23rd floors were compared. According to the findings, the 13th floor had the highest indoor air temperature, CO2 concentration, and absolute humidity due to a lack of air circulation at the neutral pressure level, driven by the stack effect.

Within a building, vertical air movement is generated as cold air warms up. Stack flow occurs even with minimal temperature differences (Heiselberg, 2004). On the

other hand, enhanced thermal gradients affect the stack effect in a positive way (Raji, Tenpierik, and van-den-Dobbelsteen, 2016). Denser and colder outdoor air tends to move inside through lower openings, and relatively less dense and warmer air tends to move upward, called buoyancy-driven flow, as seen in Figure 24 (Allocca, Chen, and Glicksman, 2003).

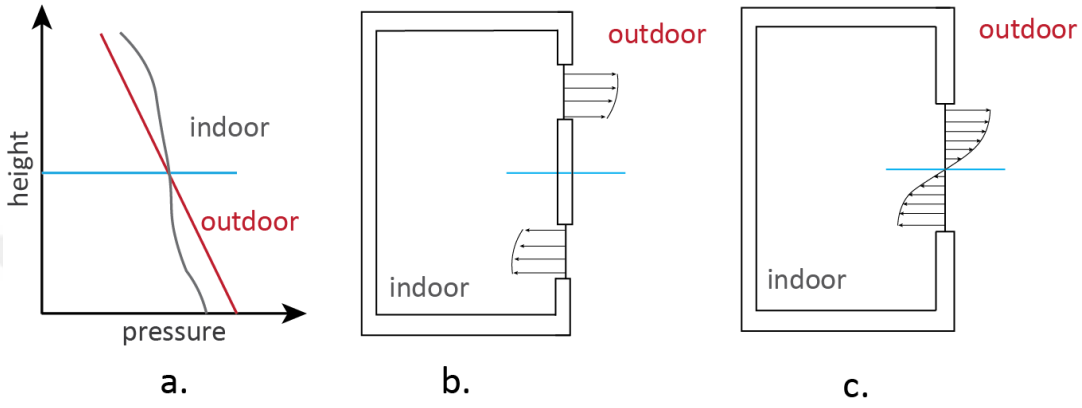

Figure 24. Representation of the relationship between airflow pressure and height in (a) a sectional view of a room with vertically aligned identical openings, (b) a room with a single opening (c) (Park et al., 2016).

According to the study by Ural, Akgün, and Ertürk (2020), CFD was used to model the airflow passing through a window vent in a kitchen with a combination boiler, which provides both central heating and hot water. During winter, cold outdoor air enters the indoor space through the lower part of the vent, while warm indoor air flows out through the upper part of the vent, as seen in Figure 25.

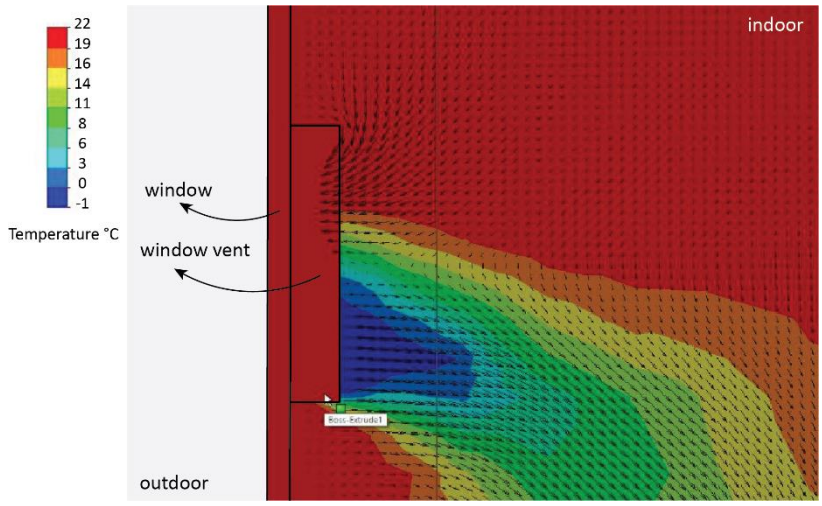

Figure 25. Airflow temperature and direction through window vent (Adapted image from Ural, Akgün, and Ertürk, 2020)

On the other hand, if the pressure difference is lower, there are improving applications for stack ventilation. For instance, in a hot and humid climate, a solar roof collector seen in Figure 26, is the most preferred solution among Trombe walls, solar chimneys, and solar collectors (Yusoff, Sapian, Salleh, Adam, and Hamzah, 2014)

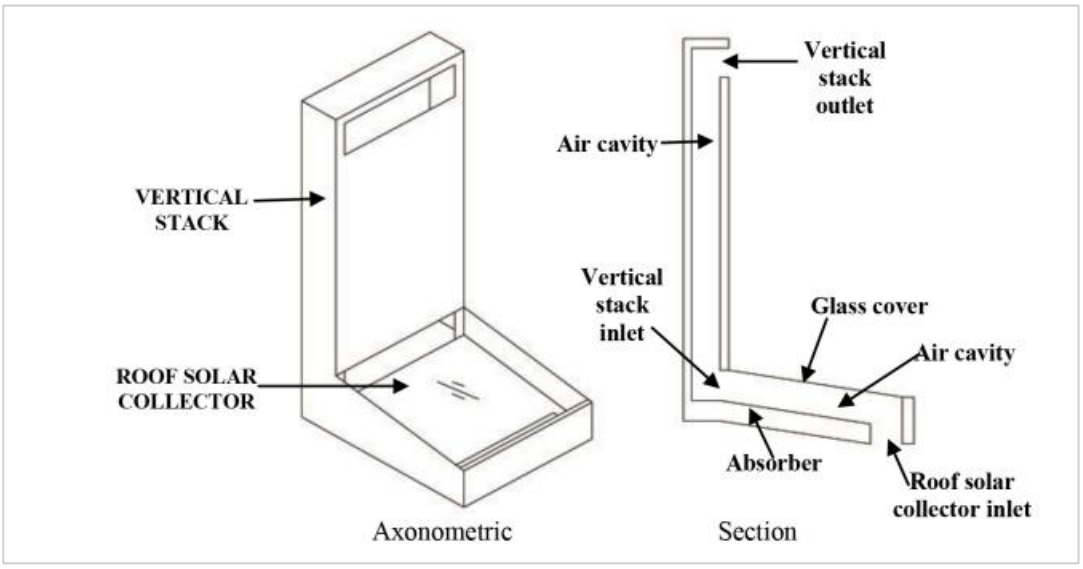

Figure 26. Solar-induced air collector (Yusoff et al. 2014).

2.2.1.3 Natural Ventilation by Combined Wind and Stack Effect

The airflow path in buildings varies depending on whether the stack effect or wind effect is dominant. According to Liddament (1996), the airflow paths within buildings depend on the interaction between stack and wind effects (Figure 27). Four scenarios were examined to illustrate this interaction. In scenario (a), with no wind, airflow enters from below and exits from above due solely to the stack effect. In scenario (b), with the introduction of low wind speeds, air enters through lower openings and exits through upper openings; the wind effect strengthens the stack effect at openings 1 and 3 while weakening it at openings 2 and 4. In scenario (c), as wind speed increases further, airflow continues from lower to upper openings; however, the intensified wind reduces the stack effect at openings 2 and 4, resulting in a decreased air change rate. In scenario (d), at even higher wind speeds, airflow exits simultaneously from both lower (1 and 2) and upper openings (3 and 4); nevertheless, the stack effect persists at openings 1 and 3, restoring the air change rate to 0.48

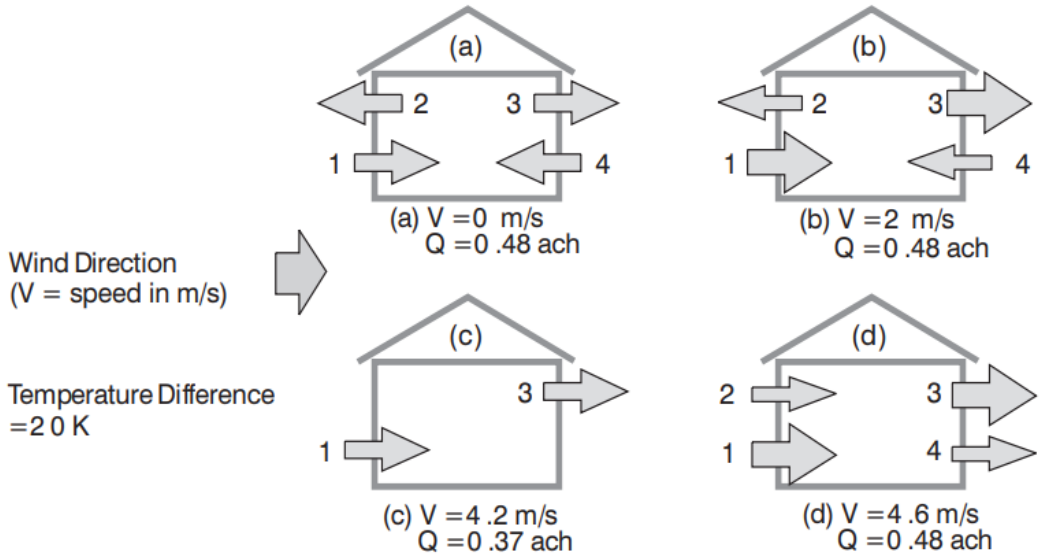

Figure 27. The relationship between airflow paths in buildings and the interaction of stack and wind effects is illustrated through scenarios (a)–(d), from stack-dominated to wind-dominated conditions (Liddament, 1996)

In a study conducted by Seo, Lee, Song, and Kato (2010), it was observed that in 20-storey buildings in Korea, particularly during winter and on upper floors, used air from lower floors flows in through stairwells or elevator shafts into housing units located above the neutral plane due to the stack effect. Additionally, the flow rate of mechanical ventilation of kitchens above the neutral plane decreases due to the stack effect, resulting in increased CO_2 concentrations (Figure 28).

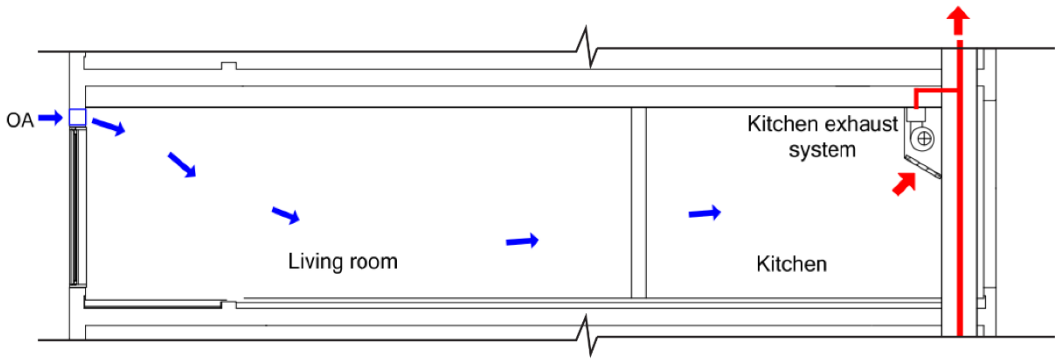

Figure 28. The kitchen section illustrates the ventilation system in which air was supplied through natural ventilation and exhausted using mechanical ventilation in the kitchens of the measured apartment building (Seo, Lee, Song, and Kato, 2010)

In another study conducted in Korea by Song, Yoon, Jeong, Kim, and Lim(2019), heat, vapour, and CO_2 concentrations were examined in a 31-storey building through measurements taken during the winter season. This study compared results from the 7th, 13th, and 29th floors, observing heat, vapour, and CO_2 concentrations. The measurement sensors were placed in the elevator hall of the measured floors at a height of about 1.6 meters. According to the results, heat, vapour, and CO_2 concentrations were highest on the 13th floor, which is closest to the neutral plane (Figure 29).

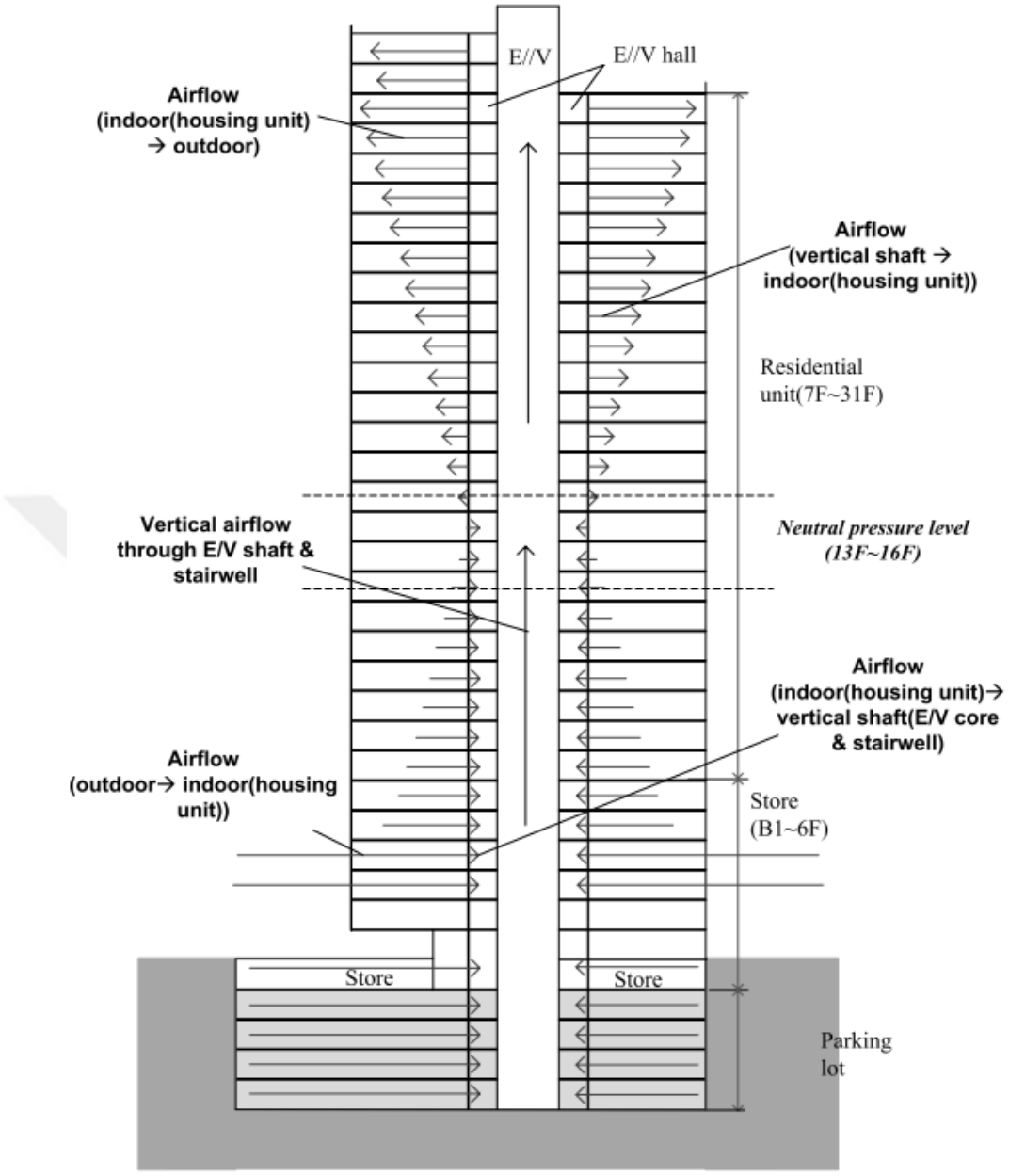

Figure 29. Airflow distribution through housing units, elevator shafts, and stairwells under the stack effect in a 31-storey residential building with underground parking and stores in Korea (Song, Yoon, Jeong, Kim, & Lim, 2019)

In situations where natural ventilation is inadequate, mechanical ventilation becomes necessary; primarily, mechanical ventilation systems such as exhaust air systems in kitchens are employed in multi-story dwellings. (Lee, Lee, Park, Kim, and Lee, 2011).

2.2.2 Mechanical Ventilation

Mechanical ventilation is categorized into three main types: exhaust ventilation, supply ventilation, and mixed-mode ventilation(Chartered Institution of Building Services Engineers Guide B, 2001). Without sufficient natural driving forces and access to fresh air through windows, mechanical ventilation emerges as an adjustable and controllable option (Hu, Liu, Ai, and Zhang, 2023). In order to run the mechanical ventilation system, electricity consumption is necessary (Davidsson, Bernardo, and Hellström, 2013). On the other hand, mechanical ventilation efficiency is not a fixed value in multi-story residential buildings due to the stack effect (Seo et al., 2010). In mechanical ventilation, balanced supply and extract are the most commonly applied systems. Other options rely on natural air movement to achieve this balance, such as mechanical extract with natural supply, and mechanical supply with natural extract (Chartered Institution of Building Services Engineers Guide B, 2001).

2.2.2.1 Exhaust Ventilation

In exhaust ventilation, the building is under-pressurised, and make-up (balancing) air, which is natural supply air, flows in from outdoors through vents and leakage openings. Thus, areas where fresh air enters become clean zones, while areas from which polluted air is extracted become contaminated zones. Indoor air cannot be completely clean; however, the airflow direction for contaminated air is intentionally designed from the clean zone toward the contaminated zone, as illustrated in Figure 30 (Chartered Institution of Building Services Engineers Guide A, 2006).

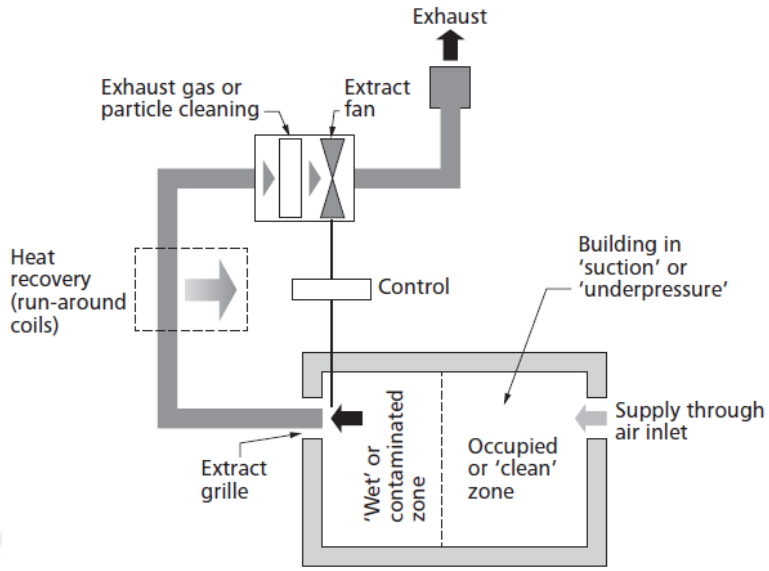

Figure 30. Diagram of the air circulation in an exhaust ventilation system with mechanical extract and natural supply (CIBSE Guide A, 2006).

It works as a part of a centralised exhaust system or, individually, in an allocated room, or a combination of both at the same time by considering the windward and leeward direction of the wind while locating the exhaust outlet (Secretary of State, The Building Regulations, 2010).

The building function is also considered a need and efficiency for an exhaust system. In the case of residential buildings, if mechanical exhaust ventilation exists, it is located in the kitchen and bathrooms due to the activities that require more ventilation to provide a healthy environment. In the bathroom case, it requires removing water vapour, causing mould growth and spreading odours to adjacent spaces; thus, exhaust ventilation performance is crucial (Kim and Yang, 2016) In order to prevent airborne transmission between spaces like the hospital, due to the cross-infection potential, airflow orientation is intended to be managed (Qian and Zheng, 2018).

In the case of the kitchen, since cooking produces a variety of pollutants, including fine particles, ultrafine particles, and volatile organic compounds, it requires greater exhaust ventilation (Chen, Zhao, & Zhao, 2018). According to the Secretary of

State's Building Regulations F(2010), if a cooker hood extracts air directly(Figure 31-a) to the outside and operates intermittently, the extraction rate should be 30 l/s during operation. However, if a recirculating cooker hood is used, an extraction rate of 60 l/s should be provided elsewhere(Figure 31-b).

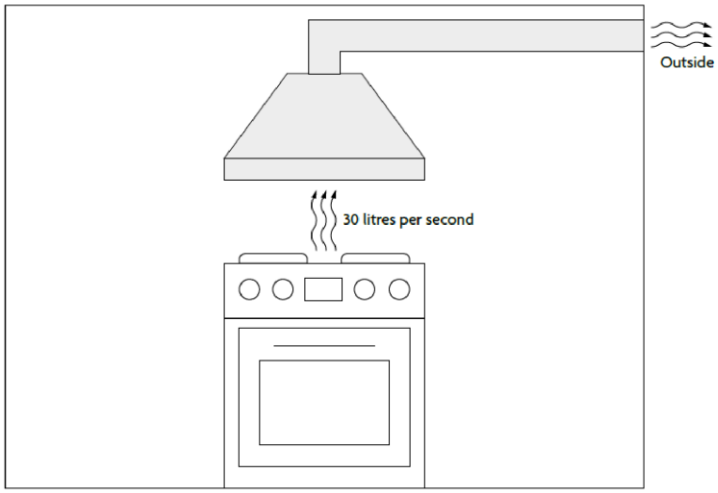

a. Cooker hood exhaust to outside

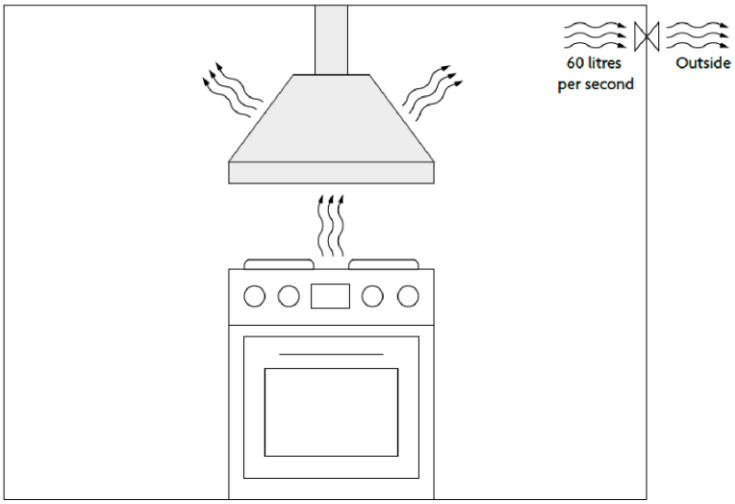

b. Recirculating cooker hood

Figure 31. Minimum ventilation rates according to cooker hood extraction type: (a) cooker hood extracting directly to the outside, (b) recirculating cooker hood (Secretary of State's Building Regulations F, 2010)

If the cooker hood extracting to the outside operates continuously, the minimum extract rate for the kitchen should be 13 l/s; however, this rate may increase

depending on the number and function of other rooms(Secretary of State's Building Regulations F, 2010).

2.2.2.2 Supply Ventilation

In mechanical supply ventilation, mechanical supply provides fresh air into the occupied spaces, and natural extraction allows air to diffuse out through leakages or purpose-provided vents, as seen in Figure 32 (Chartered Institution of Building Services Engineers Guide B, 2001).

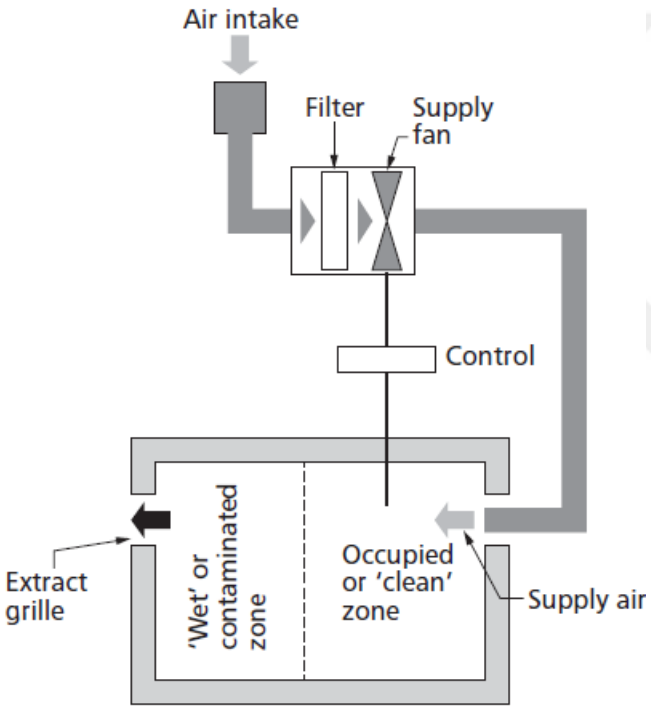

Figure 32. Diagram of air circulation of supply ventilation with mechanical supply and natural extract (Chartered Institution of Building Services Engineers Guide A, 2006).

Mechanically supplied air pressurises the space and prevents air ingress from the outdoors and connected spaces. Thus, it ensures controllability in areas where indoor air needs to be clean and filtered. The ventilation rate and air distribution system requirements for supply ventilation depend on the functions of specific areas, such

as classrooms, offices, and conference halls (Russell, Sherman, & Rudd, 2007). For example, Khankari (2018) investigated the effect of supply airflow rate in a hospital operating room by varying the diffuser discharge air velocity from 0.1, 0.15, and 0.2 m/s, corresponding to 15, 23, and 31 ACH, respectively, using Computational Fluid Dynamics (CFD), as seen in Figure 33. Since the exhaust air rate was lower than the supply air rate, the room was maintained at positive pressure. The goal of extracting air from the room without recirculation was achieved at 31 ACH, whereas at 15 and 23 ACH, the airflow path recirculated around the outer edge of the operating room.

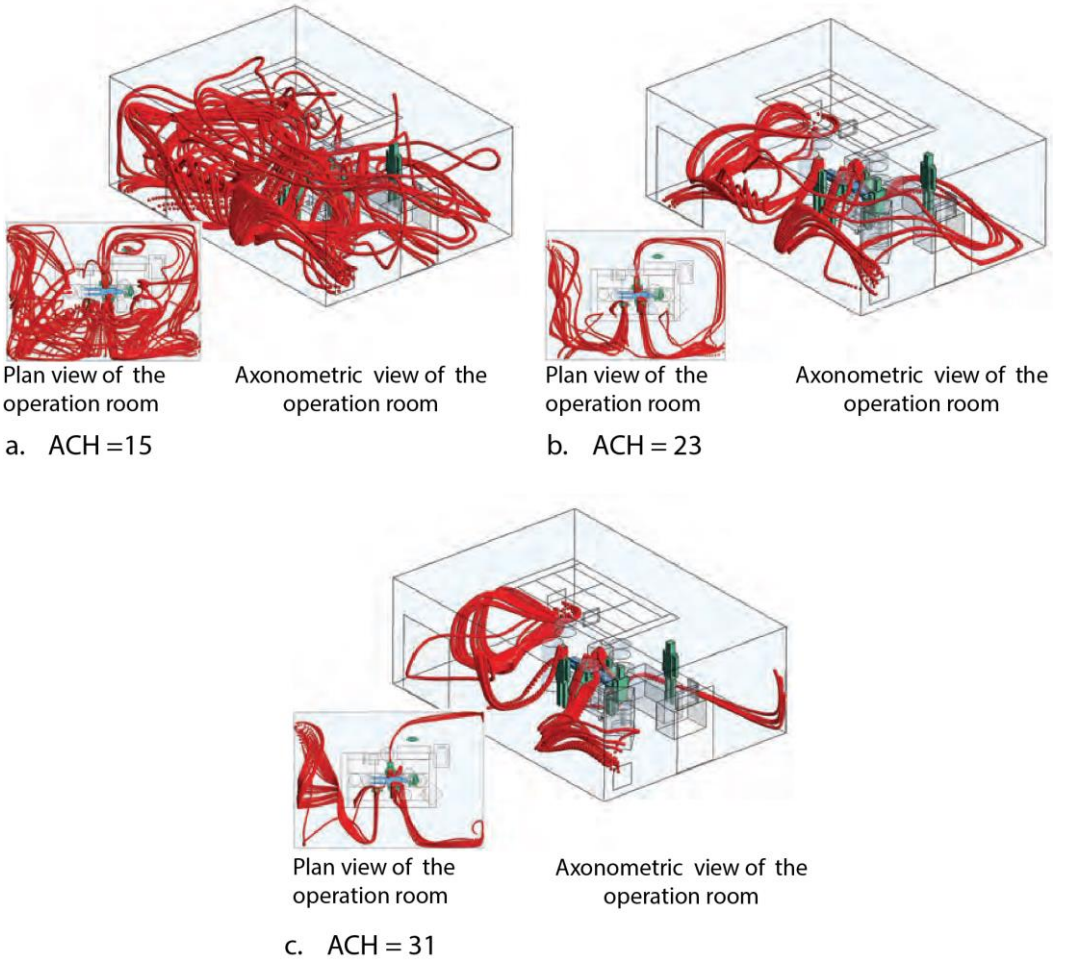

Figure 33. CFD simulation illustrations of airborne particulate flow paths from occupants in an operating room at three different ACH levels: (a) 15 ACH, (b) 23 ACH, and (c) 31 ACH. (Khankari, 2018)

Personalized supply ventilation is not only a concern for building ventilation but also a key aspect of aircraft ventilation. The significant benefit of personalized supply ventilation is that it delivers fresh air directly to the inhaled area of individuals, ensuring efficient ventilation and reducing contamination (Elmaghraby, Chiang, & Aliabadi, 2017).

2.2.2.3 Balanced Ventilation

Under-pressurisation in mechanical extract or over-pressurisation in mechanical supply ventilation is regulated in balanced ventilation by equalising the flow rates. In balanced ventilation systems, a heat recovery unit is mandatory under certain regulations in some countries with cold climates, as seen in Figure 34 (Chartered Institution of Building Services Engineers Guide B, 2001).

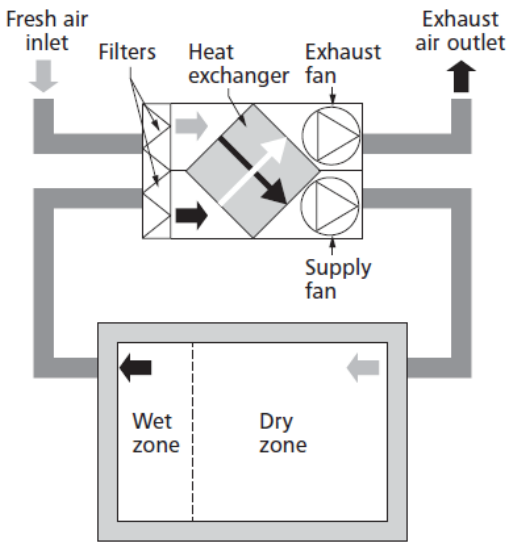

Figure 34. Diagram of air circulation of balanced ventilation with mechanical supply and extract, and heat exchanger (Chartered Institution of Building Services Engineers Guide A, 2006)

While designing a commercial kitchen, cooking heat is usable with a run-around coil system with 40% efficiency (Don, and Rich, 2014). In the context of kitchens, balanced ventilation is achieved by introducing supply ventilation - also called

“make-up air” - to counterbalance the air extraction of the cooker hood. The supply and exhaust ventilation systems operate simultaneously, transferring heat and providing occupants with a specific thermal comfort range (Flaga-Maryanczyk, Schnotale, Radon, and Was, 2014). In another definition, make-up air refers to the additional supply of air used to maintain balance and prevent building under-pressurization, which would otherwise reduce the efficiency of exhaust ventilation (Ventilation Committee of the Inter-Agency Review Council, 2010). According to Livchak, Schrock, and Sun (2005), a CFD simulation was conducted in a commercial kitchen to investigate how directly supplying outdoor air at different temperatures (hot, cold, or moderate) as make-up air influences cooker hood performance (Figure 35). The findings showed that providing make-up air at 23.9°C prevented the formation of a thermal plume at the cooker hood. At 10°C, although the cooker hood’s performance was efficient, it was uncomfortable for occupants. Finally, at 37.8°C, both cooker hood performance and occupant comfort were negatively impacted, making it the least favourable scenario.

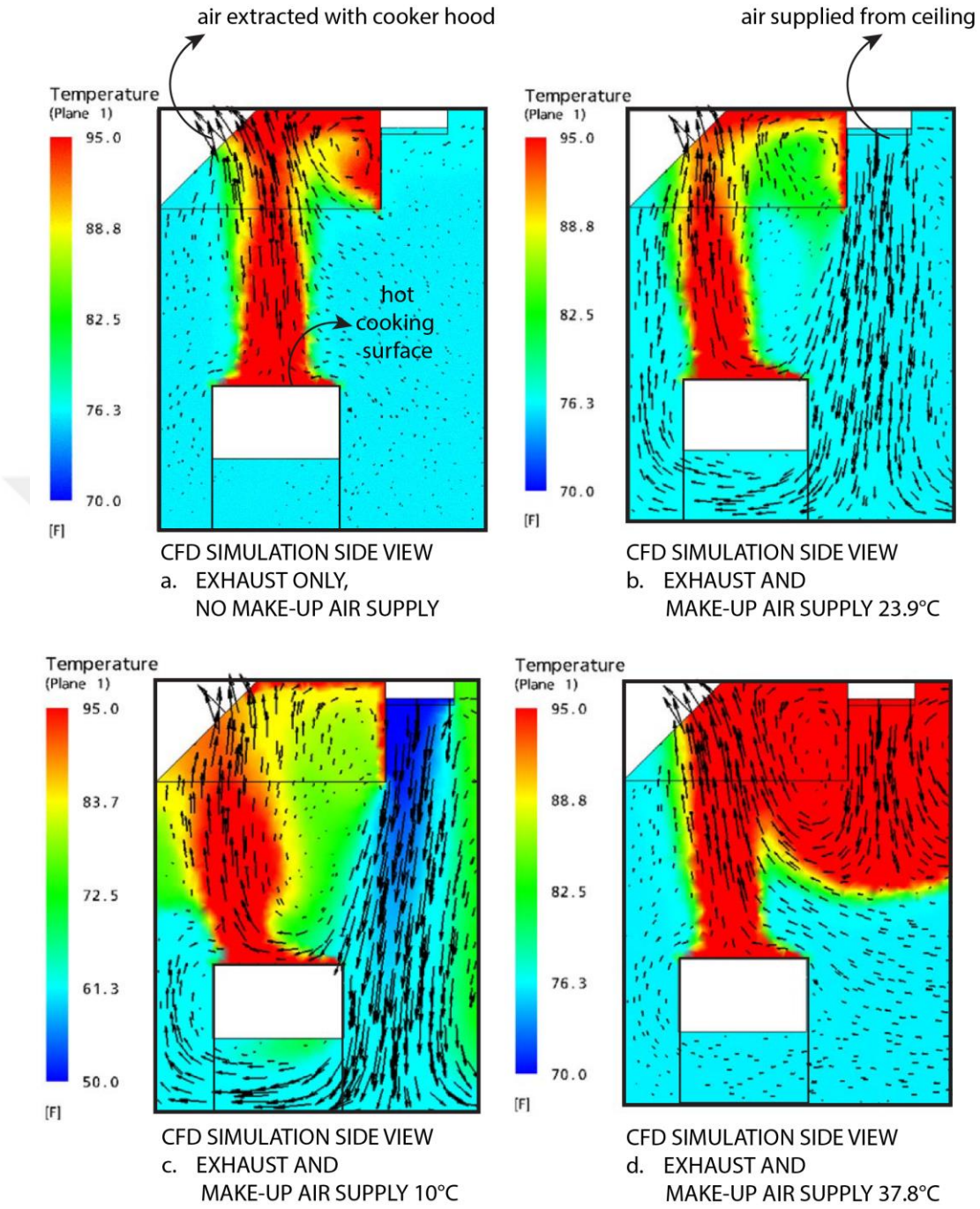

Figure 35. Cooker hood performance with (a) no air supply and with different supply air temperatures: (b) 23.9°C, (c) 10°C, and (d) 37.8°C (Livchak, Schrock, and Sun, 2005).

In an experiment using cooking oil to test exhaust rates in a Chinese residential kitchen, He, Gao, Chen, Zeng, Zhang, Zhang, Xu, and Guo (2021) found that opening a window created cross-flow and overflow, thereby negatively affecting the removal of cooking oil fumes. It was highlighted that the most effective strategy was to supply make-up air from a floor-mounted system, with a top-mounted system as the second-best option, as both approaches increased airflow rates and enhanced exhaust efficiency (Figure 36).

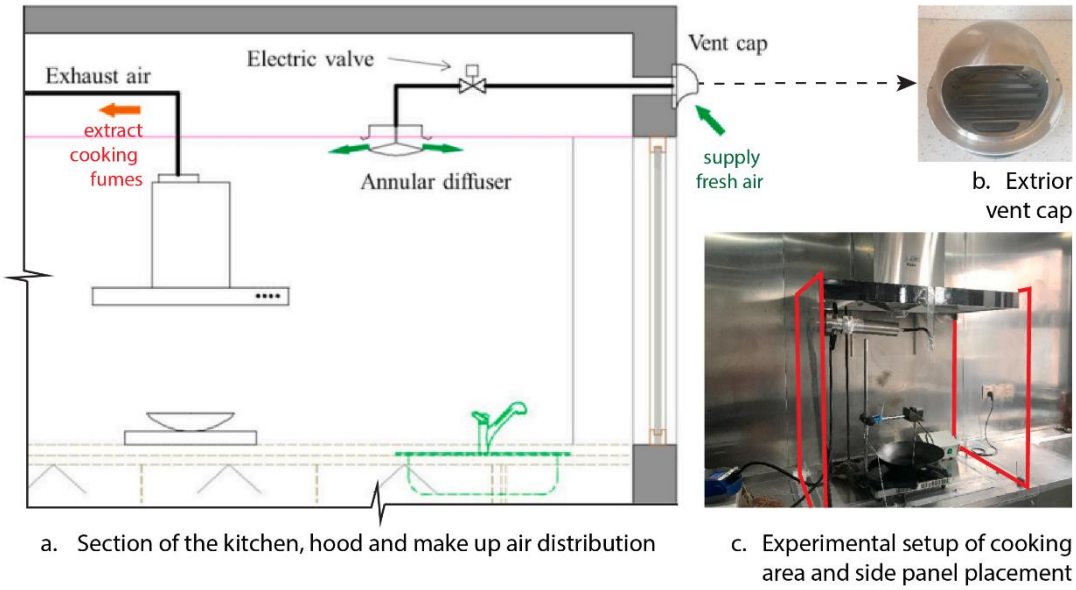

Figure 36. (a) Illustration of the kitchen airflow distribution, and (b)exterior vent cap and (c) actual details of the experimental setup (He et al., 2021)

2.2.3 Mixed Mode Ventilation

Mixed-mode ventilation combines both natural and mechanical ventilation. When natural ventilation is insufficient, mechanical ventilation operates as a supplementary system. In some cases, both natural and mechanical ventilation may function together in a complementary manner to meet ventilation requirements. Alternatively, depending on environmental conditions, either mechanical or natural ventilation may be used, switching between the two as necessary(Chartered Institution of Building Services Engineers Guide B, 2001). Soebiyan (2021)

emphasizes that the mixed-mode ventilation system is designed based on the climate period and duration, taking into account natural ventilation methods. Raji et al. (2016) point out that mixed-mode ventilation design improves the efficiency of natural ventilation by supplementing it with mechanical ventilation. Meanwhile, Heiselberg (2004) states that mixed-mode ventilation not only consumes less energy compared to solely mechanical ventilation but also provides greater stability than a system relying solely on natural ventilation.

2.3 Indoor Air Quality Measurements

Pollution is where the space with an envelope is more remarkable than exterior space; the reason for occupants and their activities in making a fire, especially in emerging countries, building materials, interior events, etc., are the primary reason for ventilation demand and the argument for indoor air quality(Sundell, 2004).

2.3.1 Air Pollutants

In an experimental study conducted in nine homes in California by Singer, Pass, Delp, Lorenzetti, and Maddalena (2017), the combustion of natural gas cooking burners was examined, and the concentrations of various indoor air pollutants—including carbon dioxide (CO_2), nitric oxide (NO), nitrogen oxides (NO_x), nitrogen dioxide (NO_2), particles with diameters of 6 nm or larger (PN), carbon monoxide (CO), and fine particulate matter ($PM_{2.5}$)—were measured in both kitchen and bedroom areas. The results showed that these pollutants significantly dispersed beyond the kitchen space. The one-hour interval during which CO_2 reached its highest concentration was used to determine the timing of peak exposure for other pollutants. On the other hand, the ASHRAE Board of Directors (2025) states that indoor CO_2 concentration is not a definitive indicator of indoor air quality (IAQ); however, it can serve as a tool when considering its relationship with other pollutants. An increase in CO_2 concentration indicates that it requires more

ventilation. In workplaces, the United States Occupational Safety and Health Administration (OSHA) (2017) sets a safe exposure limit for carbon dioxide (CO_2) at 5,000 ppm, based on an average of 8 working hours. Similarly, the National Institute for Occupational Safety and Health (NIOSH) (1976) suggests the same limit for 8 hours but also gives a short-term limit of 30,000 ppm for up to 10 minutes.

Sun and Wallace (2021) also point out that cooking is one of the most obvious sources of air pollution, especially in terms of particle emissions. The way of cooking, such as boiling or frying, and with the gas or electric stove, and low or high temperature causes a different range of ultrafine particles, in other words, $PM_{2.5}$ (particulate matter size less than 2.5 microns). Cooking at high temperatures with a gas stove produces a top value of ultrafine particles while frying rather than boiling (Zhang, Gangupomu, Ramirez, and Zhu, 2010). Moreover, deep frying causes more $PM_{2.5}$ concentration than pan frying, stir-frying, boiling, and steaming (Wu, Xiu, Wang, and Xue, 2016). Also, cooking causes a progressive rise in CO2 levels (Lee et al., 2011). According to Buonanno, Morawska, and Stabile's (2009) research, the emission rate depends on the oil type, whether olive oil or sunflower oil, while frying, considering the cooking pot surface area, on a gas or electric stove. It is also observed a greater emission rate of frying with sunflower oil on a gas stove with a larger pot surface area (Gao, Cao, Wang, Song, Zhou, Yang, and Zhang, 2013). On the other hand, cooking styles with the same material result in different emission rates; Western-style cooking using oil has a lower emission rate than Eastern-style cooking oil (Kang, Kim, H., Kim, D., Lee and Kim, T., 2019).

According to Zhang et al. (2010), exhaust fans significantly positively impact reducing emission concentration. Besides, the indoor air quality of the kitchen improves in a shorter duration with natural ventilation than with mechanical exhaust ventilation by considering the CO2 rate (Lee et al., 2011). Furthermore, the dirt on the mechanical ventilation duct system is another source of pollution (Heiselberg, 2004). Expecting mechanical ventilation to operate and clean the air can lead to a further decline in indoor air quality. Moreover, indoor air quality in a multi-story building is better in summer than in winter. The upper floors are less dense in interior

particle rate than the upper floors (Fu, Kim, Chen, and Sharples, 2021). On the other hand, according to Sui, Tian, Liu, Chen, and Wang, (2021) research, natural ventilation through the window for half an hour raised interior $PM_{2.5}$ because of the higher emission rate of the exterior $PM_{2.5}$ ratio, as seen in Figure 37.

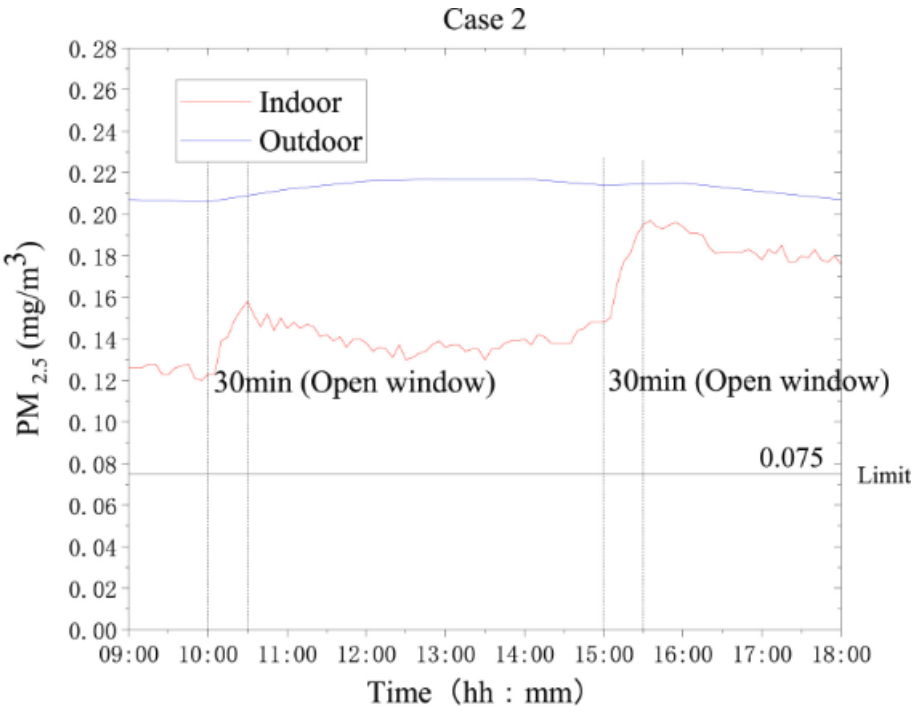

Figure 37. The relation between indoor PM2.5 concentration change and 30-minute window ventilation was measured during two distinct time intervals (Adapted table from Sui et al., 2021).

While the $PM_{2.5}$ rate is the most significant factor in interior air pollution, in different rooms apart from the kitchen, nitrogen dioxide, volatile organic compounds, toluene, benzene, and formaldehyde are also indicated (Yin, Liu, Zhang, Li, and Ma, 2019). Considering other living spaces in the house, ventilation in the kitchen is necessary for creating indoor air quality and a healthy living environment.

2.3.2 Air Filtration

Houses depend on natural ventilation without filtration, and if the air quality regarding the particulate matter is better outdoors than in the interior, then natural

ventilation is proper (Kang et al., 2020). On the other hand, natural ventilation through windows increases the $PM_{2.5}$ ratio due to the polluted exterior air in Xi, China (Sui et al., 2021). For example, if the outer $PM_{2.5}$ rate is denser than the interior while cooking, the make-up air provides a significant increase in the $PM_{2.5}$ rate, incorporated with the range hood (Xia, Bian, Shi, Zhang, and Chen, 2020). In the research conducted by Xia et al. (2020), using nanofiber screens on the window to provide filtered natural make-up air creates resistance to flow and adversely affects the range hood's performance, as seen in Figure 38.

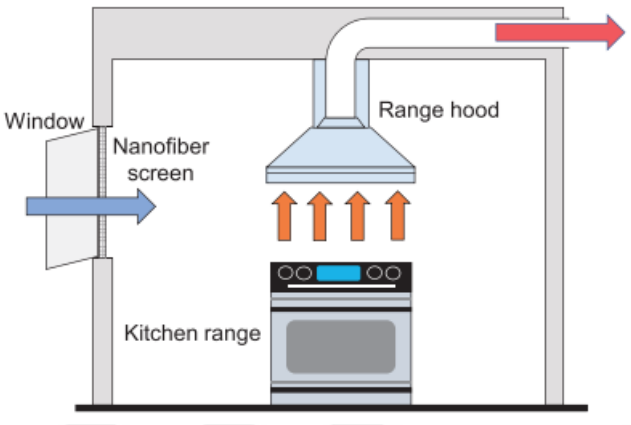

Figure 38. Natural ventilation with nanofiber screen and kitchen range hood schematic diagram (Xia et al., 2020).

Furthermore, in order to prevent particle accumulation in a range hood duct, the critical element is a filter. A filter in the range hood affects particle accumulation in the range hood duct, as seen in Figure 39; thus, periodic control is essential to provide ventilation efficiency (Zhao and Chen, 2006).

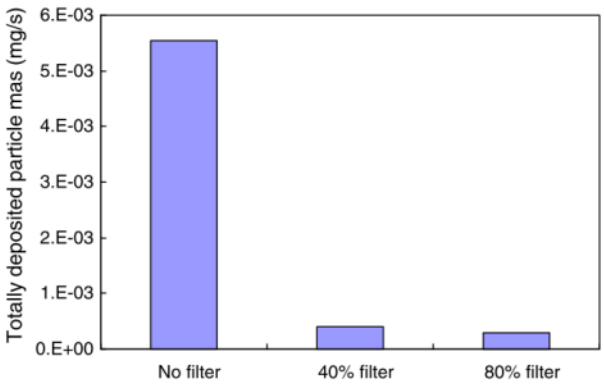

Figure 39. Relation between deposited particle mass and different filtration scenarios: no filter, 40% filter, and 60% filter (Zhao and Chen, 2006).

According to the research by Huang, Peng, Chen, and Nian(2010), cross draft inside the kitchen range hood duct forces the pollution outside of the hood due to the interior balance fluctuation caused by natural or mechanical forces. There are porous elements to use as a filter in several textiles, membranes, density, and expansion to take particles away from the airflow path (Mata, Martins, Calheiros, Villanueva, Alonso-Cuevilla, Gabriel, and Silva, 2022). In the case of a highly polluted exterior, a double air filter increases the indoor air quality by considering particle concentration (Fu et al., 2021)

2.3.3 Air Quality Control Mechanism

The air quality control mechanism for natural ventilation essentially comes down to opening or closing doors and windows. However, this situation becomes somewhat more complex for areas with low outdoor air quality. According to Costanzo, Yao, Xu, Xiong, Zhang, and Li (2019) research, if the outdoor temperature is between 10 and 28 degrees Celsius, the interior and exterior temperature difference is more than 2 degrees Celsius, and the $PM_{2.5}$ rate is lower than 0.075 mg/m^3-China limit, natural ventilation is allowed as seen in equation below.

$$\begin{cases} 10 < T_{outdoor} < 28 \\ T_{indoor} - T_{outdoor} > 2 \\ \text{PM2.5 concentration} < \text{threshold} \end{cases}$$

In this equation, considering the values, the outdoor air temperature, the temperature difference between inside and outside, and the particulate matter density outside mark off the potential of a manual control system for natural ventilation.

2.4 Indoor Thermal Comfort Measurements

The thermal comfort range varies by culture, age, gender, and perception. There are basic parameters that affect thermal comfort individually, which are temperature, velocity, and humidity of the air when ventilation occurs (Manshoor, Zaman, Asmuin, Ramlan, and Khalid, 2014)

2.4.1 Occupant's Satisfaction

The degree of the occupant's satisfactory interior air temperature relies on factors like environment, culture, and individual perception (Raji et al., 2016). The Predicted Mean Vote (PMV) is used as a universal comfort criterion index for introducing a suitable range for the interior to the mechanical ventilation, and the adaptive thermal model defines the proper operating range for natural ventilation of the buildings (Raji et al., 2016). The adaptive thermal model draws comfort zone temperature boundaries for distinctively different locations, while the minimum value refers to the coldest month and the maximum value to the warmest value, as seen in Figure 40. The comfort temperature range varies with the outdoor temperature range and tolerance limit dependently (Raji et al., 2016).

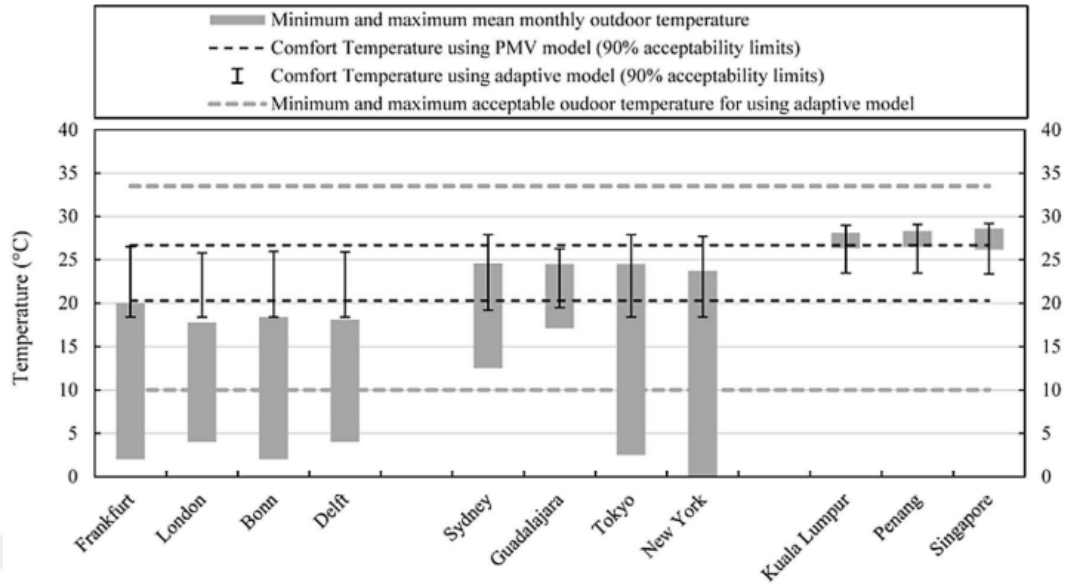

Figure 40. Comparison of mean monthly outdoor air temperature with comfort temperatures based on adaptive and predicted mean vote (PMV) models across 11 different cities (Raji et al., 2016)

According to the research by Chen, Xin, and Liu (2020), the kitchen environment examined varying exhaust air volume and increased exhaust volume of the kitchen range hood, which reduces the Predicted Mean Vote (PMV), indicating a better environment for occupants, as seen in Figure 41.

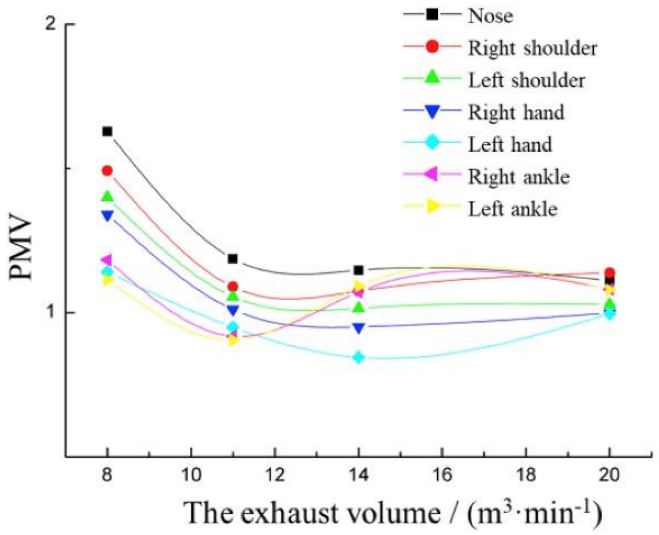

Figure 41. Predicted Mean Vote (PMV) values of various parts of the human body temperatures (Chen et al., 2020)

2.4.2 Thermal Comfort Control Mechanism

According to the U.S. Department of Energy (2015), in order to manage kitchen range hoods' Heating, Ventilating, and Air Conditioning systems (HVAC), considering the cooking activity, the mechanism is run by sensor data transmission through the range hood and HVAC system, as seen in Figure 42.

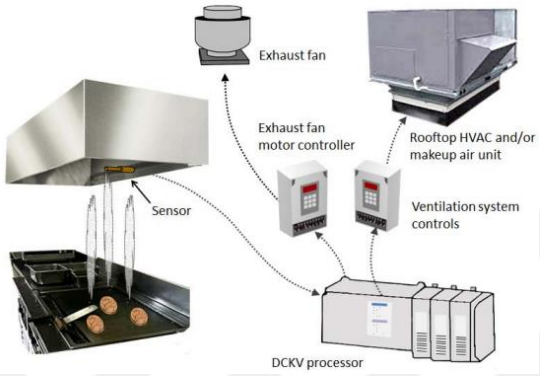

Figure 42. The kitchen mechanical ventilation control schema (U.S. Department of Energy, 2015).

On the other hand, in multi-story residential units, the kitchen exhaust system is turned on when the particle rate increases through cooking. Understanding the range hood usage cycle helps to automate the ventilation system to prevent particles' harmful effects on occupants (Zhao, Chan, Delp, Tang, Walker, and Singer, 2020). The optimum timing to operate the kitchen hood is to turn it on before cooking and turn it off after cooking (Nagda, Koontz, Fortmann, and Billick, 1989). On the other hand, most of the occupants turned on at the same time cooking started and turned off at the time cooking ended, as seen in Figure 43 (Sun et al., 2021).

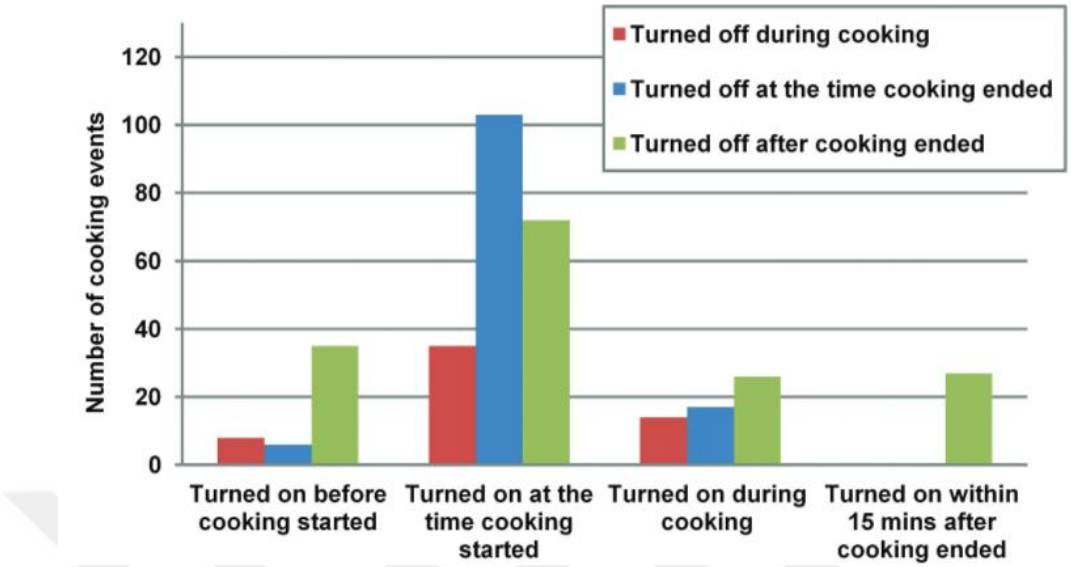

Figure 43. Mechanical ventilation habits of occupants in the kitchen (Sun et al., 2021)

Most of the time, occupants prefer opening the window rather than turning on the range hood, but for the extended duration of cooking, they do not prefer natural ventilation, especially in winter (Sun et al., 2021)

CHAPTER 3

MATERIAL AND METHOD

The Materials section initially presents the climate data, detailing the environmental conditions relevant to the study. Subsequently, the analysis progresses with the building data, adopting a sequential approach. This sequential examination begins with the overall building, followed by the kitchen data as a subordinate unit, and further narrows down to the flue data, a subcomponent of the kitchen. The method section describes the simulation processes of the material, which undergoes a two-stage analysis. These processes include the Apache Dynamic Simulation and the MicroFlo (CFD) Simulation.

3.1 Material

The research materials consist of climate data, building data, kitchen data, and flue data. Initially, these materials were used as inputs in Apache Dynamic Simulation to determine the kitchen flue airflow volume and direction. Apache Dynamic Simulation then generated the airflow data for the kitchen flue, which became one of the materials for the CFD simulation. Together with cooking data and kitchen interior component data, the airflow data formed the complete set of materials for the CFD simulation.

3.1.1 Climate Data

Simulation weather data for Ankara is embedded in the IES VE simulation program, and the weather file is based on International Weather for Energy Calculation (IWEC) data. According to ASHRAE & White Box Technologies (2008), IWEC climate data represents weather records spanning at least 12 years and up to 25 years.

The weather file contains information about dry-bulb temperature, wet-bulb temperature, solar radiation (global, direct, diffuse), relative humidity, dew point temperature, atmospheric pressure, sky cover, cloud cover, precipitation data, wind speed and wind direction. Wind data is analysed using VistaPro to determine the wind direction, speed, and frequency (Figure 44). The prevailing wind directions are from the North, with a 15% frequency and a maximum speed of 6–9 m/s. The North-East direction experiences the highest wind speed and the most frequent occurrence, making it the windward side. In contrast, the South-East and North-West directions have the lowest wind speed and frequency, designating them as the leeward sides.

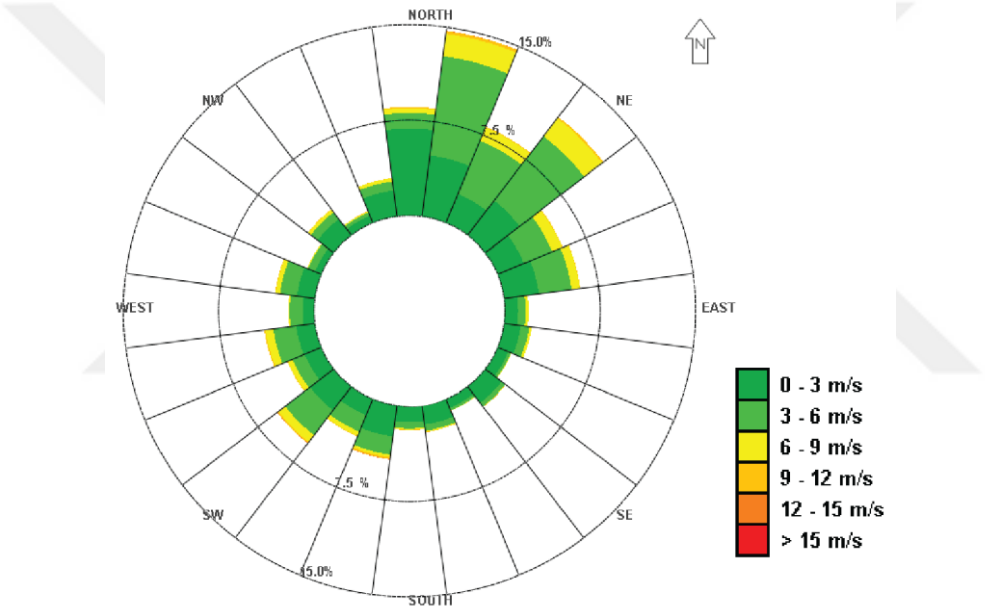

Figure 44. Wind rose diagram based on Ankara climate data from IES VE (Created using IES VE Vistapro tool)

3.1.2 Building Data

The residential unit plan is based on an existing building layout that includes four units; however, for the sake of simplicity, only two were modelled. It is assumed that the building is isolated, with no surrounding structures or shading. The building has a footprint of 15m x 15m and a height of 30m. The ten-story apartment building utilises two distinct plan layouts depending on whether it employs a vertical or

horizontal flue. To prevent exhaust backflow into the interior, the horizontal flue building's outlets are intentionally oriented away from the prevailing wind. Consequently, two distinct horizontal-flue configurations — one leeward and one windward — were developed, each resulting in its unique plan layout. The vertical-flue configuration uses a single plan layout. Consequently, three unique plan layouts were developed to represent the four scenarios. The horizontal flue's external opening is designed to remove kitchen fumes and is therefore consistently oriented on the leeward side, which is a negatively pressurised area. Consequently, when the apartment building is oriented toward the windward side, the horizontal flue assumes an L-shaped configuration as seen in Figure 45-H2, an apartment with horizontal flue. "V" denotes a vertical-flue apartment building, while "H" denotes a horizontal-flue configuration. The suffix "1" represents the leeward orientation and "2" represents the windward orientation. For simplicity, each combination of flue type and wind orientation is labelled as V1, V2, H1, and H2 (Figure 45).

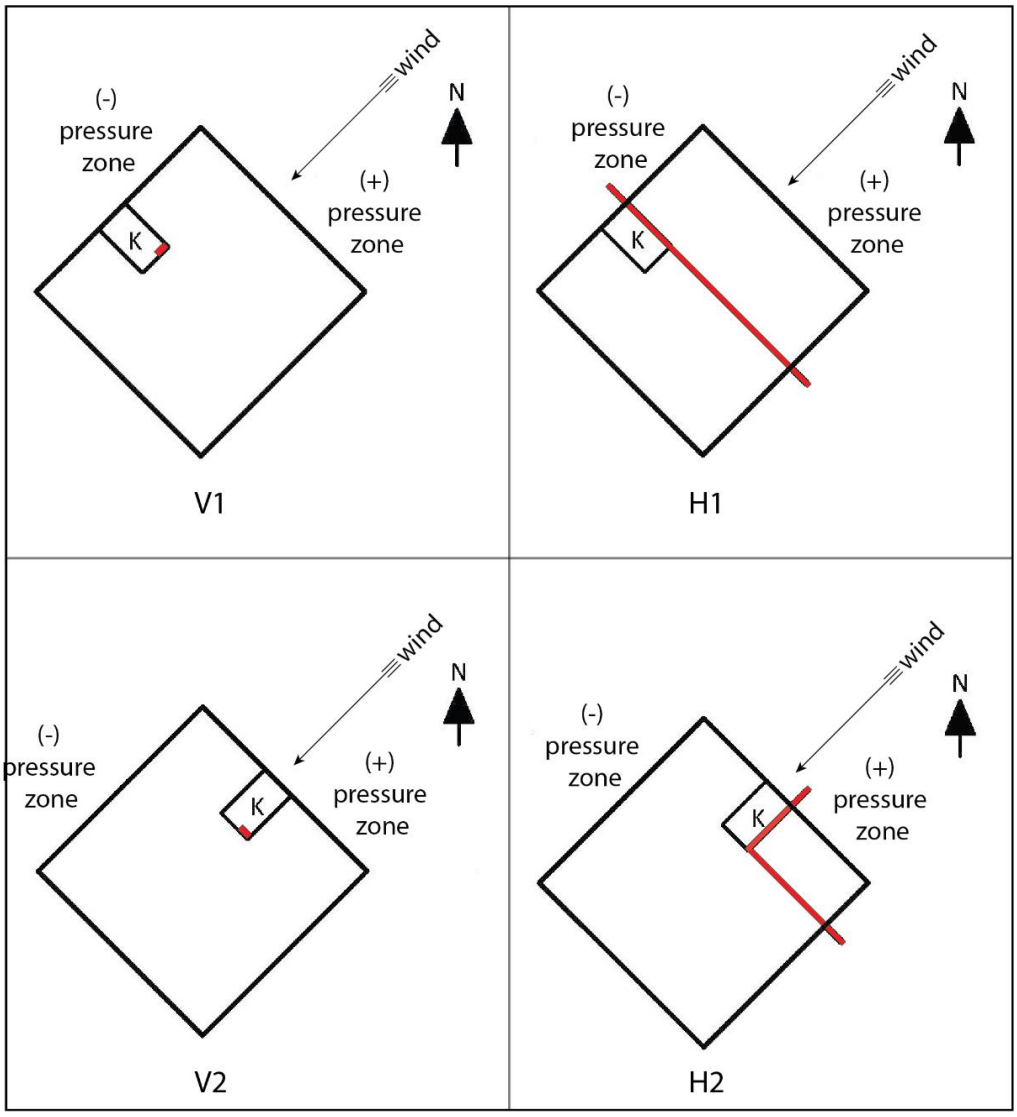

Figure 45. Plan layouts of the apartment building, differentiated by flue type and orientation.

For the apartment buildings of V1 and V2, the flue starts from the first-floor kitchen, passes through the building, and extends above the roof (Figure 46 and Figure 47).

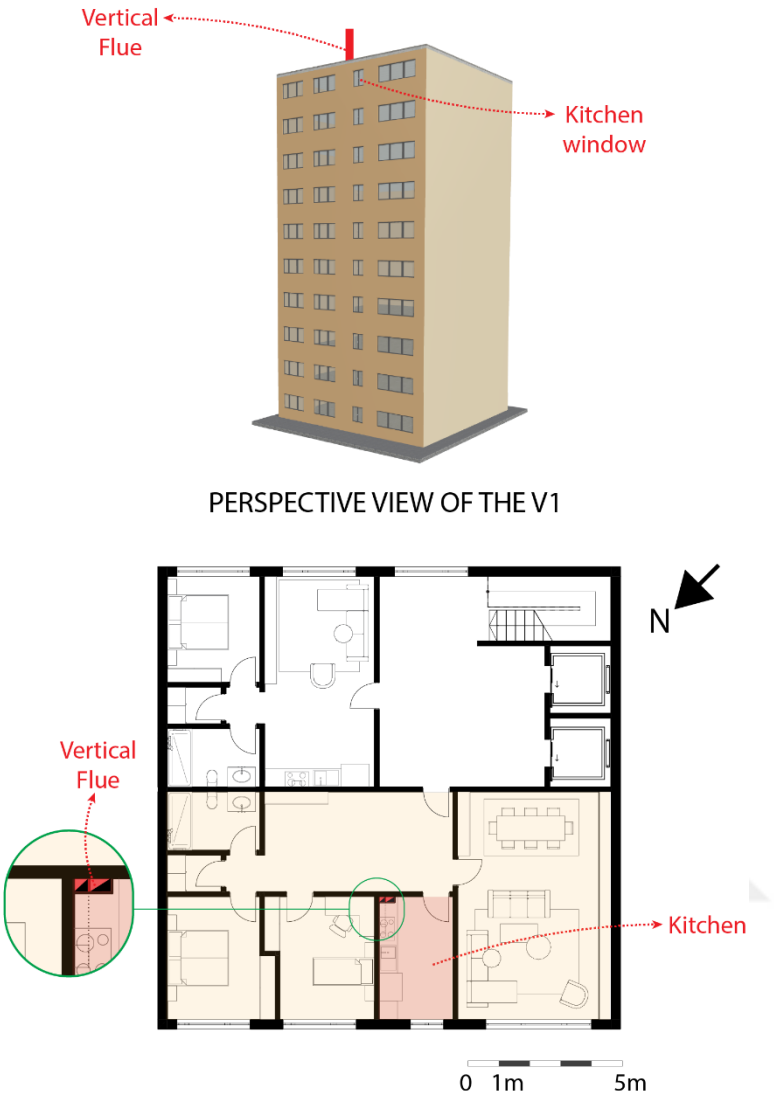

Figure 46. Leeward side oriented kitchen with a single-sided opening (natural gas vent on the window) and the vertical flue passing through the kitchen extends to the roof.

The only difference between the plan layout and the perspective view is that V1 is oriented towards the leeward side, whereas V2 is oriented towards the windward side. The perspective view and plan layout of V2 are presented in Figure 47.

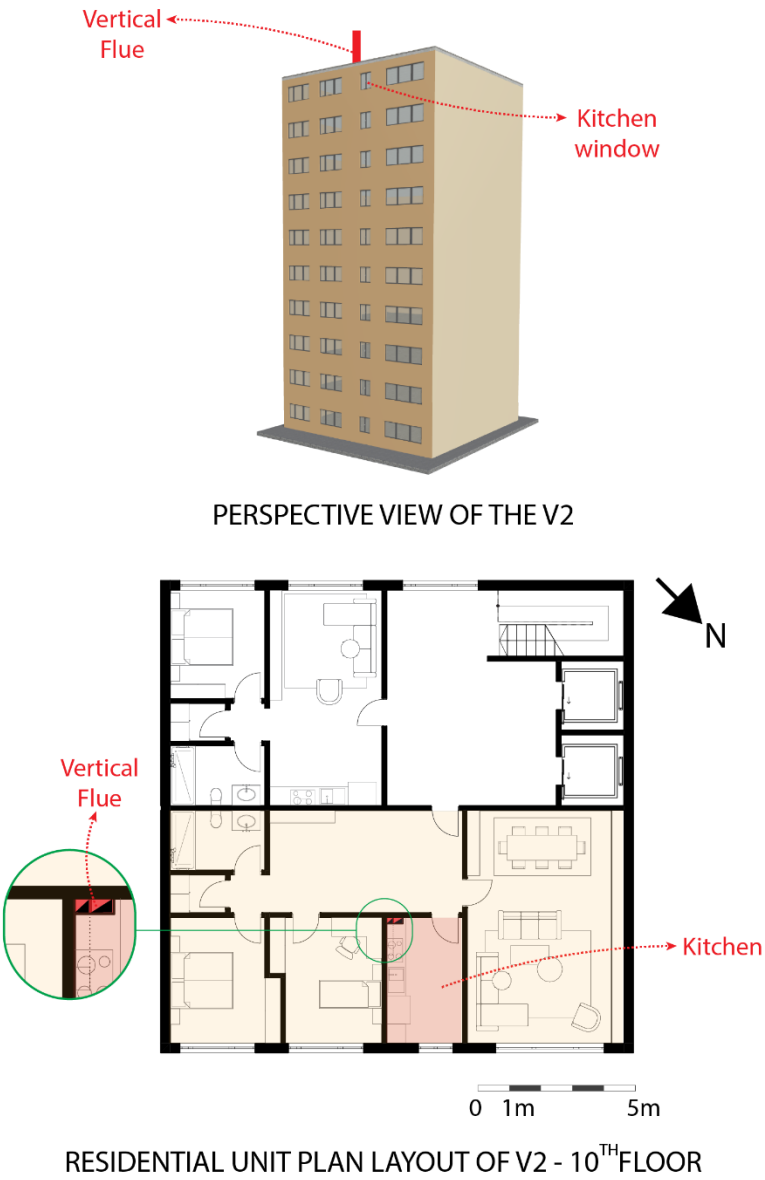

Figure 47. Windward side oriented kitchen with a single-sided opening (natural gas vent on the window) and the vertical flue passing through the kitchen extends to the roof.

For the H1, the flue enters from the kitchen facade, passes through the kitchen and adjacent spaces, and then extends to the rear facade of the building (Figure 48).

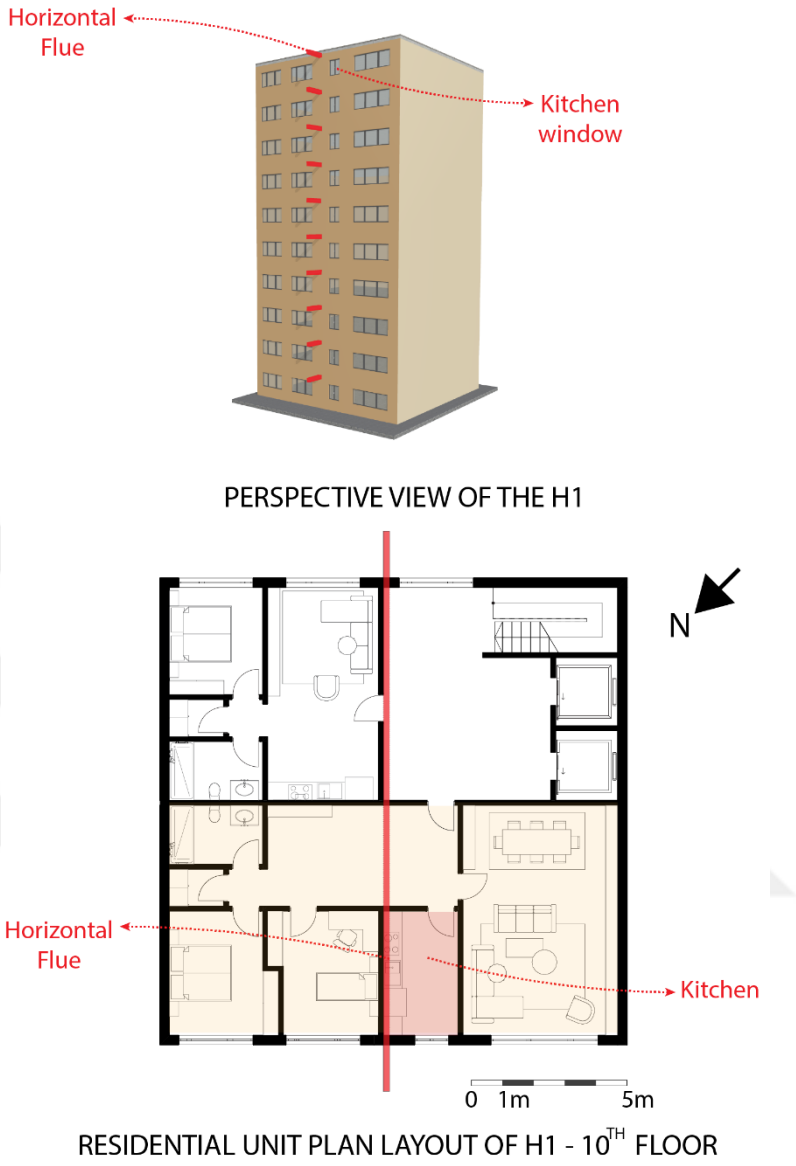

Figure 48. Leeward side oriented kitchen with a single-sided opening (natural gas vent on the window) and a horizontal flue that passes through the apartment building from one side to the other

For the H2, the flue enters from the kitchen facade, passes through the kitchen where it bends, continues through adjacent spaces, and extends to the other side of the building (Figure 49).

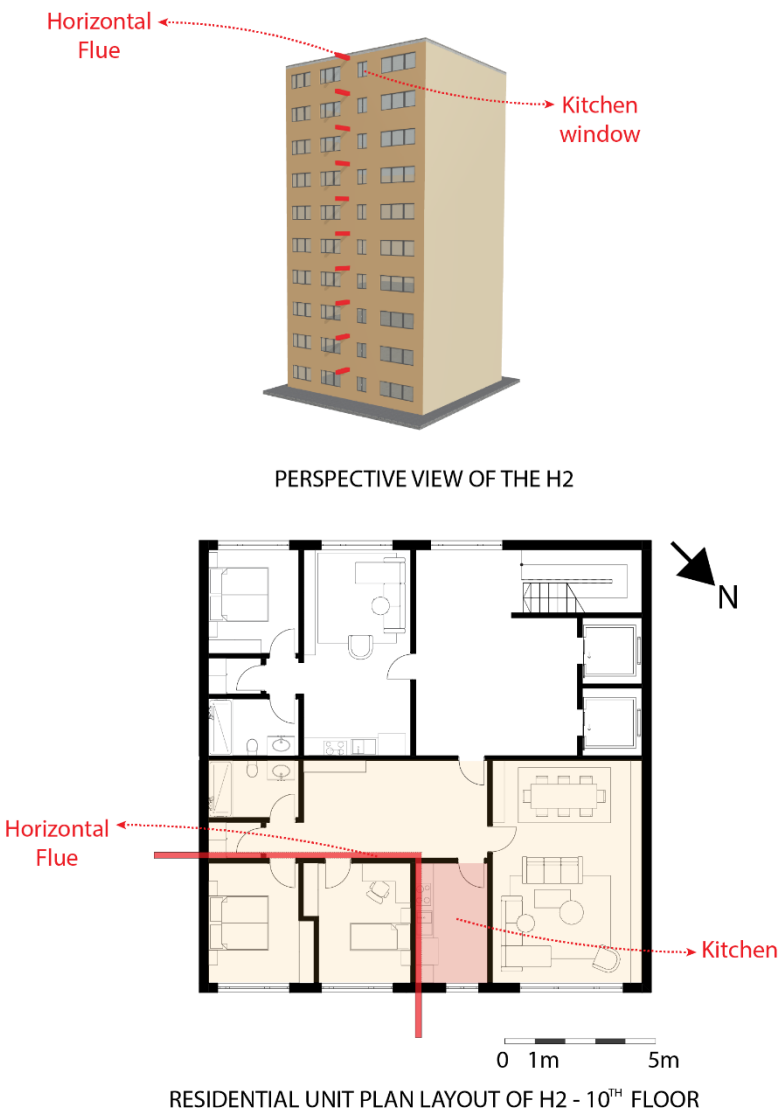

Figure 49. Windward side oriented kitchen with a single-sided opening (natural gas vent on the window) and a horizontal flue that passes through the apartment building, bending from one side to the other

Since the research focuses on the kitchen volume, the kitchen volumes are modelled individually for the IES VE ModelIT simulation, while the remaining volumes are modelled without room properties and opening specifications. The kitchen interior door is assumed to be closed, with no airflow occurring beneath it. Unlike the architectural drawings, the simulation model illustrates the natural gas vent

positioned above the window instead of within it. Top, front, and back views of the horizontal- and vertical-flue simulation models are presented in Table 5.

Table 5.Top, front, and back views of the simulation model

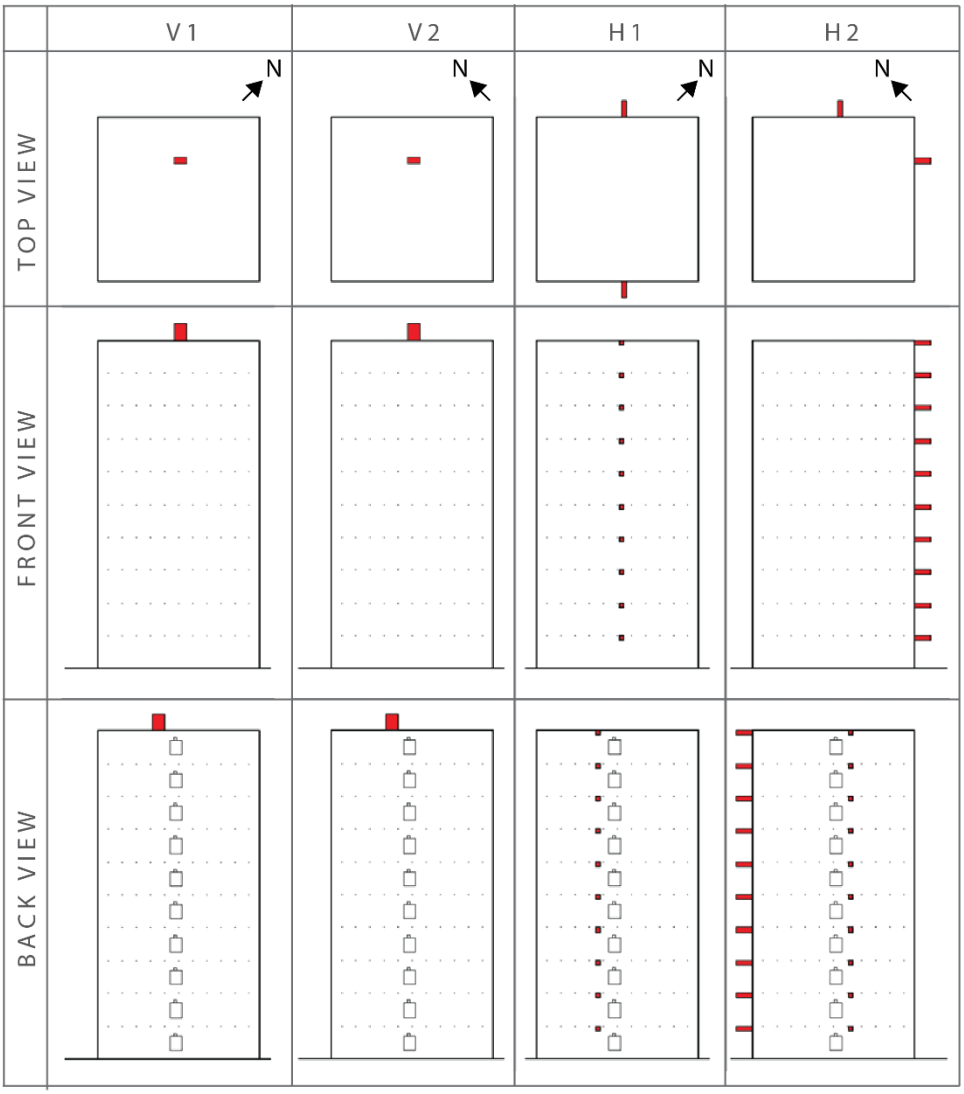

3.1.2 Kitchen Data

The I-type kitchen layout, presented in Section 2.1.2, is the most basic kitchen plan from which other layouts are derived. Due to the variability in furniture placement and window openings in open kitchen plans, the simulation is planned based on an enclosed kitchen type to provide a general overview of the effects of cross-flow and

stack-induced flow without incorporating the variables of interior design. The kitchen plan layout and sections for V1, V2, H1, and H2 are presented respectively in Figures 50, 51, 52, and 53. Additionally, the placement of kitchen components is also shown.

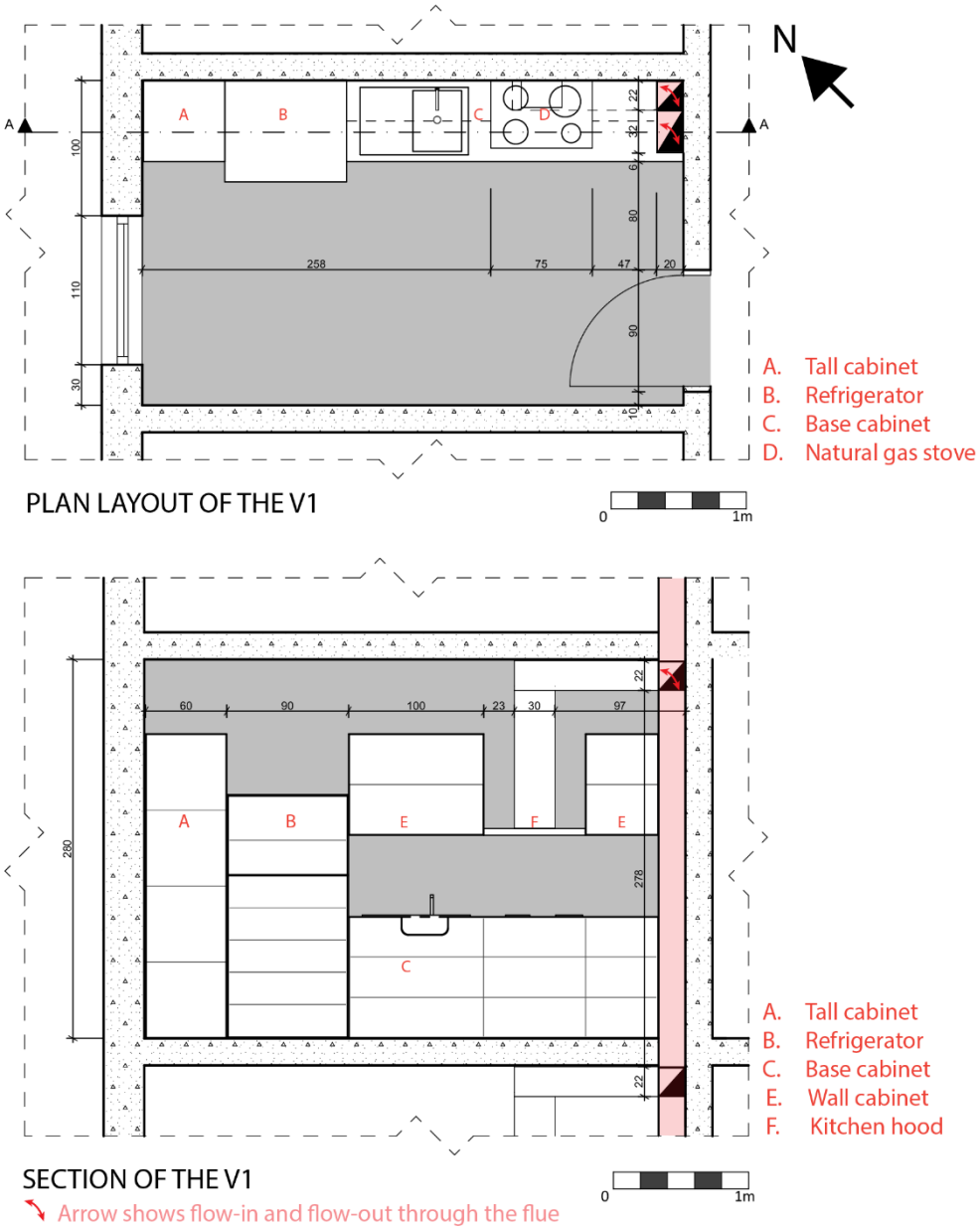

Figure 50. The vertical flue is positioned vertically next to the interior wall of the kitchens of V1

The V2 plan layout is identical to V1; only the building orientation has changed, as indicated by the north arrow.

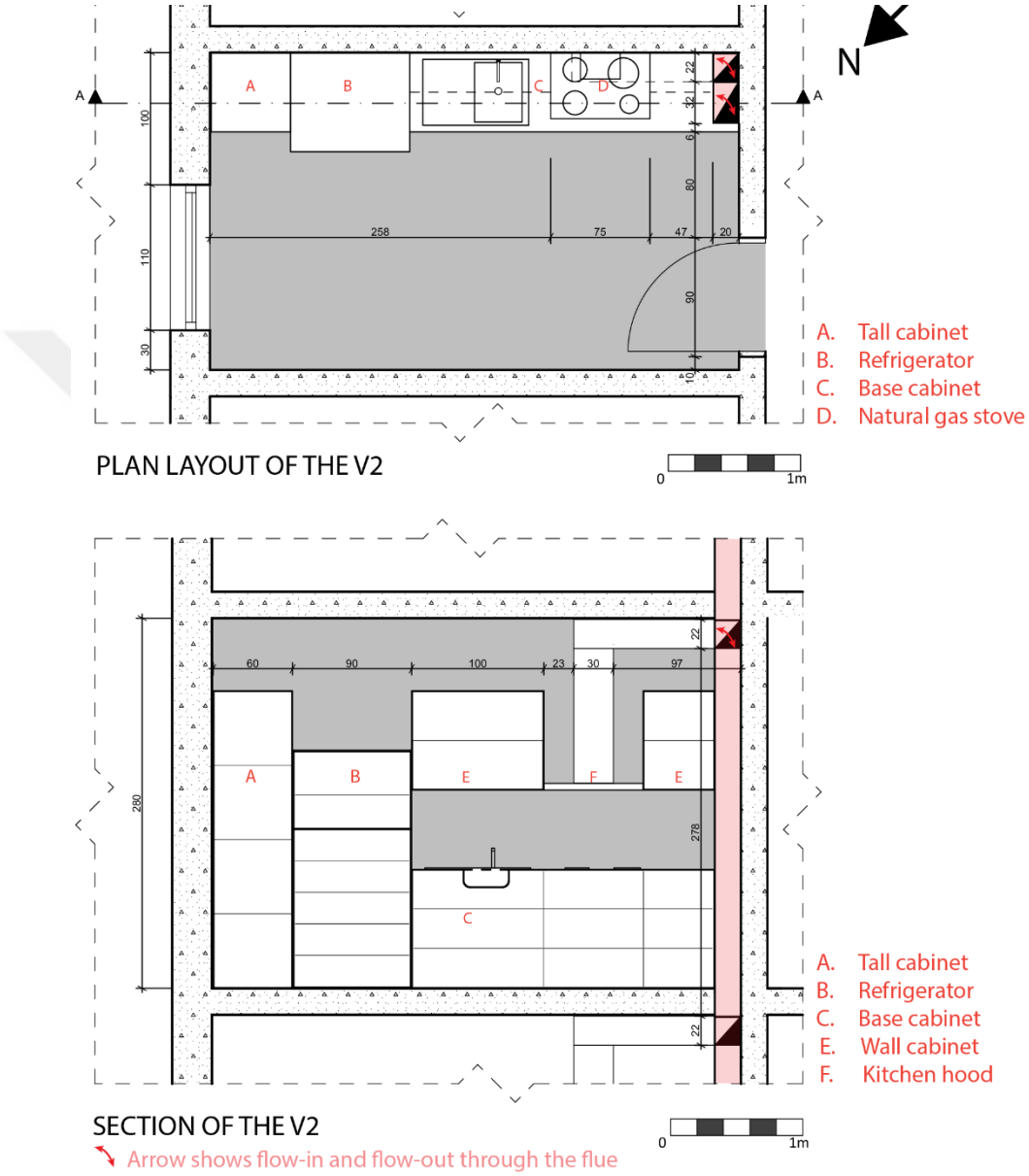

Figure 51. The vertical flue is positioned vertically next to the interior wall of the kitchens of V2

In the H1 plan layout, the ventilation flue is positioned vertically at the top; it serves that floor only and is not connected to the floors above or below.

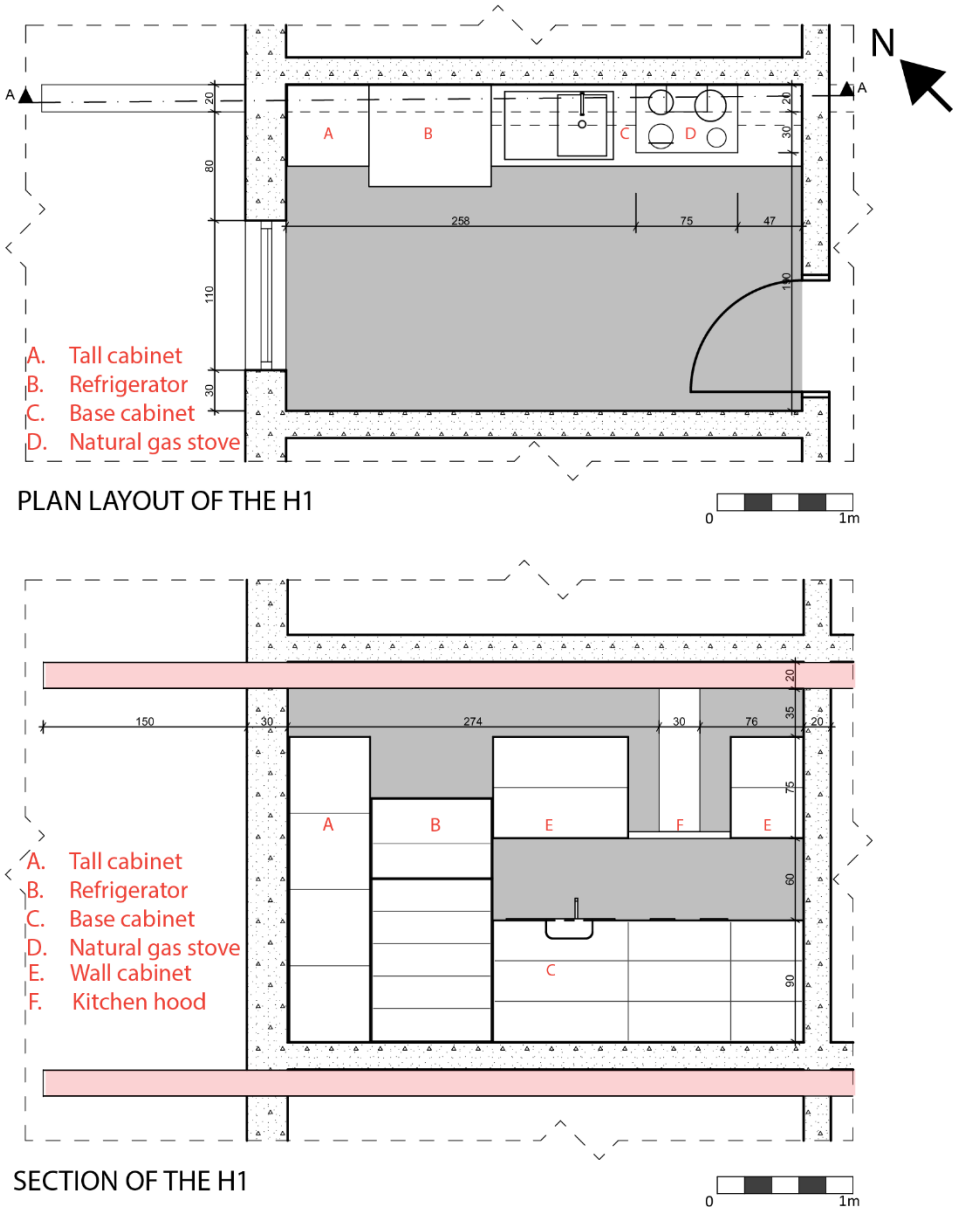

Figure 52. The horizontal flue is positioned horizontally beneath the ceiling of the I-type kitchen and passes directly through the adjacent spaces.

H2 has the same plan layout as H1; only the building orientation has changed, as indicated by the north arrow.

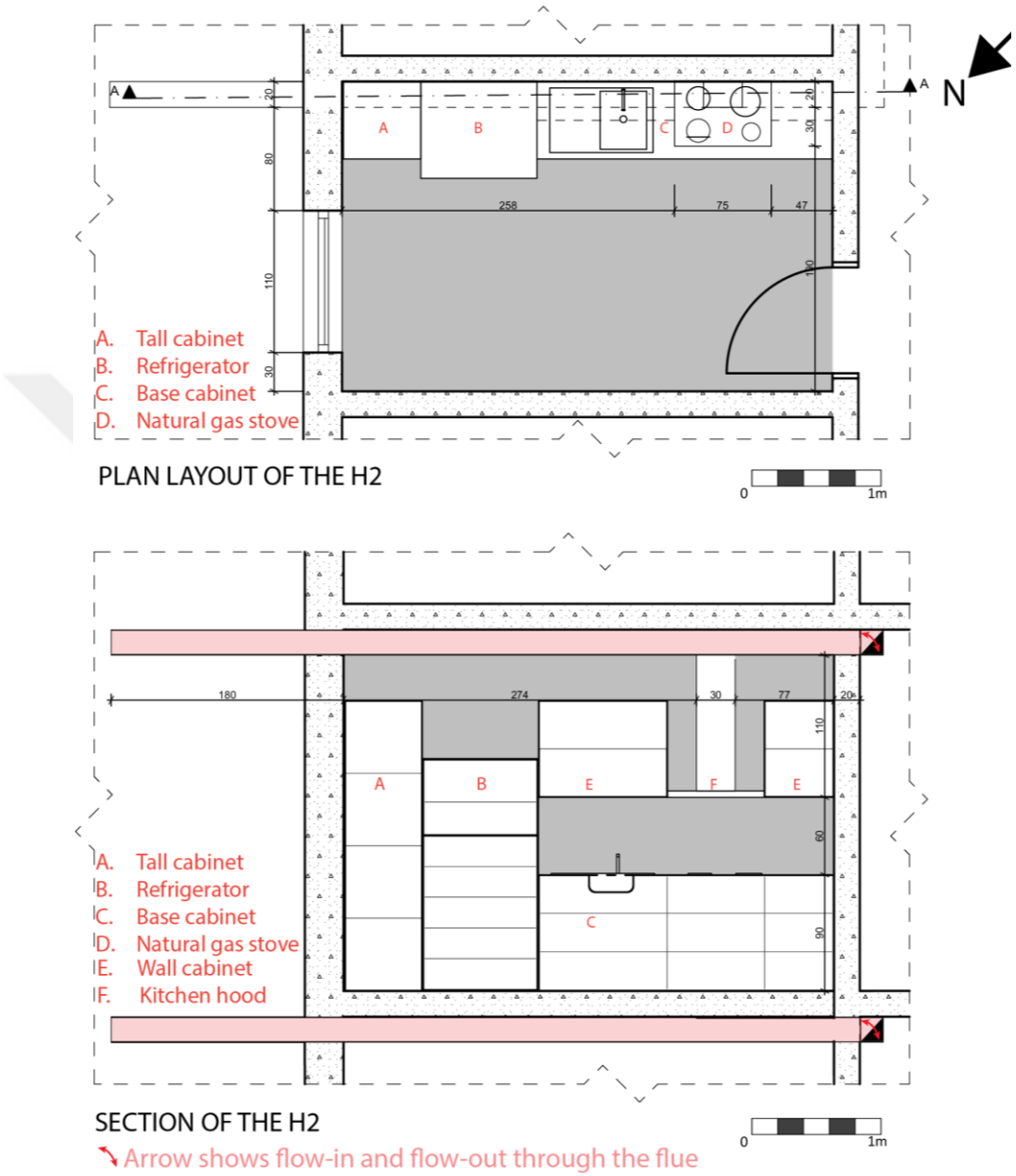

Figure 53. The horizontal flue is positioned horizontally beneath the ceiling of the I-type kitchen and passes directly through the adjacent spaces.

In the simulation model, the kitchen window is not planned to be operable, and therefore, it is not shown as an opening in the kitchen. Airflow is planned to be achieved through the natural gas vent opening and flue opening (Figure 54).

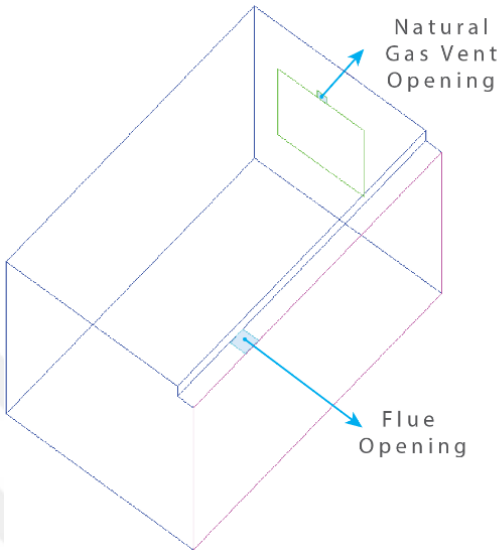

Figure 54. Axonometric view of the kitchen IES-VE simulation model shows kitchen openings for natural ventilation

3.1.3 Flue Data

The flue has been planned in three ways in the apartment buildings (Table 6). Firstly, for the apartment building with a vertical flue, as a shunt flue system shown in Section 2.1.3, Figure 16, it has been planned in the same way for both V1 and V2. Secondly, for the H1, the horizontal flue is planned to be horizontal and linear. Thirdly, for the H2, the horizontal flue is planned to be horizontal and to turn 90 degrees along the X-axis.

Table 6.The 3 different configurations of the flue in the apartment building.

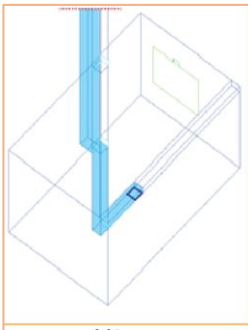	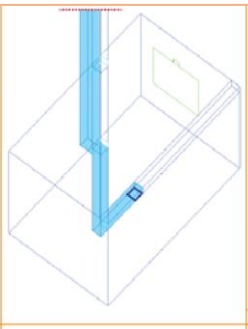	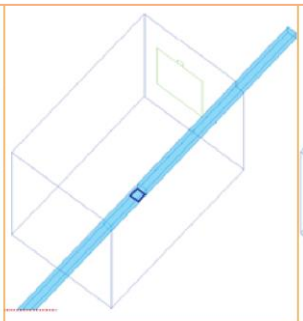	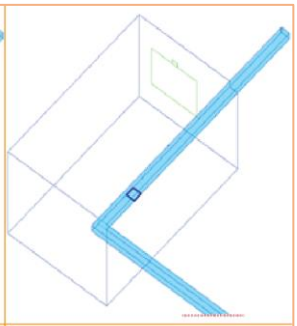
V1	V2	H1	H2
Flue type 1	Flue type 1	Flue type 2	Flue type 3

The vertical flue is modelled as a shunt flue system. Each floor consists of a vertical, 3-meter-long side flue connected to a central flue. The central flue starts from the 1st-floor side flue and extends to a height of 27.2 meters, reaching 1.5 meters above the roof. The side flue has a cross-sectional area of 0.2 m × 0.2 m, while the central flue has a cross-sectional area of 0.2 m × 0.3 m (Figure 55).

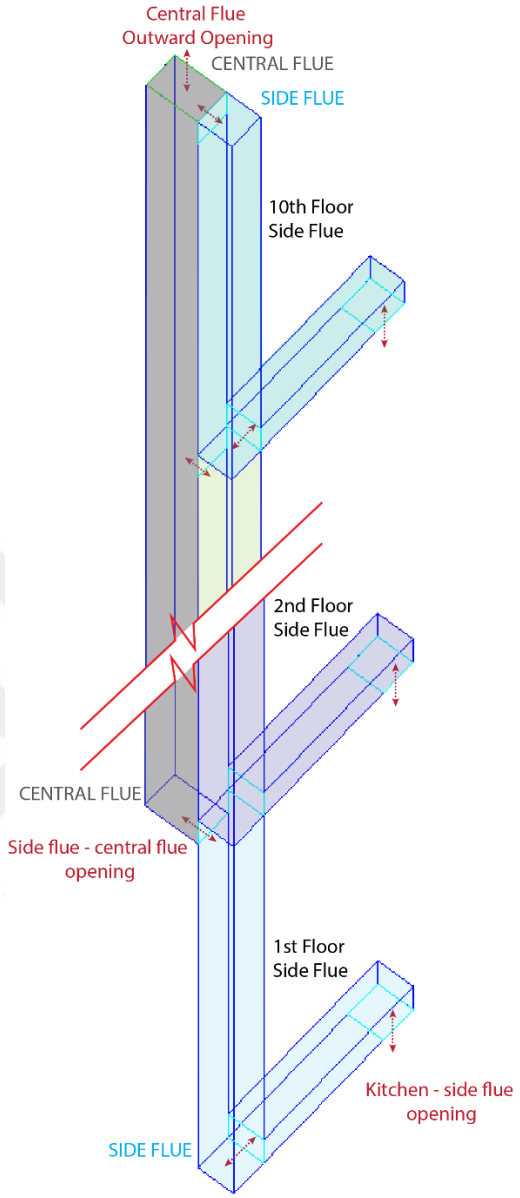

Figure 55. Simulation Model of Vertical Flue

The horizontal flue is designed as separate horizontal flues for each flat. It is configured in two ways for wind-oriented scenarios. For H1, it starts from the kitchen flue opening and extends outward horizontally in both directions. It extends 1.5 meters from the facade, with a total length of 18 meters and a cross-sectional area of 0.2 × 0.2 m (Figure 41). For H2, it starts from the kitchen flue opening and extends outward horizontally in two directions, but 90 degrees from each other(Figure 56).

The L-shaped horizontal flue has a total length of 14 meters for this scenario and retains the same cross-sectional area.

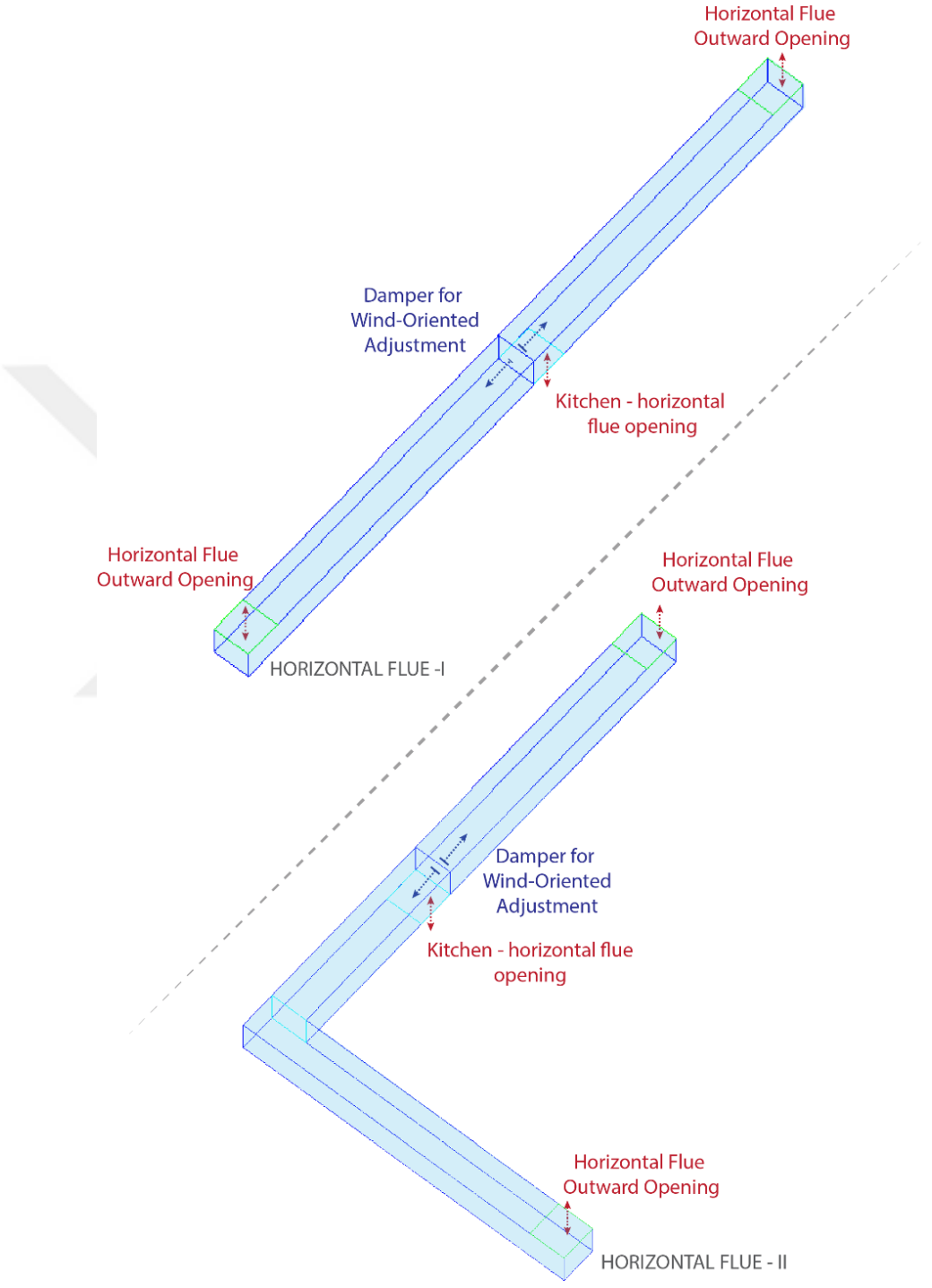

Figure 56. Simulation Model of Horizontal Flue I and II

3.2 Method

Most research studies address kitchen ventilation to understand airflow movement under specific environmental conditions within a defined volume, considering indoor air quality or thermal comfort. This is achieved through the utilization of Computational Fluid Dynamics (CFD) simulation programs or physical experimental setups. This research progresses through the use of simulation programs, given the challenges involved in designing and implementing a horizontal experimental setup for ventilation ducts in apartment buildings. This research employs the IES VE Apache Dynamic Simulation Tool and MicroFlo CFD Tool, for the building performance simulation, to investigate the indoor air quality of apartment kitchens during cooking.

- Phase 1: In the first simulation with the Apache Dynamic Simulation tool, the natural ventilation airflow at building openings in an apartment was comparatively analyzed across horizontal and vertical flue types and floors (from the 1st to the 10th), considering both windward and leeward orientations. Airflow was evaluated by considering the frequency of backflow(flow-in rate) and mode value of the flow over the year, through the interior opening of the kitchen which connects the flue and hood. Based on the flow-out rate performance, the apartment building with a vertical flue and the apartment building with a horizontal flue were selected for comparison under the same scenario. For both the 1st and 10th floors of each building, the day on which each kitchen reaches its potential (mode value occurs) over the year was determined and that day was designated as the design date for the CFD.
- Phase 2: A CFD analysis was conducted with MicroFlo on four kitchens, comparing cooking fumes and odours under both natural ventilation systems using indicators such as CO_2 levels and their spatial distribution, H_2O levels and their spatial patterns, temperature variations, airflow

direction and velocity, the local mean age of air, and particle tracking (Figure 57).

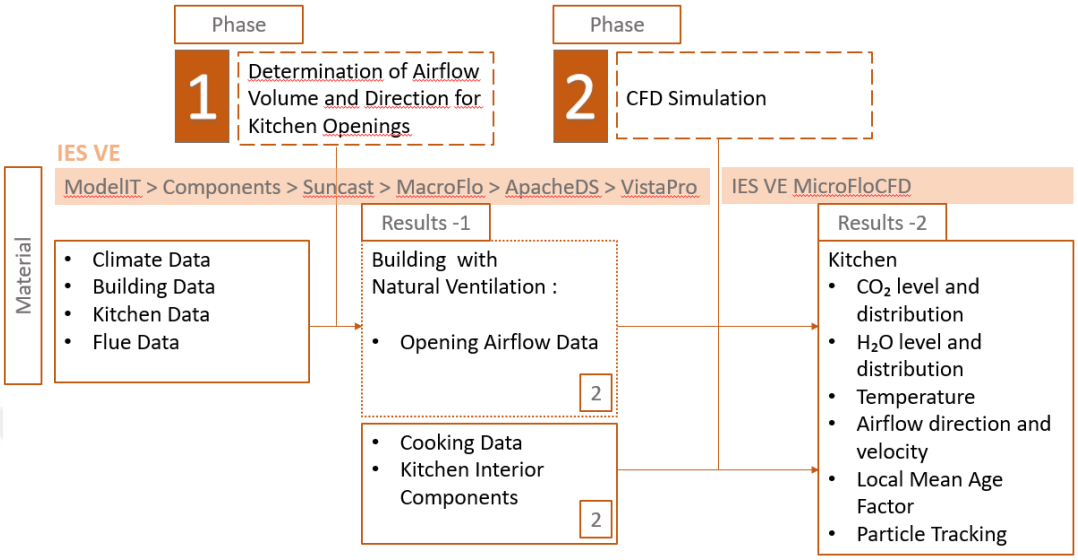

Figure 57. Material and method flow diagram

3.2.1 Phase 1: Investigation of Airflow Through Openings

In a 10-story apartment building, airflow patterns in the kitchen interior through both the horizontal flue opening, the vertical flue opening, and the natural gas vent opening are investigated throughout the year during the designated cooking hour (17:00–18:00). Wind and buoyancy forces, along with thermal forces from cooking and seasonal heating, generate airflow in an apartment building. The input data for the natural ventilation calculation during cooking (with Apache Dynamic Simulation software) is prepared as described below.

The wind direction, speed, and frequency are analysed using VistaPro, from the climate data. The wind data is visualised as a wind rose to orient the apartment building openings to the leeward side in V1 and H1 and to the windward side in V2 and H2.

There are two openings in the kitchen: an interior opening for the flue and an exterior opening as a natural gas vent opening (Section 3.1.2, Figure 50). Natural ventilation

is planned through two openings. The first is the natural gas vent, which is set to 99% open (the highest level) and remains on at all times in the simulation model. The second is an interior opening—the flue opening—modelled as a "hole" in the simulation, also always on and 100% open. The kitchen's exterior window is not defined as an airflow path; rather, it is included in the model solely as a parameter affecting thermal losses and gains. Apache Dynamic Simulation operates alongside MacroFlo, with the calculations of both tools interconnected. MacroFlo determines natural ventilation airflows driven by wind and buoyancy pressure through the openings in the building envelope.

3.2.1.1 Wind-Driven Airflow

The factors affecting the wind pressure applied to the building include wind speed, wind direction, building geometry, the surrounding terrain, and nearby obstructions. Wind speed and direction data are directly obtained from climate materials. The 30m high apartment building geometry is assumed to be located in terrain characteristics that indicate that more than 50% of the buildings within a 3000m radius exceed a height of 21m. It is assumed that there are no obstructions around the apartment building.

3.2.1.2 Buoyancy-driven Airflow

The pressure created by the air density at a given height is buoyancy-driven. While it is related to height inside the building, the buoyancy pressure in the outside air is influenced by both height and wind. The stack effect occurs when pressure changes with height, creating height-related pressure imbalances between air masses at different temperatures. Inside the building, seasonal heating and cooking activities are factors that affect temperature, while climatic variations are the factors that influence temperature outside the building. Cooking generates a heat load in the kitchen: according to CIBSE Guide A (2006), a hot plate with a 2-burner natural gas

stove generates a 4450 W heat load. It is assumed that cooking takes place between 17:00 and 18:00 for all kitchens in the apartment building, and a heat load has been applied for this timeframe throughout the year.

The seasonal heating period was determined as excluding the months from June to October, as seen in Figure 58, by analysing dry-bulb temperature with VistaPro in compliance with the Ankara Governorship Local Environmental Board (Ankara Valiliği Mahalli Çevre Kurulu, 2009) regulation. This regulation requires activating the central heating system when the outdoor air temperature falls below 15°C.

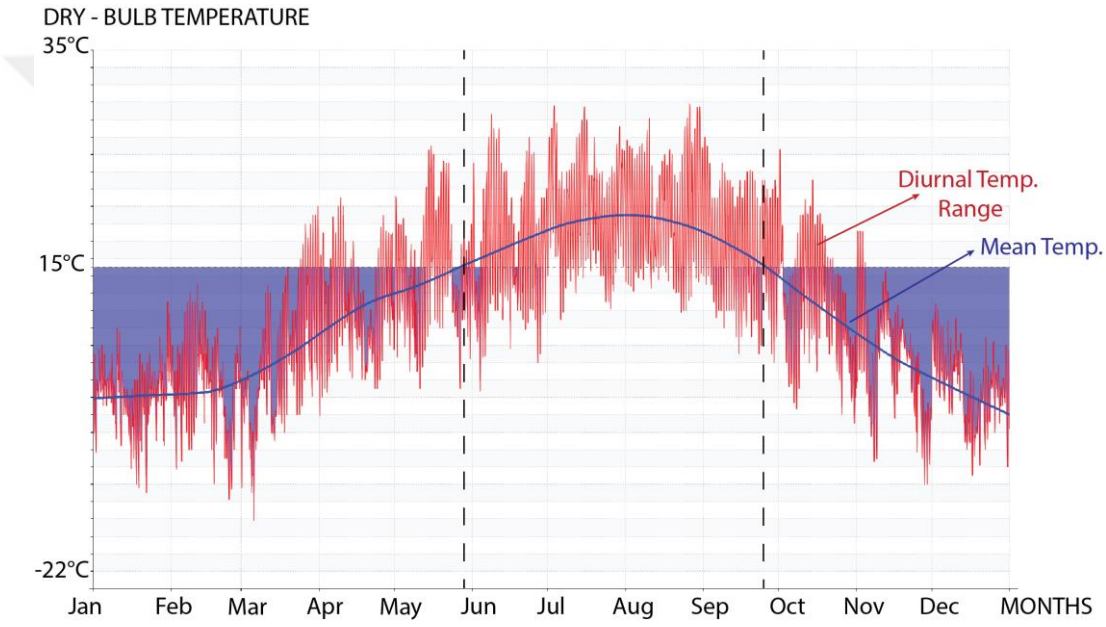

Figure 58. Annual dry-bulb temperature profile of Ankara for determining the heating period

According to Environmental Design - CIBSE Guide B (2005), operative temperature settings vary depending on the room type in residential buildings. The recommended comfort criteria are specified as 20–23°C for the living room, 17–19°C for the kitchen and bedroom, 26–27°C for the bathroom, and 19–24°C for the hall. For the research building, which is assumed to be heated by a central heating system, the main setpoint temperature during occupied times has been set to 22°C, based on CIBSE's operative temperature for living rooms. A setback temperature of 17°C has

been applied during unoccupied periods and nighttime occupancy as seen in Figure 59.

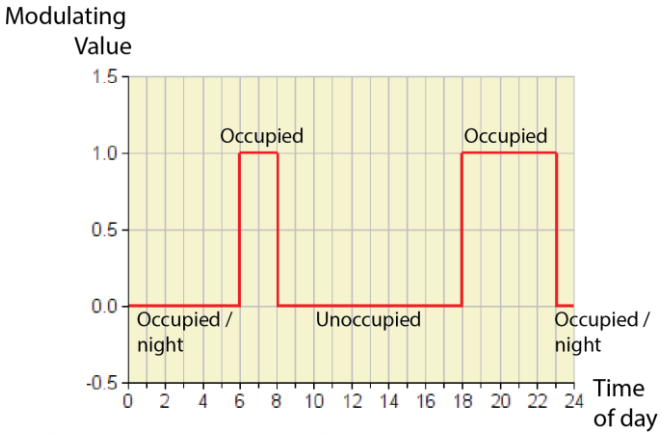

Figure 59. The IES VE graph shows the hours of the day when the building is heated. 1 represents the heating system is on, while 0 is off.

In Apache Dynamic Simulation (ADS), heat transfer by conduction, convection, and radiation is calculated separately for each building element and integrated with thermal loads and natural ventilation data. The simulation operates using climate data as input. The data is given in 10-minute intervals ranging from a single day to an entire year. The results of the ADS were analysed separately for apartment buildings with vertical flues and those with horizontal flues under scenarios V1, H1, V2, and H2. The ADS natural ventilation data was converted into numerical and graphical formats using VistaPro. In order to extract the net flow volume—representing the conditions during cooking hours over one year—which is determined by subtracting the flow-in from the flow-out at the kitchen flue opening. This net flow volume data was compared using one of VistaPro's data analysis tools, called Synopsis to determine the maximum flow-out and maximum flow-in values (i.e., the range of the net flow volume). To understand the overall behaviour of natural ventilation during cooking hours throughout the year, the net flow volume was also extracted as tabulated data, and its mode value was calculated using Excel.

Furthermore, using the Range Test tool in VistaPro (Figure 60), the percentage of instances where the net flow volume was positive (i.e. when the flow-out exceeded

the flow-in) was determined for each kitchen flue opening, defined as the flow-out rate.

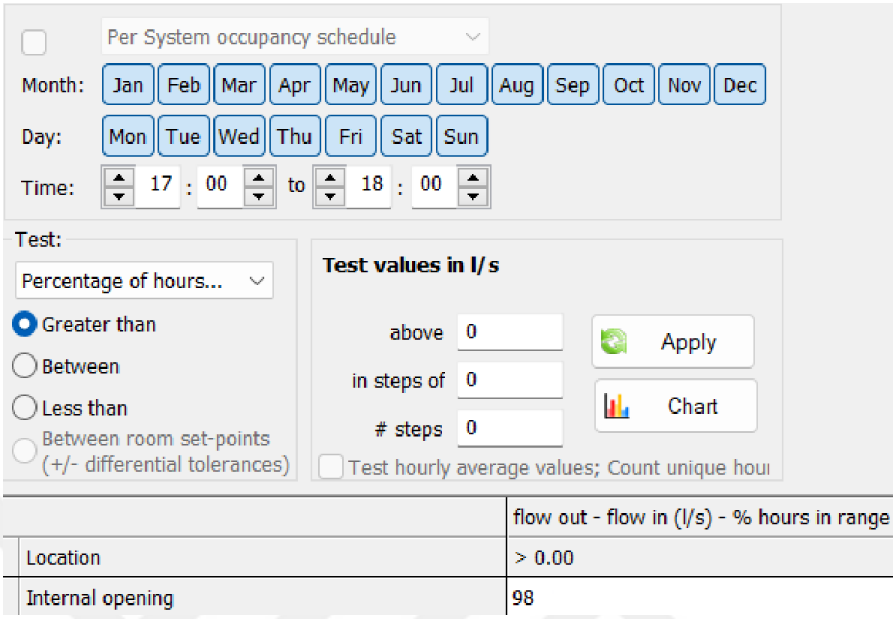

Figure 60. Dialog box of the Range Test tool in Vistapro

Subsequently, the results for the 10-floor apartment kitchens were converted into tabulated data for further comparison and evaluation.

During cooking, it was assumed that having the flue function as an extract would positively influence indoor air quality, especially in vertically flued buildings where minimising the transfer risk of cooking fumes and odours is critical. In the scenario chosen for CFD analysis, the primary criterion was the flow-out (extract) rate data, while the mode value of the flow volume was used to define the overall character of natural ventilation in the kitchen and to select the design date.

3.2.2 Phase 2: Cooking Fume Flow in the Kitchen: CFD Simulation

To assess the performance of stack-induced airflow through vertical flue ventilation, climate data for the selected cooking-hour interval and the corresponding ventilation-opening boundary conditions were exported from the VistaPro Analysis tool as a BCF (boundary condition file) and imported into Apache Dynamic Simulation (Figure 61).

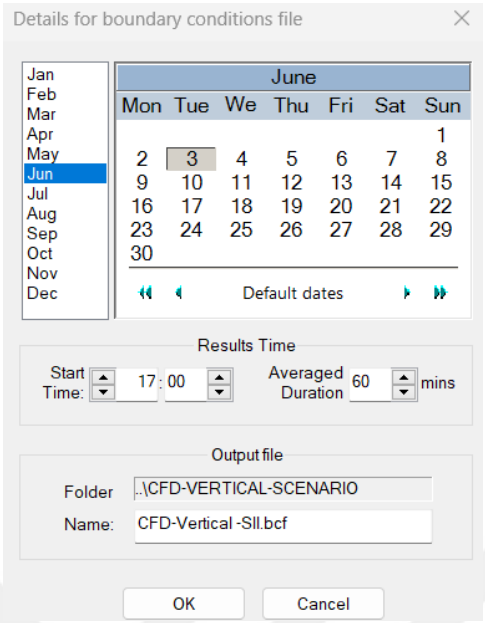

Figure 61. Boundary condition month, day, time and duration selection (From VistaPro dialog box)

To simulate the cooking event in the kitchen, component objects were added as obstructions, solid heat sources, and H_2O and CO_2 sources. A grid mesh was generated, and the simulation was run. The CFD monitor was examined to ensure the reliability of the results. CFD results were displayed using the MicroFlo Viewer tool, displaying velocity, temperature, CO_2 mass fraction, H_2O mass fraction, local mean age factor, and particle tracking.

3.2.2.1 Component Phase

For the MicroFlo (CFD) simulation, components were created using the IES VE Component tool and defined as either objects or openings for the kitchen. Components are defined as objects that affect airflow based on their physical state. Solid objects create surfaces that act as obstructions to airflow. The ability of objects to act as sources depends on whether they are solid or non-solid. Solid objects can be defined as heat and temperature sources. On the other hand, non-solid objects can be defined as sources of H_2O, CO_2, or CO.

The kitchen hood is placed as an object, with mechanical ventilation set to off, affecting airflow only as an obstruction. The occupant is placed as an obstruction, and its heat and moisture sources are disregarded. For cooking, a saucepan and a pot were modelled as solid objects. The stove was represented as a medium-sized double-burner object, sized according to the 20 cm base diameter of the cookware, and positioned directly beneath it. Because the stove operates by natural gas combustion, it was modelled not as a solid object but as an emission source of H_2O and CO_2.

According to CIBSE Guide A (2006), a hot plate with a 2-burner natural gas stove is defined as shown in Table 7. Assuming both burners are medium-sized, the total heat gain, expressed in W, is defined as the heat source value of the stove.

Table 7.Natural gas stove and heat value (CIBSE Guide A, 2006)

Condition	Rated Power (W)	Standby Power (W)	Sensible Gain (W)	Latent Gain (W)	Total Gain (W)
Hot Plate - 2 Burners	5630	390*	3430	1020	4450
Hot Plate - 1 Burner	2815	195	1715	510	2225

CIBSE Guide A (2006), states that natural gas combustion produces H_2O at a rate of 0.16 kilograms of moisture per hour per kW of input energy. The amount of H_2O generated during the combustion process of natural gas (CH_4) with a natural gas stove producing 2225 W (2.225 kW) of heat is calculated in step 1. Thereafter, the amount of CO_2 generated by the same stove through the combustion process is calculated in step 2, based on the amount of H_2O calculated in step 1. To this end, the ratio of CO_2 to H_2O; is calculated using their molar mass (H_2o is 18 g/mol and CO_2 is 44 g/mol) the natural gas combustion equation:

$$CH_4 + 2O_2 \rightarrow CO_2 + 2\ H_2O,$$

Step 1: Moisture Production: H_2O rate of moisture production x power of stove, hence the amount of H_2O = 0.16 kg/hkW x 2.25kW =0.356 kg/h or 356g/h

Step 2: CO_2 Production: Since 1 molecule of CO_2 is produced for every 2 molecules of H_2O, the ratio of CO_2 to H_2O in g/h is equal to the ratio of their masses in g/mol; i.e. (44g/mol) / (2 x18g/mol) =1.22. Hence the amount of CO_2 produced = 1.22 x 0.356 kg/h = 0.435 kg/h

As a result, each burner has been assigned as a source of 0.435 kg/h of CO_2, 0.356 kg/h of H_2O, and a 2225 W heat source.

According to CIBSE Guide A (2006), natural gas combustion produces H_2O at a rate of 0.9–3 kilograms of moisture per hour per kW of input energy for cooking three meals. For a 2225 (W 2.225 kW) system, the calculation is explained below:

Minimum rate: 0.9 kg/h per kW so; minimum H_2O: 2.225 × 0.9 = 2.00 kg/h

Maximum rate: 3.0 kg/h per kW so; Maximum H_2O: 2.225 × 3.0 = 6.68 kg/h

The result H_2O Production Range: 2.00–6.68 kg/h for cooking three meals

Cooking two meals H_2O production range is 1.34–4.45 kg/h. In the research kitchen, the cooking style, such as deep frying, stir-frying, or boiling, has not been specified, and an average value of 2.90 kg/h H_2O production is assumed. In the model, a moisture source has been defined over the saucepan and pot, each with the same base area (20 cm), at 1.45 kg/h H_2O (Figure 62).

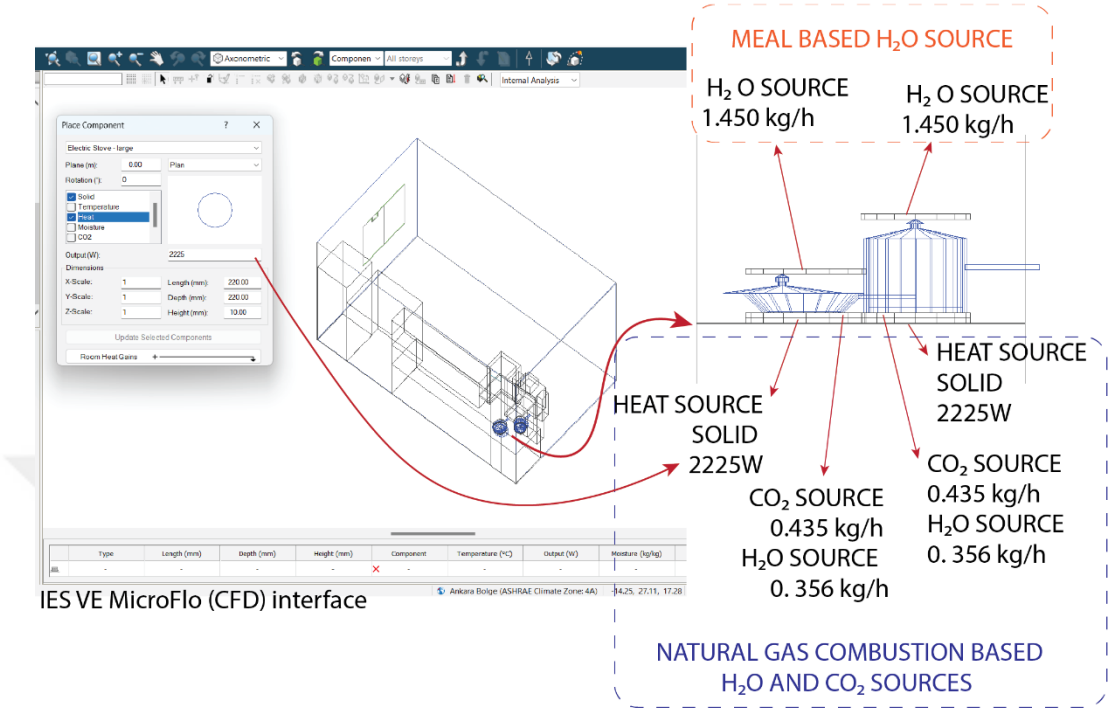

Figure 62. Assignment of heat, CO_2, and H_2O sources to kitchen stoves and meals

3.2.2.2 Boundary Conditions Phase

Boundary Conditions for apartment buildings - Apache Dynamic Simulation Results Exported from VistaPro Analysis Tool (03 June 17:00–18:00) (Figure 59). While importing boundary conditions into the MicroFlo (CFD) tool, the import room gains box was not ticked because it already included previously calculated room heat gain, seasonal heating load, and cooking heat load. For June, there is no seasonal heating load; however, the cooking load was added as a heat source within the natural gas stove component in the CFD model. To avoid double calculation, the heat load from boundary conditions was not included (Figure 63).

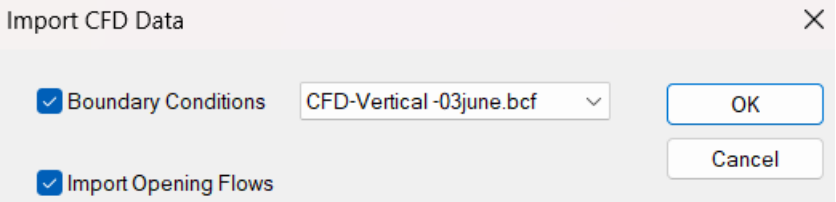

Figure 63. MicroFlo import dialog box

With the import of boundary conditions, kitchen openings were defined as supplying or extracting air based on the flow-in or flow-out conditions determined by the program, depending on the simulation duration, day, and month.

In the CFD analysis, to avoid oscillations in the simulation graph caused by the nozzle jet effect at the opening connecting the kitchen hood and the flue, the airflow rate at the flue opening was recalculated and then assigned to the kitchen hood's opening to the kitchen. If the flue opening airflow is directed inward, it is defined as a supply; if it is directed outward, it is defined as an extract, as seen in Figure 64. The opening connecting the kitchen hood to the flue was defined with a zero-value pressure boundary, thereby creating an aperture in the component that only allows air to pass through.

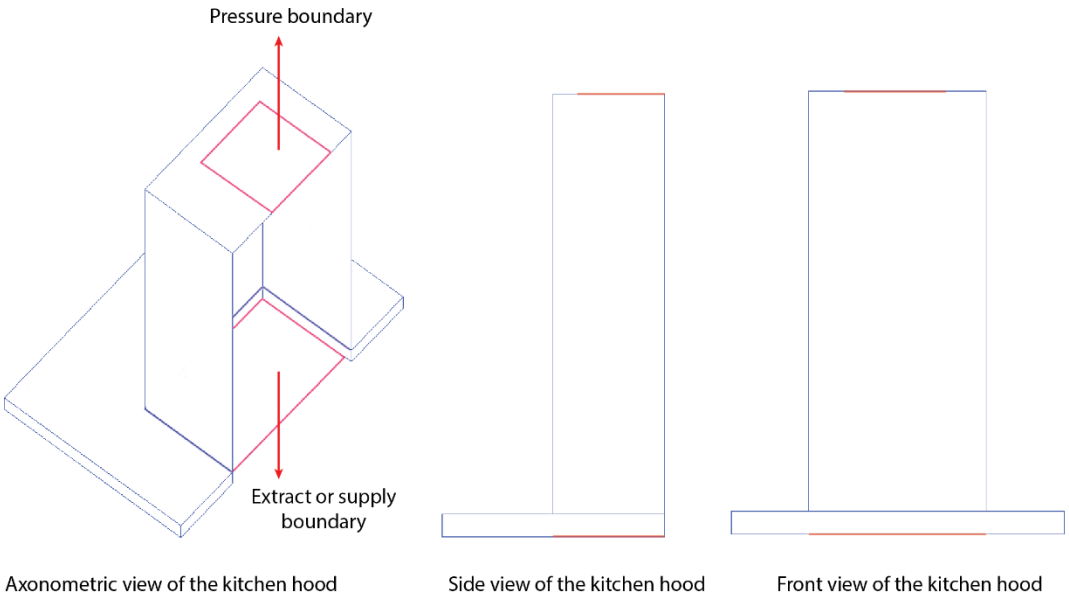

Figure 64. Kitchen hood boundary conditions

The analysis was conducted under the assumption that the kitchen hood contained no filtration layer and no flow obstructions on the inner volume.

In the event of flow-in from the flue opening to the kitchen—where air enters from the flue—the CO_2 concentration within the flue was assigned as the supply airflow property. In the ADS, the fresh air CO_2 concentration is considered to be 400 ppm. According to the ADS natural ventilation analysis results, the flue connected to V1-F10 exhibited an average CO_2 concentration of 512 ppm during the cooking hour.

3.2.2.3 Grid Meshing and Simulation

The grid mesh is checked to ensure that the kitchen opening areas have a mesh grid in each x, y, and z direction. The model grid aspect ratio value is within the acceptable range (Figure 65).

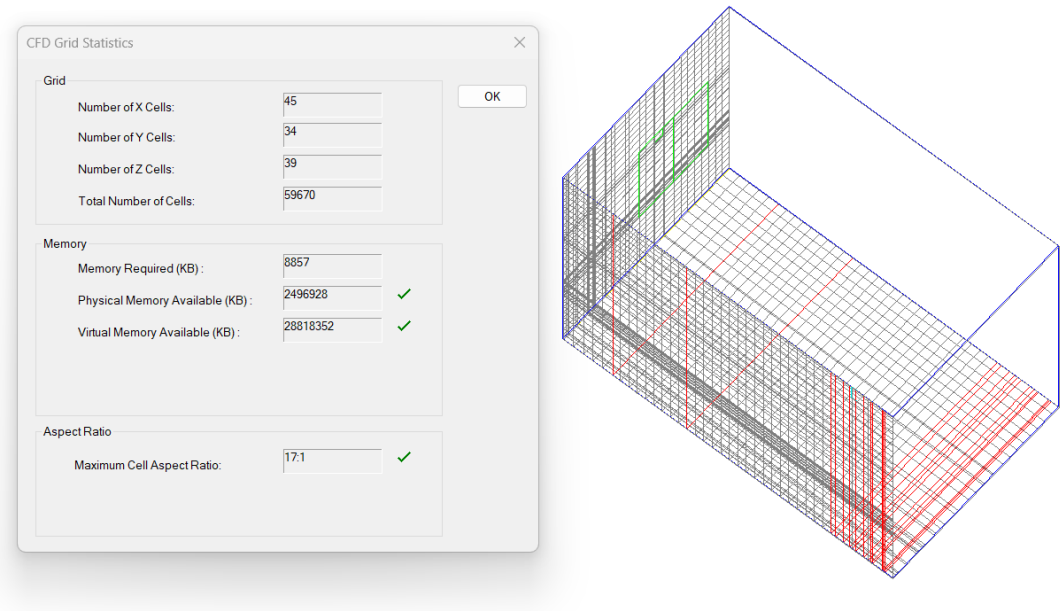

Figure 65. CFD grid statistics and model mesh in the MicroFlo tool.

There are two different turbulence models: the k-ε turbulence model and the constant effective viscosity turbulence model. In the k-ε turbulence model, k represents the turbulent kinetic energy and ε refers to the rate of dissipation. According to the IES

VE MicroFlo User Guide (n.d), the k-ε turbulence model allows the use of more advanced features compared to the constant effective viscosity turbulence model; therefore, the k-ε model was selected.

After the simulation run, residuals were checked for convergence or divergence using the MicroFlo CFD Monitor. According to Buckley (2021), in CFD: Hospital Operating Room *(On-demand online training presentation)*, residuals should decrease by the end of iterations for an acceptable graph, as seen in Figure 66.

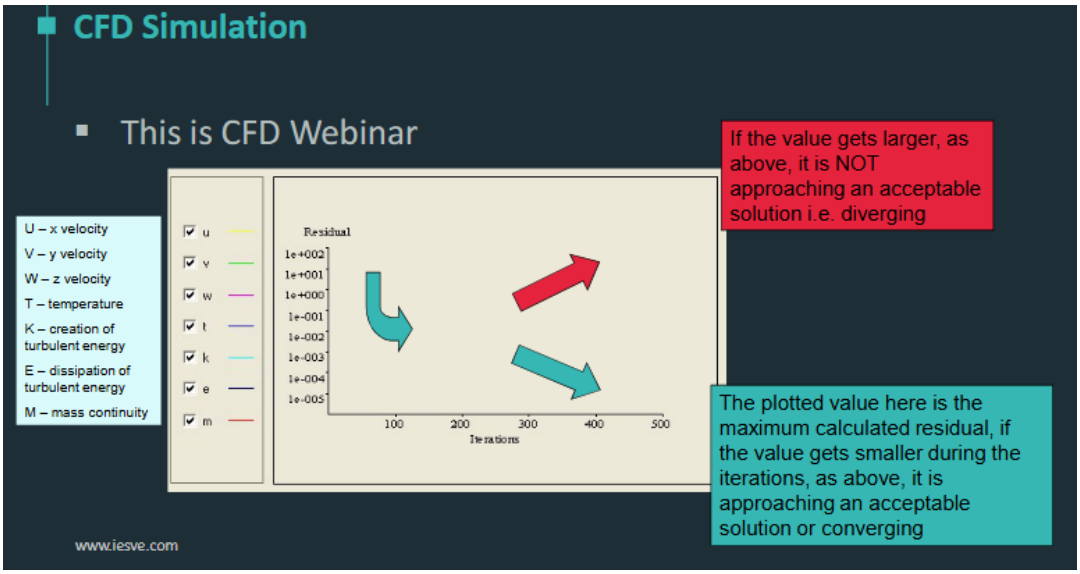

Figure 66. CFD Monitor residual feature overview (Buckley, 2021)

When the CFD monitor is examined, it can be observed that the residuals are decreasing; thus, it is considered converged (Figure 67).

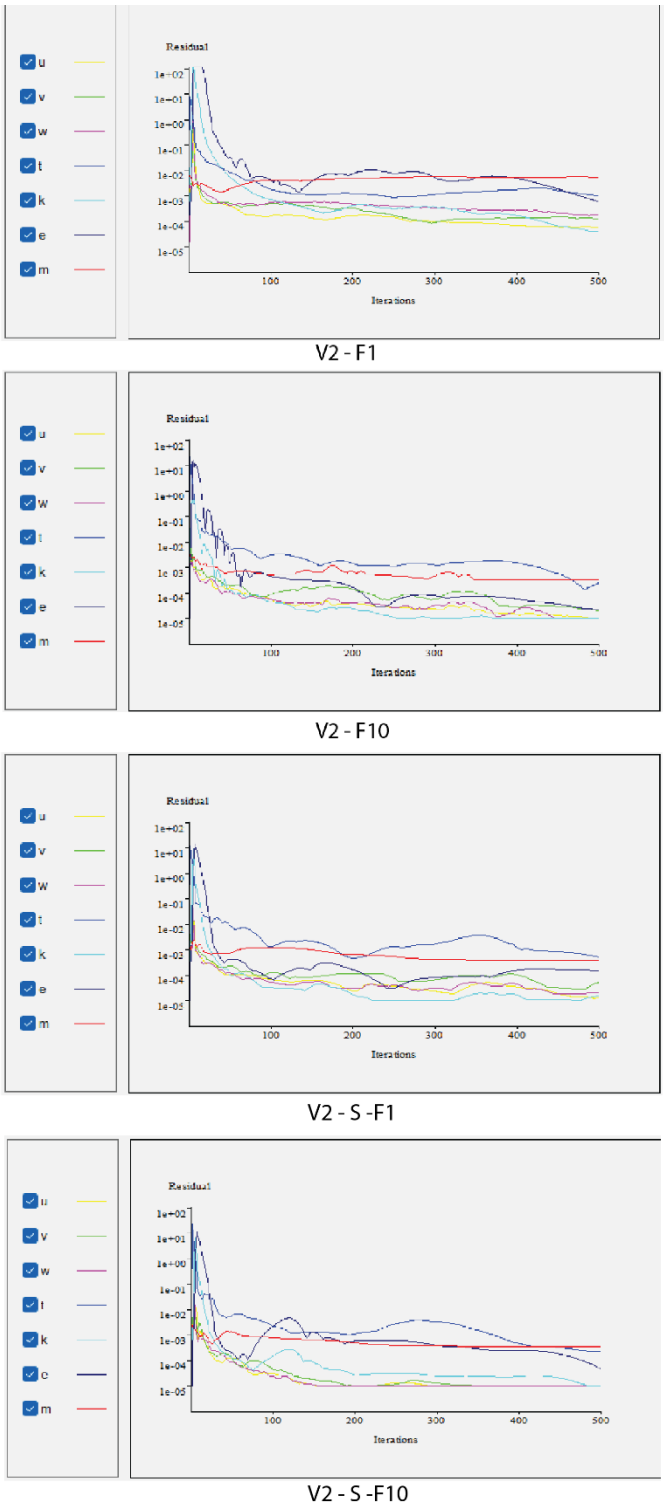

Figure 67. The calculated residuals decrease throughout the iterations (As obtained from the MicroFlo Tool)

RESULTS AND DISCUSSION

4.1 Results of Apache Dynamic Simulation

The results of the ADS were analyzed using the VistaPro tool as tabulated data, separately for apartments V1, V2, H1, and H2. Maximum flow-out volume, maximum flow-in volume, the mode value of the flow volume, and flow-out rate data were evaluated for each floor's kitchen. These results were then compared within the context of V1-V2 and H1-H2, leading to the selection of the scenario for CFD analysis.

4.1.1 Scenario I (V1 and H1)

Table 8 shows the flow volume (l/s) throughout the year for the time interval between 17:00 and 18:00. Blue-coloured values represent flow-out (extract), indicating airflow from the kitchen to the flue. While red-coloured values represent flow-in (supply), indicating airflow from the flue into the kitchen. The indicators presented in Table 8 are correspondingly applicable to Table 9. In Scenario I, two apartment configurations facing the windward side were simulated: a vertical-flue building (V1) and a horizontal-flue building (H1). The horizontal flue of H1 was analysed from the damper boundary, with its short and long segments evaluated separately. For the sake of simplicity, the horizontal-flue apartment configurations will be designated H1-S (short flue) and H1-L (long flue).

In Scenario V1 (Table 8), the maximum flow-out volume ranges from 20 L/s to 47 L/s, with the highest value recorded on the 1st floor and the lowest on the 6th floor. The flow-in volume varies between 8 L/s and 37 L/s, reaching its minimum on the 4th floor and its maximum on the 7th and 8th floors. The mode of flow volume

for the 1st–7th floors corresponds to flow-out, ranging from 7 L/s to 31 L/s; within this range, the highest mode value occurs on the 1st floor and the lowest on the 7th floor. For the 8th–10th floors, the mode corresponds to flow-in, ranging from 10 L/s to 22 L/s, with the highest mode on the 10th floor and the lowest on the 8th floor. The flow-out rate decreases with elevation: on the 1st–7th floors it ranges from 78% to 99%, peaking on the 4th floor; on the 8th–10th floors, it ranges from 13% to 19%, with the highest value on the 7th floor and the lowest on the 10th floor.

In Scenario H1-S (Table 8), the maximum flow-out volume ranges from 33 to 94 L/s — lowest on the 7th and 8th floors and highest on the 10th floor. The flow-in volume varies between 14 and 41 L/s, reaching its minimum on the 1st through 4th floors and its maximum on the 7th and 8th floors. The mode value across all ten floors corresponds to flow-out and remains constant at 8 L/s. The flow-out rate varies from 1% to 26%, with its lowest values on the 7th and 8th floors and its highest value on the 10th floor.

In Scenario H1-L (Table 8), the maximum flow-out volume ranges from 74 L/s to 86 L/s — lowest on the 1st–6th floors and highest on the 9th and 10th floors. The flow-in volume ranges from 13 L/s to 41 L/s, with its minimum on the 1st–4th floors and its maximum on the 7th and 8th floors. The mode flow volume value across all 10 floors corresponds to flow-out, varying between 5 L/s and 8 L/s; it is lowest on the 6th floor and identical — at its highest value — on the 1st–5th floors and the 10th floor. The flow-out rate remains constant at 99% on every floor.

Table 8.Maximum inflow and outflow, mean flow volume, and outflow rate for the configurations V1, H1-S, and H1-L.

Floor Number	Max Flow-out Volume (l/s)	Max Flow -in Volume (l/s)	Mode of flow vol. (l/s)	Flow-out rate (%)	LEEWARD SIDE / APARTMENT WITH VERTICAL FLUE **V1**
1	47	12	31	99	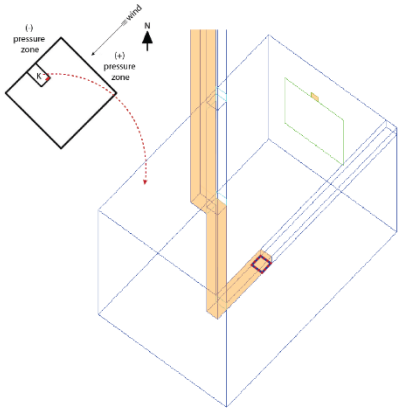
2	45	11	28	99	
3	43	10	27	99	
4	42	8	23	99	
5	25	10	13	97	
6	20	12	13	97	
7	32	37	7	78	
8	31	37	10	19	
9	38	25	16	17	
10	37	27	22	13	
Floor Number	Max Flow-out Volume (l/s)	Max Flow-in Volume (l/s)	Mode of flow vol. (l/s)	Flow-out rate (%)	LEEWARD SIDE / APARTMENT WITH HORIZONTAL FLUE(SHORT) **H1-S**
1	80	14	8	24	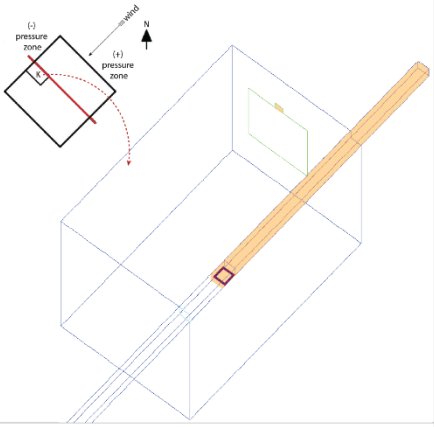
2	80	14	8	24	
3	80	14	8	24	
4	80	14	8	24	
5	80	28	8	21	
6	80	28	8	21	
7	33	41	8	1	
8	33	41	8	1	
9	37	37	8	2	
10	94	25	8	26	
Floor Number	Max Flow-out Volume (l/s)	Max Flow-in Volume (l/s)	Mode of flow vol. (l/s)	Flow-out rate (%)	LEEWARD SIDE / APARTMENT WITH VERTICAL FLUE(LONG) **H1-L**
1	74	13	8	99	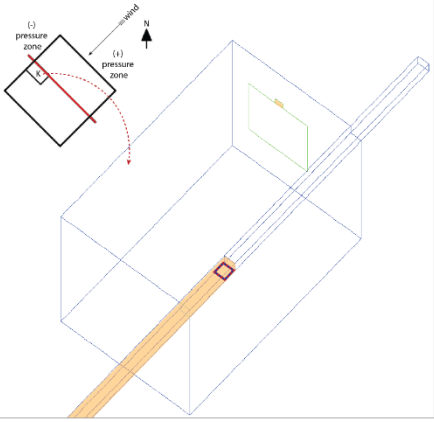
2	74	13	8	99	
3	74	13	8	99	
4	74	13	8	99	
5	74	26	8	99	
6	74	26	5	99	
7	81	41	7	99	
8	81	41	7	99	
9	86	24	6	99	
10	86	23	8	99	

4.1.2 Scenario II (V2 and H2)

In Scenario II, two apartment configurations facing the leeward side were simulated: a vertical-flue building (V2) and a horizontal-flue building (H2). The L-shaped horizontal flue of H2 was analysed from the damper boundary, with its short and long segments evaluated separately. For the sake of simplicity, the horizontal-flue apartment configurations will be designated H2-S (short flue) and H2-L (long flue) as seen in Table 9.

In Scenario V2 (Table 9), the maximum flow-out volume ranges from 18 L/s to 44 L/s, with the highest value recorded on the 1st floor and the lowest on the 6th floor. The flow-in volume varies between 6 L/s and 25 L/s, reaching its minimum on the 6th floor and its maximum on the 10th floor. The mode of flow volume for the 1st–7th floors corresponds to flow-out, ranging from 7 L/s to 30 L/s; within this range, the highest mode value occurs on the 1st floor and the lowest on the 7th floor. For the 8th–10th floors, the mode corresponds to flow-in, ranging from 11 L/s to 20 L/s, with the highest value on the 10th floor and the lowest on the 8th floor. The flow-out rate decreases with elevation: on the 1st–7th floors it ranges from 87% to 97%, peaking on the 4th floor; on the 8th–10th floors, it ranges from 24% to 36%, with the highest value on the 8th floor and the lowest on the 10th floor.

In Scenario H2-S (Table 9), the maximum flow-out volume ranges from 75 L/s to 88 L/s — lowest on the 1st floor and highest on the 10th floor. The flow-in volume varies between 0.4 L/s and 0.7 L/s, with its minimum on the 10th floor and peak values on the 2nd–6th floors. The mode value across all 10 floors corresponds to flow-out, ranging from 8 to 9 L/s; it is lowest on the 1st and 5th–10th floors, and highest on the 2nd–4th floors. The flow-out rate remains constant at 100% on every floor.

In Scenario H2-L (Table 9), the maximum flow-out volume ranges from 8 L/s to 82 L/s — lowest on the 5th and 6th floors and highest on the 9th and 10th floors. The flow-in volume is constant at 1 L/s on every floor. The mode value across all 10

floors corresponds to flow-out, ranging from 7 L/s to 8 L/s; it is lowest on the 5th and 6th floors and identical — at its highest value — on all other floors. The flow-out rate varies between 99% and 100%, reaching its minimum on the 5th and 6th floors and its maximum on the remaining floors.

When determining which kitchens to select for CFD analysis, kitchens within each group: V1 with V2 and H1 with H2 were compared. In both V1 and V2, the lower floors' flue openings exhaust air while the upper floors function as air supply. However, configuration V2 exhibits higher flow-out rates on the upper floors. Consequently, it was selected because it more closely aligns with the intended natural ventilation strategy, whereby the natural gas vent functions as the supply and the flue opening serves as the extract. To analyze the three key points of ventilation performance in the building, the 1st floor, where the flow-out is highest, and the 10th floor, where the flow-out is lowest, were selected for CFD analysis.

Similarly, for H1 and H2, when comparing the short-flued and long-flued versions using the same parameters, the H2-S scenario was chosen due to its highest flow-out rates. Although there is no direct correlation between the number of floors and the flow-out rate or mode flow volume, the 1st and 10th floors were selected for CFD analysis to facilitate a comparison with Scenario II (See Appendix for detailed flow volume data throughout the year for V2 - F1, V2 - F10, H2-S-F1, and H2-S-F10).

Table 9.Maximum inflow and outflow, mean flow volume, and outflow rat for the configurations V2, H2-S, and H2-L.

Floor Number	Max Flow-out Volume (l/s)	Max Flow-in Volume (l/s)	Mode of flow vol. (l/s)	Flow-out rate (%)
1	44	12	30	98
2	42	11	27	98
3	41	10	25	98
4	40	9	23	99
5	24	7	17	97
6	18	6	14	97
7	31	11	7	87
8	30	16	11	36
9	38	23	16	30
10	37	25	20	24

LEEWARD SIDE / APARTMENT WITH VERTICAL FLUE **V2**

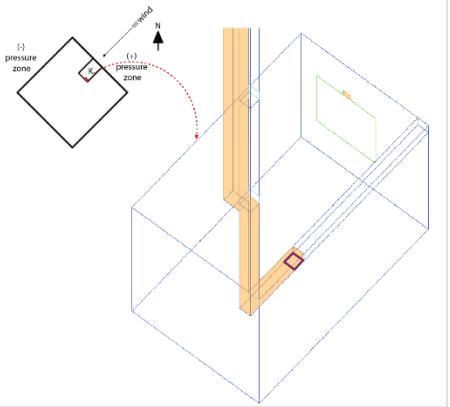

Floor Number	Max Flow-out Volume (l/s)	Max Flow-in Volume (l/s)	Mode of flow vol. (l/s)	Flow-out rate (%)
1	75	0.7	8	100
2	75	0.9	9	100
3	75	0.9	9	100
4	75	0.9	9	100
5	75	0.9	8	100
6	75	0.9	8	100
7	83	0.8	8	100
8	83	0.8	8	100
9	88	0.7	8	100
10	88	0.4	8	100

WINDWARD SIDE / APARTMENT WITH HORIZONTAL FLUE(SHORT) **H2-S**

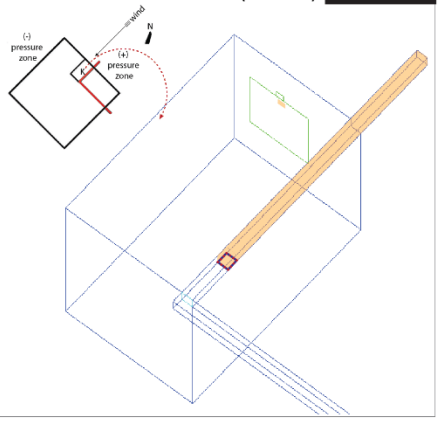

Floor Number	Max Flow-out Volume (l/s)	Max Flow-in Volume (l/s)	Mode of flow vol. (l/s)	Flow out rate (%)
1	69	1	8	100
2	69	1	8	100
3	69	1	8	100
4	69	1	8	100
5	8	1	7	99
6	8	1	7	99
7	77	1	8	100
8	77	1	8	100
9	82	1	8	100
10	82	1	8	100

WINDWARD SIDE /APARTMENT WITH VERTICAL FLUE(LONG) **H2-L**

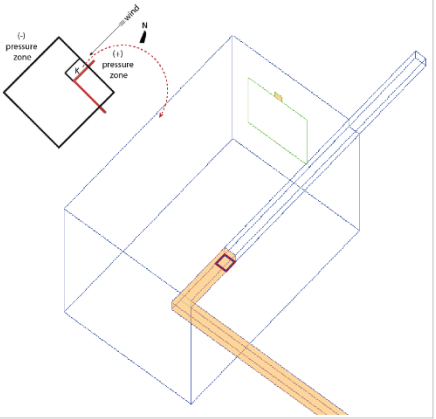

4.1.3 Determination of the Design Date

In the scenario selected for CFD analysis, the flow-out (extract) rate data was the primary criterion, while the mode value of the flow volume served to characterize the overall natural ventilation pattern in the kitchen and to determine the design date. Therefore, the flow volume mode values for V2 - F1, V2 - F10, H2-S-F1, and H2-S-F10 are 30 l/s, -20 l/s, 8 l/s, and 8 l/s, respectively, where negative values indicate flow-in and positive values indicate flow-out. The times at which the mode values occurred in the timetable were analysed for the 1st and 10th floors of each building, and the moments when these mode values occurred were marked as seen in Figure 68.

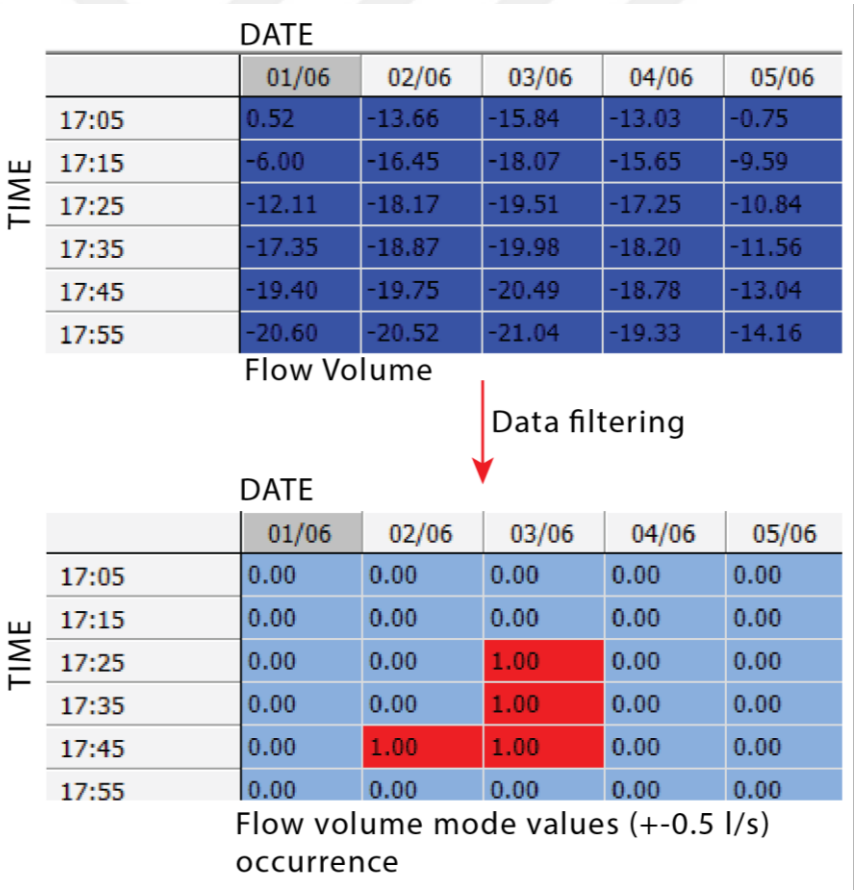

Figure 68. From flow volume to flow volume mode value occurrence process

The flow volume mode value occurrence table was analyzed on an annual basis for each selected scenario according to its unique flow volume mode value (Table 10). Each vertical interval represents the duration between 17:00 and 18:00, while the letters in the horizontal interval indicate the months from January to December. The flow volume mode value for all four scenarios occurred on 03 June, which was selected as the CFD design date.

Table 10.A timetable of the times throughout the year when each kitchen's unique mode value occurred.

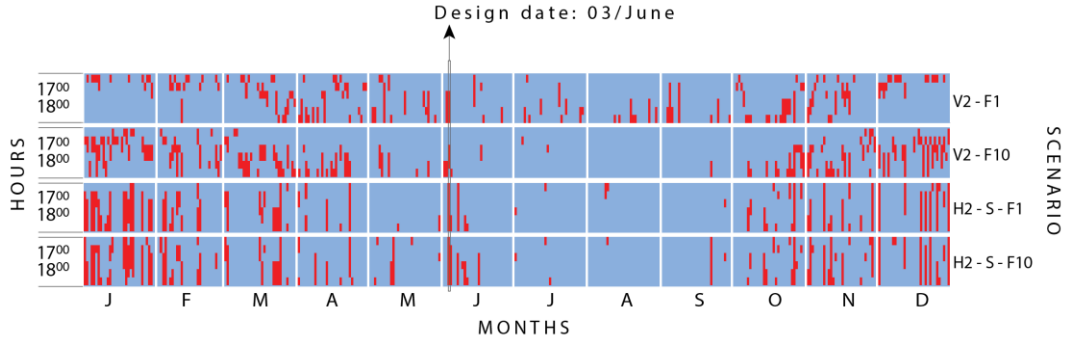

On 03 June (Table 11), between 17:00 and 18:00, the dry-bulb temperature drops from 10°C to 9.7°C. The wind speed decreases from 1.5 m/s to 0.7 m/s. On the wind-rose chart, where 0° represents north and 180° represents south, the wind blows from 180°—from the south—between 17:00 and 18:00.

Table 11.Dry-bulb temperature, wind speed, and direction on the design date for the Ankara location

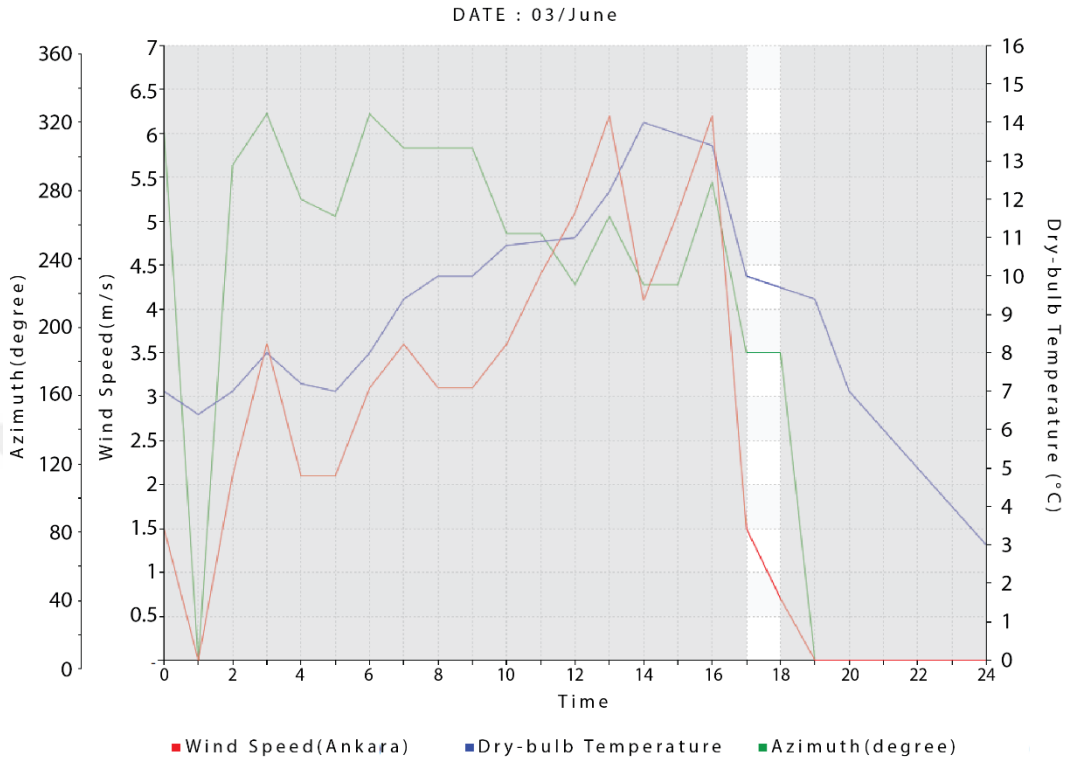

For 03 June, the flow volume mode value occurrence graphs for V2-F1, V2-F10, H2-S-F1, and H2-S-F10 are presented in Table 12. Only V2-F10 shows a negative flow volume value—indicating flow-in—while the other flue openings exhibit flow-out.

Table 12.The flow volume of selected kitchens for design date during cooking hour

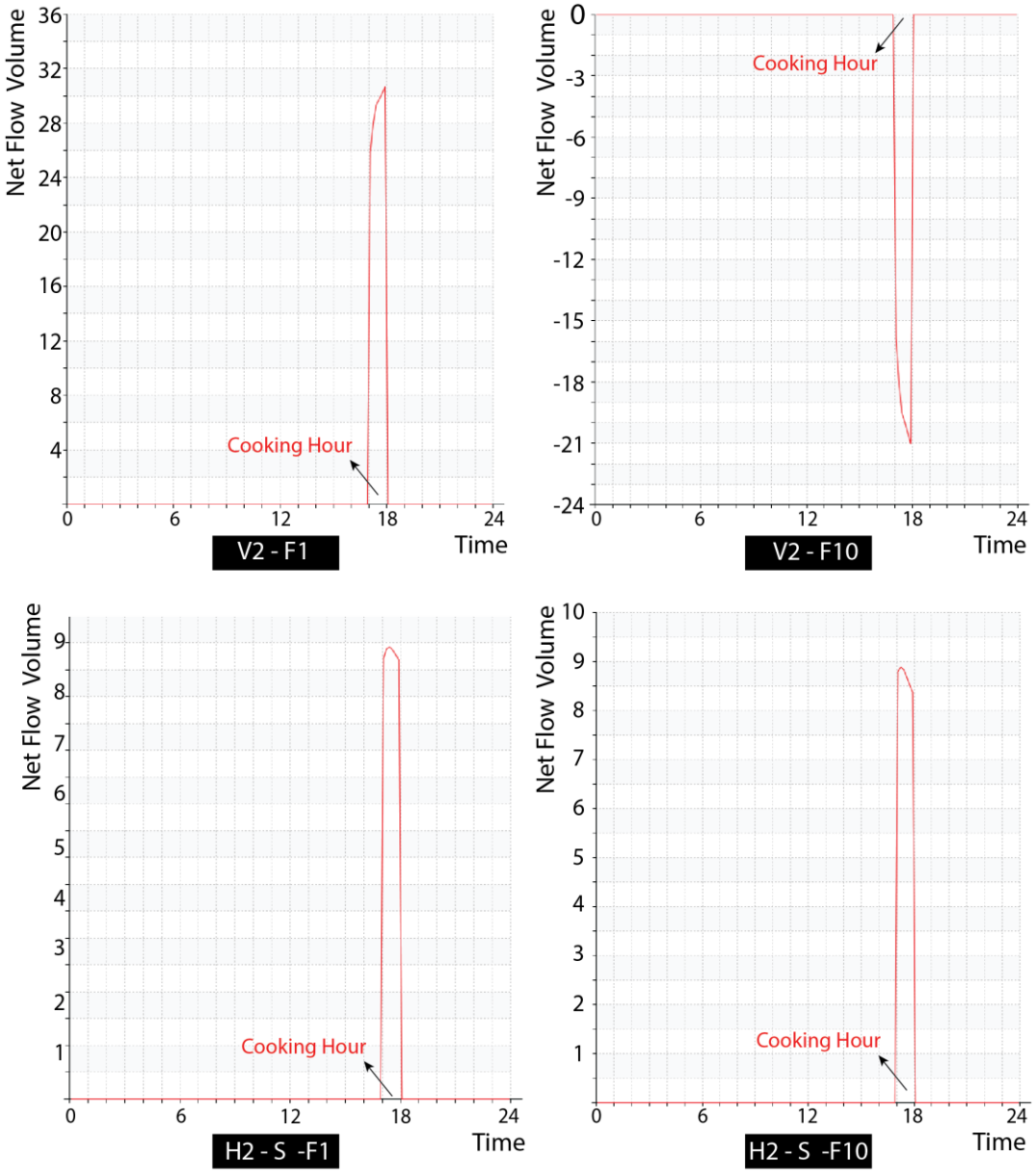

4.2 Results of CFD Simulation

In this chapter, the CFD results obtained on the design date for four kitchen configurations V2-F1, V2-F10, H2-S-F1 and H2-S-F10 are presented. The results

detail the in-kitchen airflow characteristics during cooking, including distributions of velocity, temperature, CO_2 concentration, and moisture. Airflow effectiveness is quantified using the Local Mean Age of Air, and the transport pathways of cooking fumes and odours are analysed via particle tracking results.

4.3.1 Velocity Profile of Airflow

Figure 69 shows an axonometric top view of the velocity profiles for V2-F1 and V2-F10. The airflow velocity range is 0–1.5 m/s. In V2-F1, airflow accelerates from the natural gas vent into the kitchen; as it progresses inward, it decelerates and is redirected toward the kitchen hood. Conversely, in V2-F10, the airflow at the natural gas vent is directed from the kitchen toward the outside at a uniform velocity that is significantly lower than in V2-F1.In both V2-F1 and V2-F10, cooking causes changes in airflow velocity around the kitchen hood; however, in both cases, the velocities remain within a similar range and stay below 0.95 m/s.

Figure 70 shows an axonometric top view of the velocity profiles for H2-S-F1 and H2-S-F10, which are nearly identical. In both cases, a uniform airflow—reaching a maximum velocity of 0.41 m/s—is directed from the natural gas vent into the kitchen. Around the kitchen hood, cooking causes slight variations in airflow velocity; however, as with V2-S-F1 and V2-S-F10, the velocities in both H2-S-F1 and H2-F10 remain within a similar range and stay below 0.95 m/s.

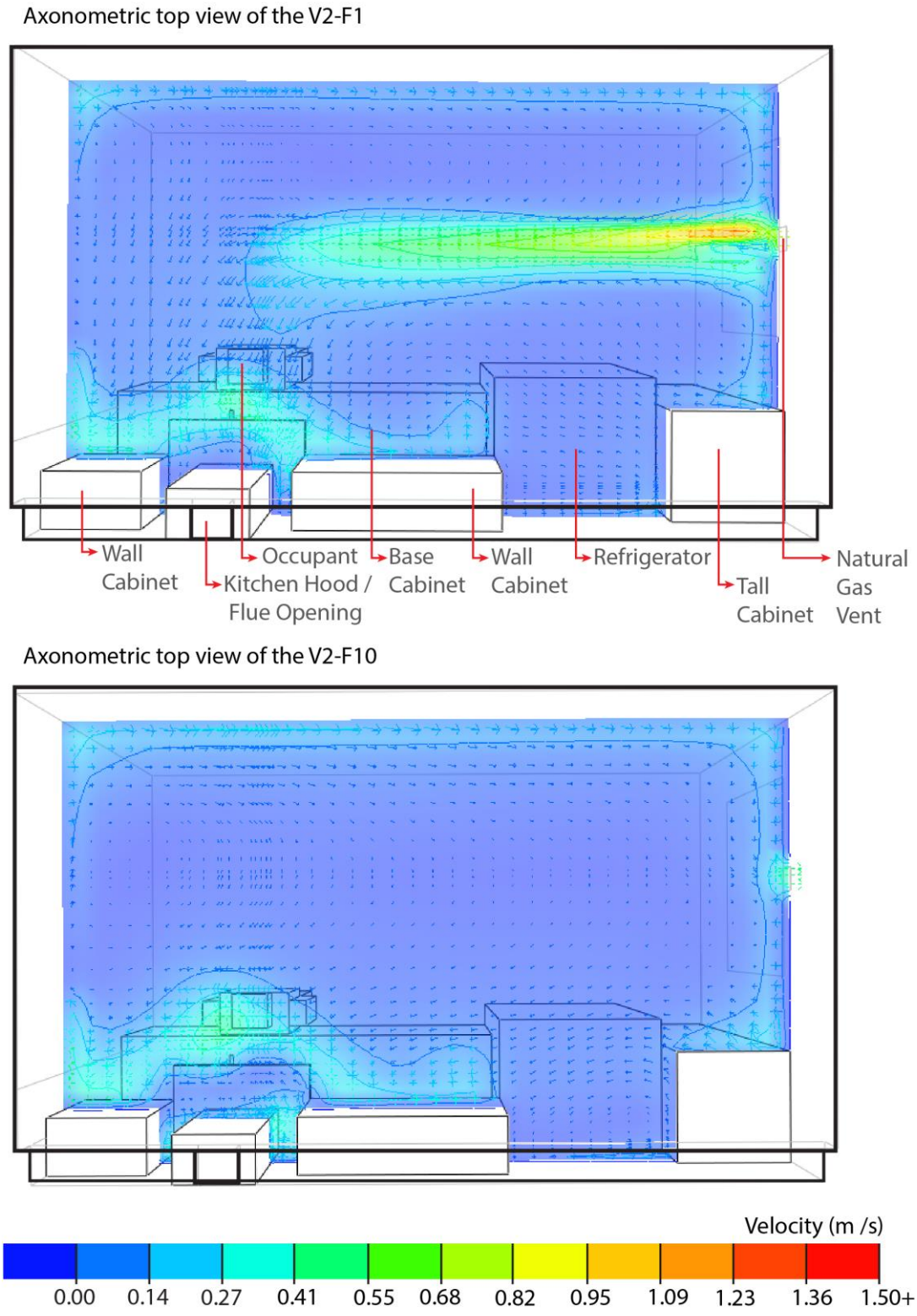

Figure 69. Axonometric top view showing the velocity profile for V2-F1(above) and V2-F10(below)

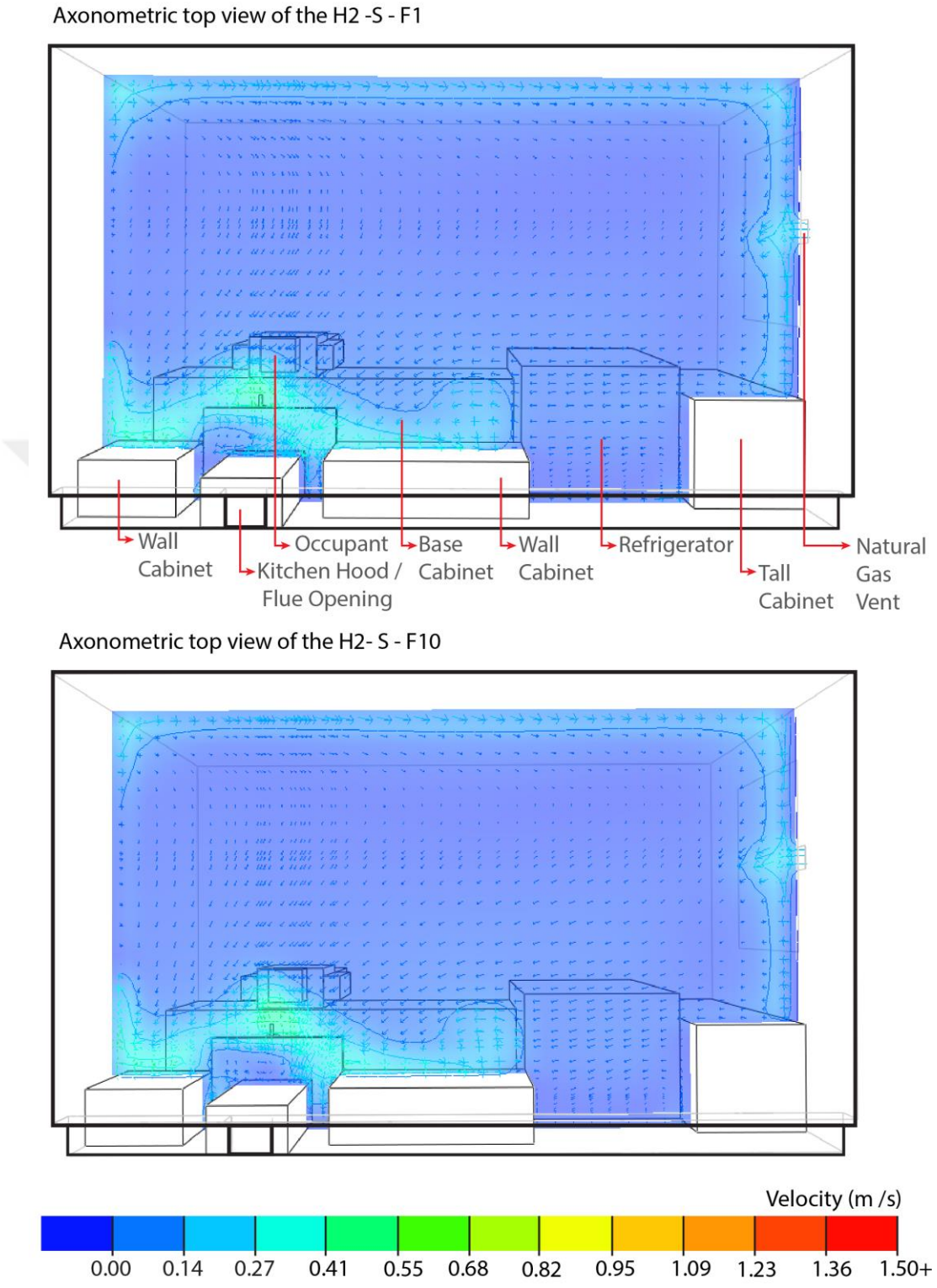

Figure 70. Axonometric top view showing the velocity profile of H2-S-F1(above) and H2-S-F10(below)

4.3.2 Temperature Profile of Airflow

Figure 71 shows an axonometric section of the temperature profiles for V2-F1 and V2-F10. The temperature range is 19–35 °C. In both cases, the use of the natural gas stove produces a vertical temperature gradient. In V2-F1, temperature contours remain largely horizontal, indicating a uniform upward gradient. In V2-F10, however, the contours curve upward toward the wall cabinets, demonstrating heat accumulation along and above the cabinets.

Figure 72 shows an axonometric section of the temperature profiles for H2-S-F1 and H2-S-F10. The temperature range is 19–35 °C. In both cases—as in V2-F1 and V2-F10—the use of the natural gas stove produces a vertical temperature gradient. Similar to V2-F1, the temperature contours in H2-S-F1 and H2-S-F10 remain largely horizontal, indicating a uniform upward gradient.

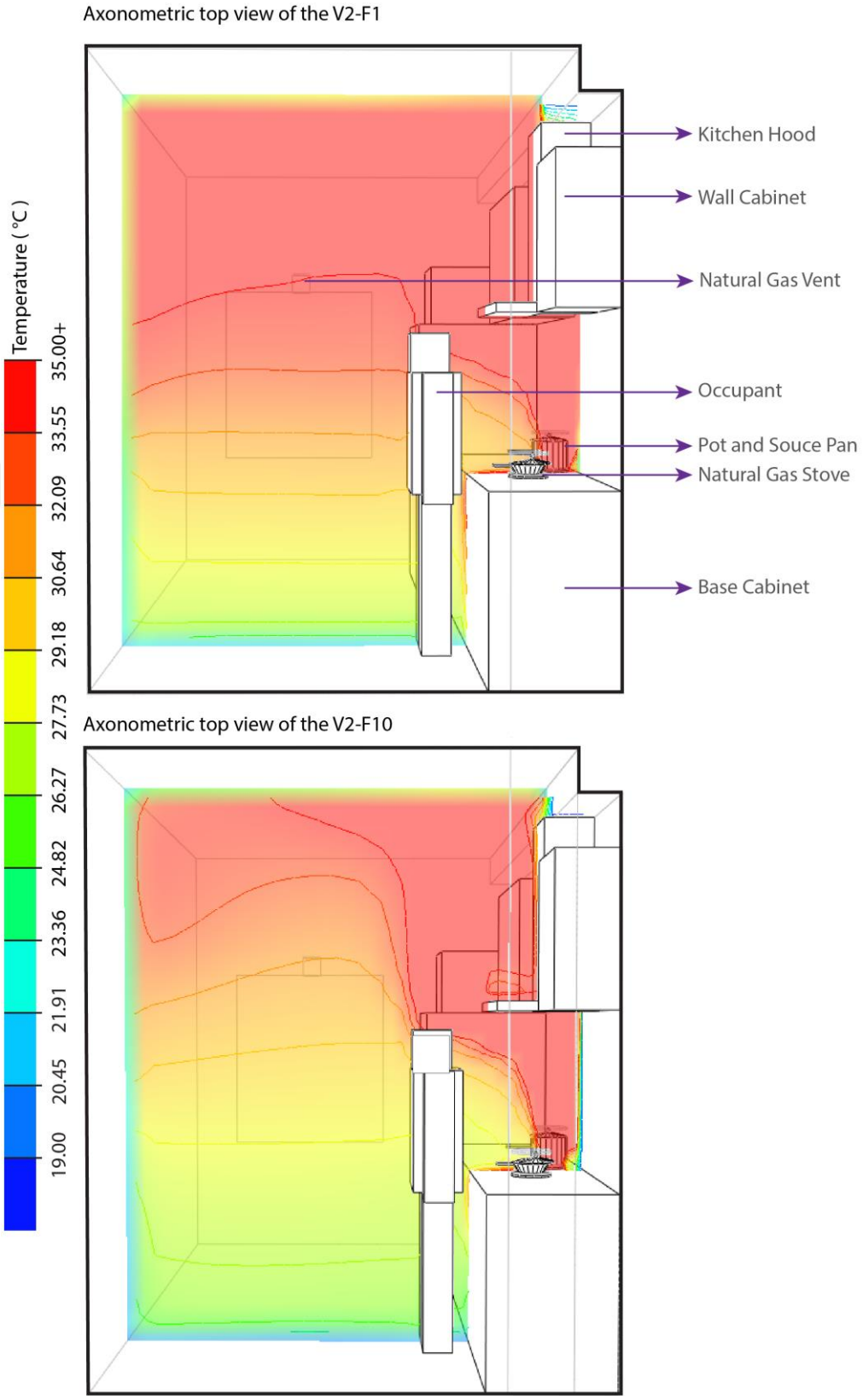

Figure 71. Axonometric top view showing the temperature profile for V2-F1 (above) and V2-F10(below)

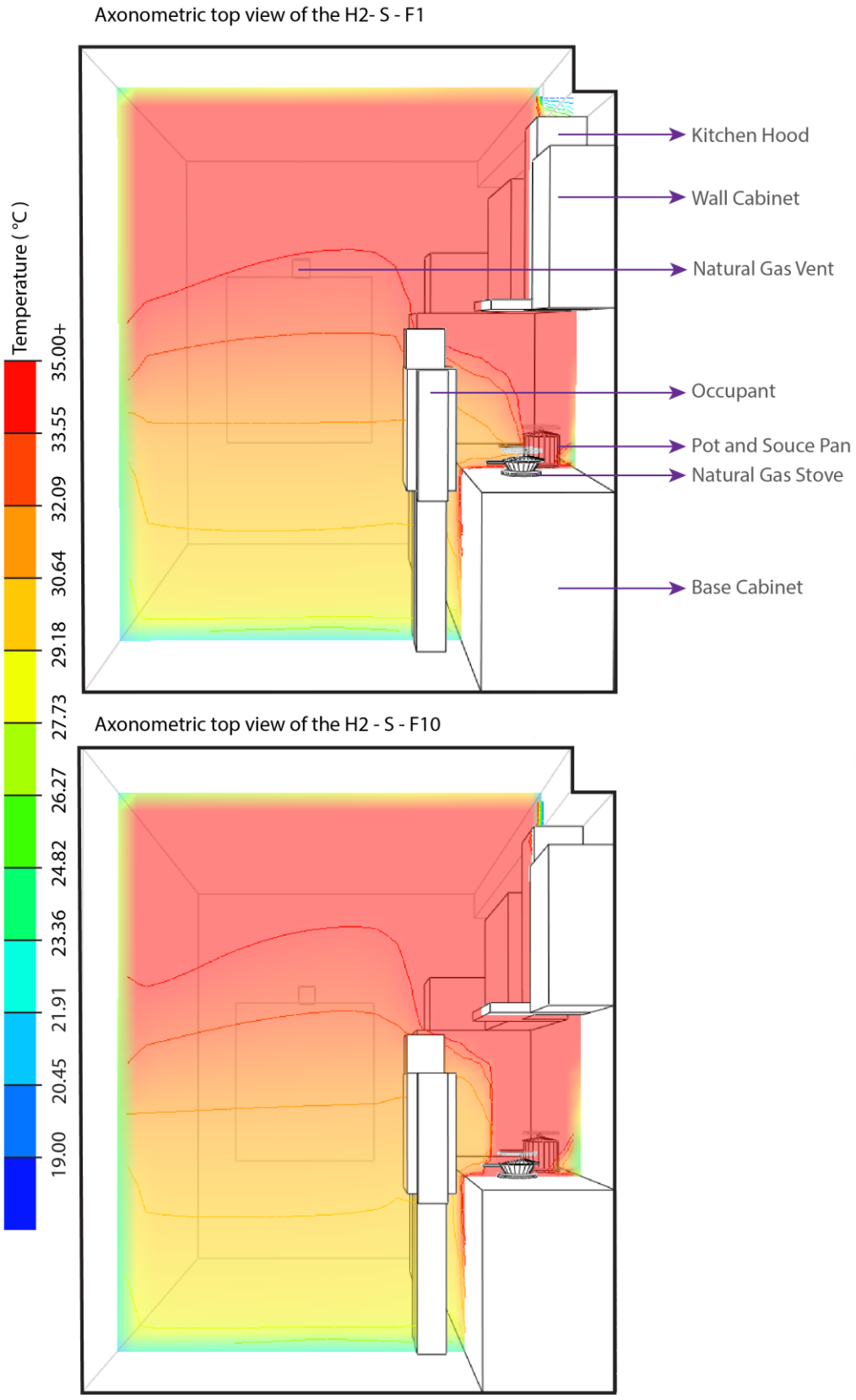

Figure 72. Axonometric top view showing the velocity profile for H2-S-F1 (above) and H2-S-F10(below)

4.3.3 CO_2 Profile of Airflow

Figure 73 shows axonometric sections of the CO_2 profiles for V2-F1, V2-F10, H2-S-F1, and H2-S-F10. The range for the CO_2 profile is 0 to 15000 parts per million(ppm). The lowest CO_2 concentration, around 8000 ppm, was measured in a part of the kitchen at V2-F1. As the distance to the CO_2 source decreased, the concentration increased significantly. Subsequently, V2-F10 showed the next elevated levels, while the highest concentrations were observed at H2-S-F1 and H2-S-F10. When considered alongside the airflow volume data, it is clear that lower airflow volume results in noticeably higher CO_2 concentrations. Although the CO_2 level of the flue opening air at V2-F10 (512 ppm) exceeds that of fresh air (400 ppm), the overall concentration remains lower at V2-F10 compared to V2 because the natural gas vent there exhausts a larger airflow volume, thereby reducing the CO_2 concentration. When comparing H2-S-F1 and H2-S-F10, even though the mode flow volume value is the same, it remains unstable over the one-hour cooking process. Although the fresh air supplied by the natural gas vent at H2-S-F1 may create a gap within the dense CO_2 mass, overall it does not appear to reduce the concentration. To validate the CO_2 concentration in the kitchen volume, the CFD model used an input of 0.870 kg h^{-1} of CO_2 generated by cooking, which was converted to parts per million (ppm) with three different calculators. CO_2 infiltration and exfiltration through the building envelope and the spread of CO_2 to other rooms through the kitchen door were disregarded. As a result, for reference calculator I(URL-3), assuming normal conditions, the CO_2 concentration was converted to 14 970 ppm (by volume) and 22 430 ppm (by weight). In reference calculators II(URL-4) and III(URL-5), the CO_2 concentration was converted to 18 281 ppm and 18 270 ppm, respectively(Appendix). The CFD analyses of the test kitchens gave lower concentrations because they account for natural ventilation through the vent and ducts. Notably, the V2 kitchens, which have a higher airflow rate, show lower CO_2 concentrations than the H2 kitchens.

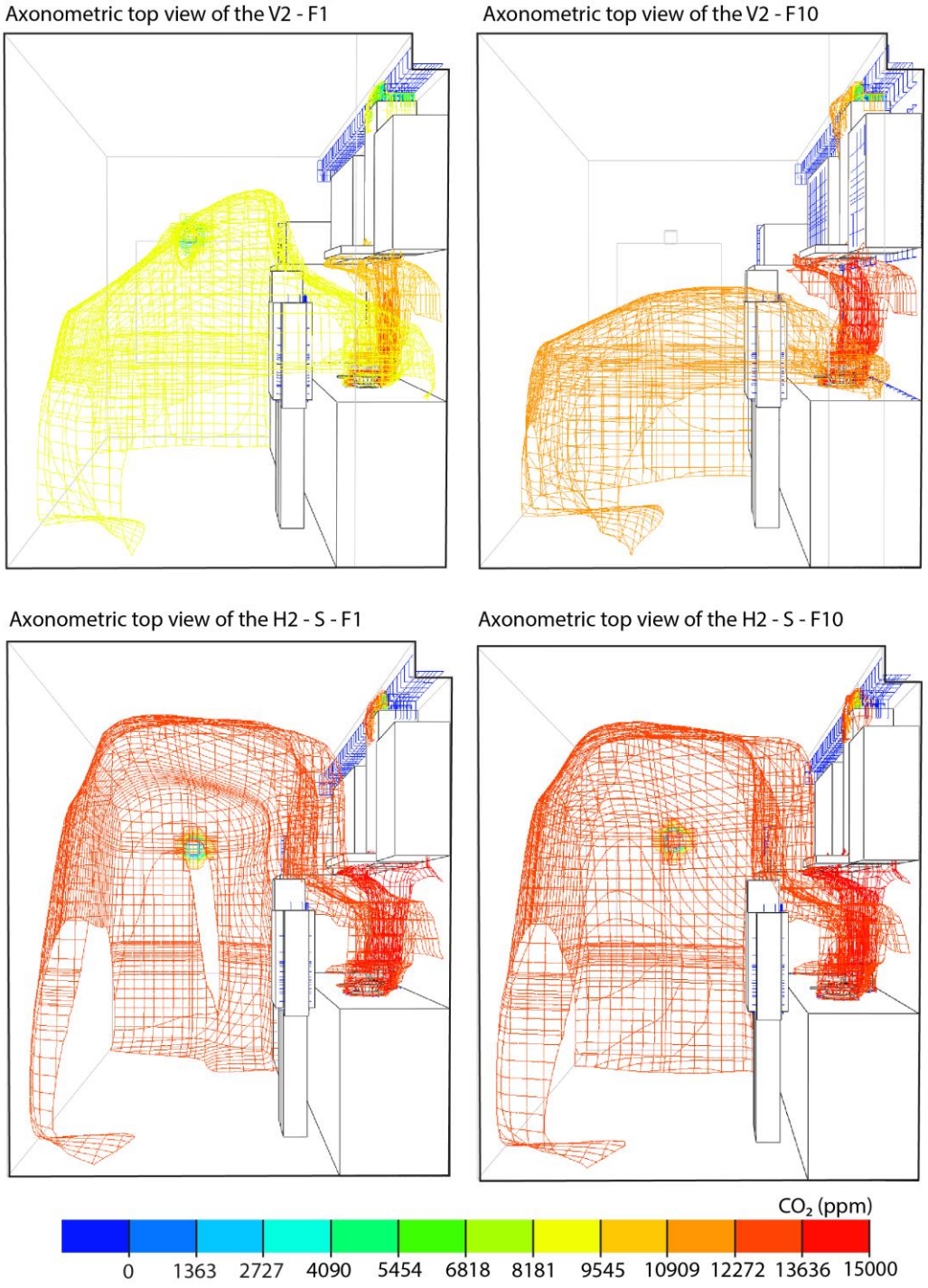

Figure 73. Axonometric top view showing the CO_2 profile for V2-F1 (top-left), V2-F10(top-right), H2-S-F1(bottom-left) and H2-S-F10(bottom-right)

4.3.4 Moisture Profile of Airflow

Figure 74 shows axonometric sections of the H_2O profiles for V2-F1, V2-F10, H2-S-F1, and H2-S-F10. The moisture concentration ranges from 0 to 0.04 kg/kg. V2--F1 and H2-S-F1 exhibit nearly identical moisture concentrations, between 0.0363 and 0.04 kg/kg. V2-F10 and H2-S-F10 show slightly lower concentrations in areas further from the stove, ranging from 0.0327 to 0.04 kg/kg. In V2-F1, the moisture contour bends upward above the fresh air entering from the natural gas vent. In contrast, in both V2-F10 and H2-S-F10, the moisture accumulates beneath the kitchen hood, while the remaining area of the kitchen maintains lower moisture concentrations.

Figure 74. Axonometric top view showing the H_2O profile for V2-F1 (top-left), V2-F10(top-right), H2-S-F1(bottom-left) and H2-S-F10(bottom-right)

4.3.5 Local Mean Age of Air

The Local Mean Age of Air (LMAA) quantifies ventilation efficiency by measuring the time required to replace indoor air. Figure 75 shows an axonometric top view of the LMAA for V2-F1, V2-F10, H2-S-F1, and H2-S-F10, with values ranging from 0 to 60 minutes. In V2-F1, the indoor air is renewed within 32–38 minutes, whereas in V2-F10, the renewal time exceeds 60 minutes. Both H2-S-F1 and H2-S-F10 exhibit nearly identical performance, renewing indoor air within 27–32 minutes. Despite the higher fresh-air velocity supplied through the natural gas vent in V2-F1, both H2-S-F1 and H2-S-F10 demonstrate enhanced ventilation performance, as evidenced by their shorter local mean ages of air.

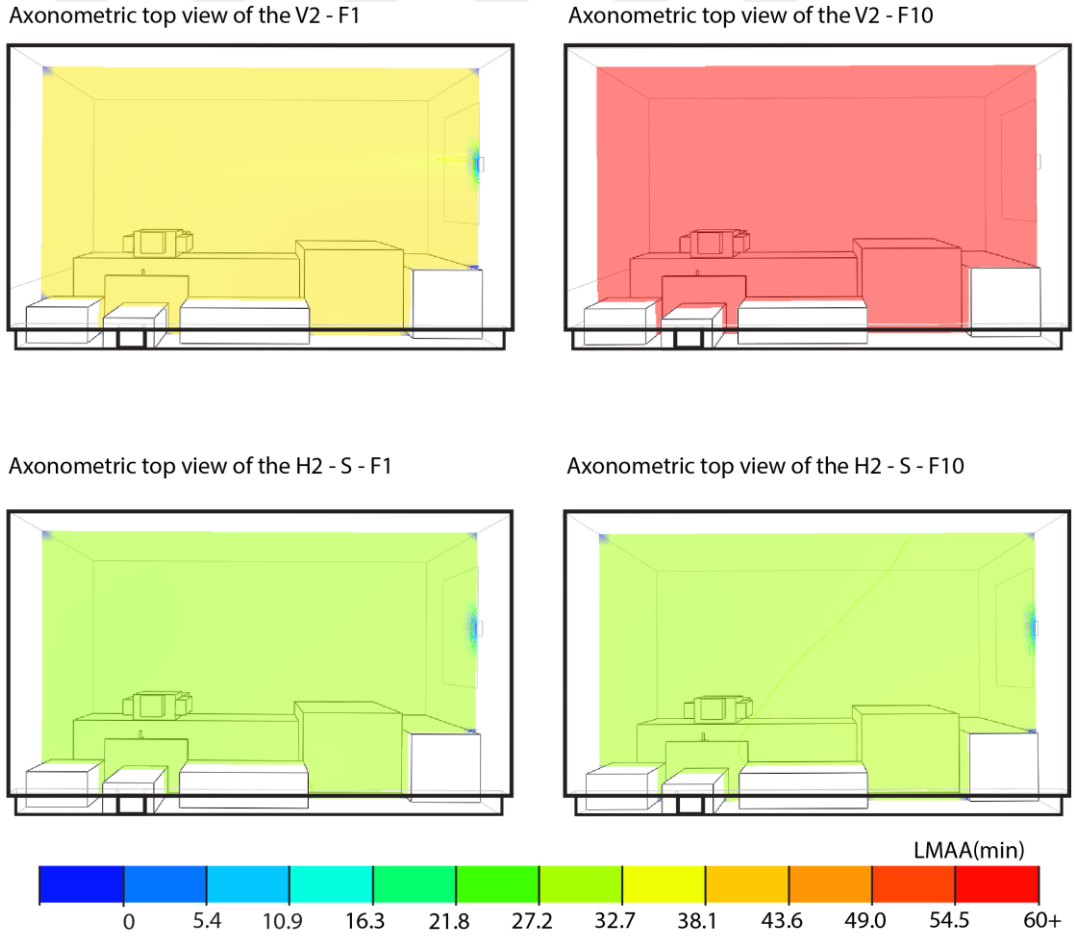

Figure 75. Axonometric top view showing the LMAA profile for V2-F1 (top-left), V2-F10(top-right), H2-S-F1(bottom-left) and H2-S-F10(bottom-right)

4.3.6 Particle Tracking of Airflow

Particle tracking illustrates each particle's path over its initial 100 m distance. The colour of the path indicates the particle velocity, as seen in Figure 76. In all cases, this path remains confined within the kitchen. In V2-F10, H2-S-F1, and H2-S-F10, particles rise as they heat and descend as they cool, following a large spiralling path from the centre of the kitchen toward the kitchen hood. In V2-F1, however, the path is irregular; it appears to be strongly influenced by the influx of fresh air from the natural gas vent.

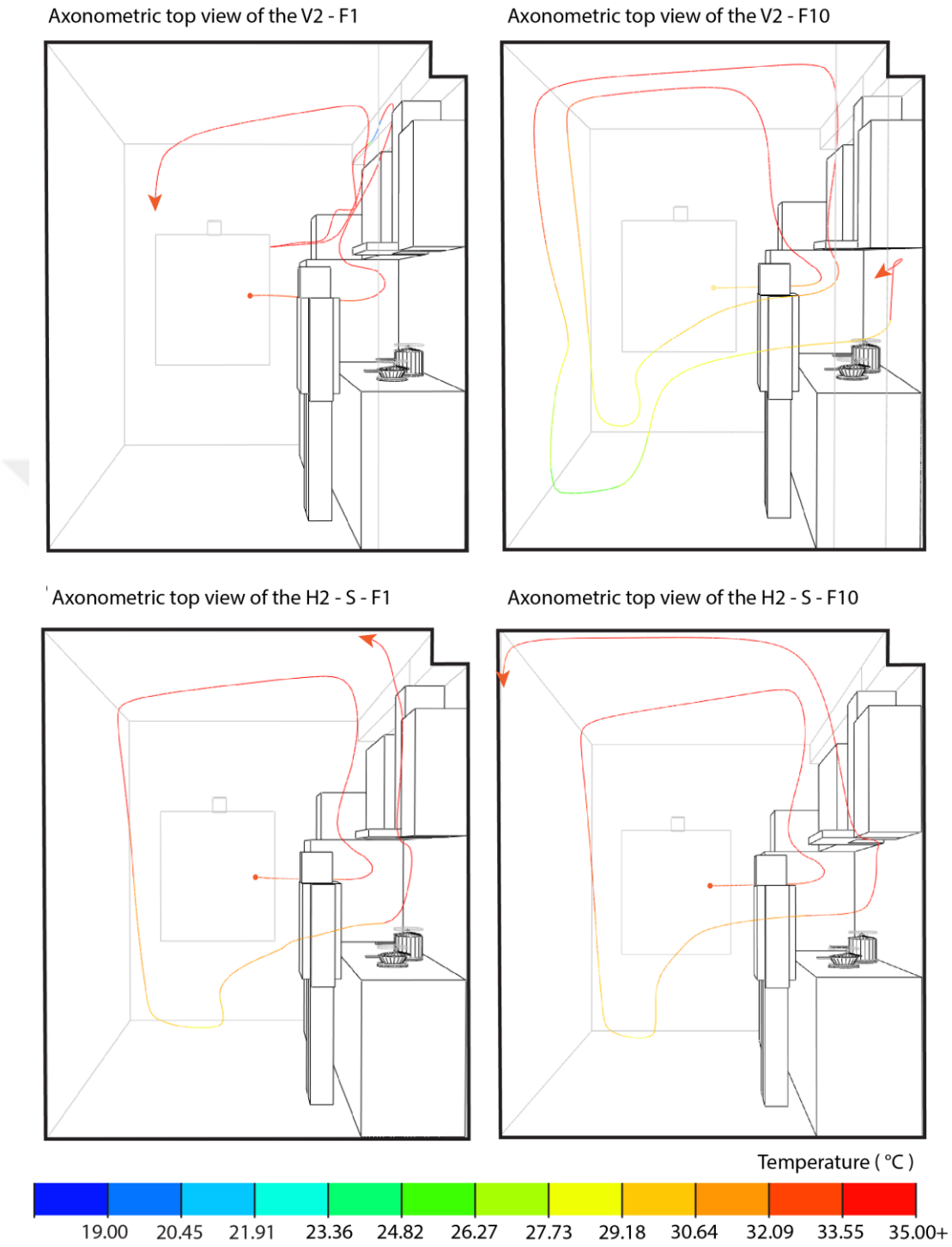

Figure 76. Axonometric top view showing the particle path profiles over the first 100 m for V2-F1 (top-left), V2-F10(top-right), H2-S-F1(bottom-left) and H2-S-F10(bottom-right)

CHAPTER 4

CONCLUSION

The research was inspired by the occurrence of cooking odours in apartment kitchens despite the absence of any ongoing cooking activity. Although the culinary culture is diverse, dishes generally consist of vegetables cooked with meat, onions, tomato paste, and tomatoes; additionally, a wide variety of spices are used, and food is typically lightly fried in oil before water is added during cooking. During this process, a natural gas stove is commonly used for cooking, while a natural gas vent located on the window supplies fresh air. In some cases, this vent is closed during winter to prevent cold air from entering. The kitchen ventilation systems in Turkey's apartment buildings depend on the combined operation of shunt flues and kitchen hoods to exhaust cooking smoke and odours. However, in some cases, either closing the balcony or designing a secondary space as a kitchenette is preferred as a solution to prevent the cooking fumes and odours caused by frying. The kitchen ventilation systems in Turkey's apartment buildings depend on the combined operation of shunt flues and kitchen hoods to exhaust cooking smoke and odours. While existing studies have largely concentrated on the efficiency of kitchen hoods—evaluated through PM2.5 measurements or CFD simulations—the literature reveals a need for further development in ventilation efficiency when the kitchen hood is not in use. The research findings indicate that under such conditions the flue opening functions as a natural ventilation opening. In vertically flued buildings, the stack effect generated by cooking activity in one kitchen affects the airflow rate and velocity of the flue openings in other kitchens connected to the same flue system to varying degrees.

This research aims to reduce the inter-floor transmission of polluted air during winter, driven by the stack effect. However, in vertically flued buildings—where the stack effect is predominant—orienting the building toward the windward or leeward direction does not significantly mitigate its impact on kitchen ventilation.

Conversely, in horizontally flued, windward-oriented building kitchens, the high flow-out rate at the connection between the kitchen and the flue opening, along with the independent design of the flues, offers an alternative strategy to reduce inter-floor transmission.

One of the aims of the study was to investigate indoor air quality. During cooking in apartment kitchens, both vertically flued and horizontally flued systems are evaluated using CO_2 concentration, H_2O concentration, and indoor air refresh duration as key parameters. The ASHRAE Board of Directors (2025) notes that indoor CO_2 levels alone are not definitive indicators of indoor air quality (IAQ), but higher CO_2 concentrations require increased ventilation. Because the H2 scenario produces a higher CO_2 concentration, the need for mechanical ventilation (kitchen hood) is greater. However, its refresh time is shorter than in V2, suggesting that it might run for a shorter period—although further research is needed. Meanwhile, V2 shows a lower CO_2 concentration but a longer refresh time, as seen in Figure 21 in Section 2.2.1.1, due to the higher airflow volume creating a strong yet non-uniform airflow within the kitchen. In contrast, H2's weaker but more evenly distributed airflow affects the kitchen air uniformly and results in an overall shorter refresh time.

Considering that today's kitchens function much like workplaces and are based on the original Frankfurt kitchen design, CO_2 threshold limits were assessed in the following way. In a work environment, the United States Occupational Safety and Health Administration (OSHA) (2017) advises keeping carbon dioxide (CO_2) levels under 5,000 parts per million (ppm) over eight hours, while the National Institute for Occupational Safety and Health (NIOSH) (1976) recommends the same long-term limit but also provides a short-term limit of 30,000 ppm for exposures up to ten minutes. In this context, the CFD-tested kitchens reach CO_2 concentrations of up to 15 000 ppm and refresh time of up to one hour. The concentration levels exceed the 5 000 ppm occupational limit for an eight-hour exposure, although they remain below NIOSH's short-term level of 30 000 ppm for ten minutes.

According to the ADS results for natural ventilation, when all floors are cooking simultaneously without using the kitchen hood, the stack effect becomes significant in vertically flued buildings. Typically, the lower floors exhaust air from the kitchens, while the opposite occurs on the upper floors, where air is supplied into the kitchens through the hood. It was also observed that orienting both the building and the kitchen's natural gas vent toward the windward side increased the flow volume. However, compared to the leeward orientation, this approach further reduced the already low flow-out rate on the upper floors relative to the lower floors, negatively impacting kitchen ventilation. In this situation, instead of supplying fresh air from the natural gas vent, it was observed that the vent was exhausting indoor air. Both the V1 and V2 scenarios exhibit a neutral pressure level between the 7th and 8th floors and exhibit lower flow, where the function of the flue opening shifts from exhaust to supply. Mijorski and Cammelli (2016), indicate that on the tested floor closer to the neutral pressure level, the lack of airflow leads to higher CO_2 concentrations. Taking into account the low airflow volume in H2, it can be inferred that floors closer to the neutral level in V2 may exhibit higher CO_2 concentrations compared to the other floors.

In the study by Xu, Xiong, Zhang, and Li (2019), an equation was presented for natural ventilation, specifying temperature and CO_2 concentration ranges aimed at preserving indoor air quality and thermal comfort. In the V2-F1 scenarios, when the flue opening supplies air into the kitchen, the CO_2 concentration is higher than that of fresh air (512 ppm > 400 ppm). This conclusion indicates a negative impact on indoor air quality in vertically flued kitchens—not due to the CO_2 concentration itself, but because of the cooking-generated particles from other kitchens in the apartment that accompany it. Considering the kitchen hood filter performance and the particles deposited in the duct, as described in Figure 39 of Section 2.3.2, it appears that the CO_2 concentration in the flue can be accompanied by both newly generated cooking particles and those previously deposited. Consequently, in terms of indoor air quality, the inter-floor transmission scenario at V2-F10 emerges as the worst case.

According to the ADS results for natural ventilation, for the vertical flue scenarios, H1 and H2—when all floors are cooking simultaneously the effect of wind direction is significant. In scenario H2, the horizontal flue exhibits more consistent results in both its short and long sections. Moreover, no significant differences in flow volume mode value and flow-out rate were observed between floors. It demonstrates that, when necessary, mechanical ventilation with the same exhaust characteristics and consistent performance—without generating opposing flow-in—can be ensured through a high flow-out rate across floors from low to high.

Based on these results, the research questions are addressed as follows:

- The research indicates that the maximum airflow volume is reached in the horizontally flued building due to wind effects; however, when considering the overall airflow characteristics (as indicated by the mode value), the vertically flued building exhibits a higher airflow volume.
- According to ASHRAE Board of Directors (2025) evaluations, kitchens generally meet acceptable CO_2 limits, but windward-oriented buildings with horizontal flues require additional ventilation due to higher CO_2 concentrations. Upper floors in both windward- and leeward oriented buildings with vertical flues emerge as the worst scenario for indoor air quality, as CO_2 levels, combined with cooking particles and duct deposits, create heightened pollution. Leeward oriented buildings with horizontal flues are slightly better than that worst case but still exhibit high CO_2 levels due to similar low airflow, plus the kitchen's own cooking particles. Meanwhile, the best scenario is on lower floors of windward- and leeward oriented buildings with vertical flues, which maintain lower CO_2 concentrations and more efficient removal of cooking particles. Finally, windward oriented buildings with horizontal flues are considered the second best scenario overall, as any additional cooking particles are not compounded by further deposits from the flue. In horizontally flued buildings, natural ventilation performance is significantly influenced by whether the building is oriented towards the

windward or leeward side. The worst scenario occurs when both the horizontal flue outlet and the natural gas vent are oriented toward the same leeward direction, whereas the best performance is achieved when both are oriented towards the windward side. In contrast, for vertically flued buildings, the windward/leeward orientation has only a minimal effect on natural ventilation performance.

- In horizontally flued buildings, the natural gas vent generally functions as an air supply—except when both the horizontal flue outlet and the natural gas vent are oriented toward the same leeward direction. In contrast, in vertically flued buildings, the natural gas vent typically supplies fresh air on the lower floors, while it acts as an exhaust on the upper floors.

For apartment buildings with a horizontal flue, the main issue is that low airflow volume leads to higher CO_2 levels, and it is assumed that cooking-related particles also disperse in a pattern similar to CO_2 concentration within the kitchen. In a windward-oriented kitchen, airflow volume can be increased by using a kitchen hood, and because there is no stack effect, efficient ventilation can be achieved. However, in a leeward-oriented scenario, mechanical ventilation can encounter reverse airflow at different times of the year, affecting different floors variably and resulting in lower performance than in the windward-oriented scenario. To implement a horizontal flue system effectively, the building's and flue's wind orientation, as well as local climate data, should be assessed in the design phase. In different locations, considering daily and annual wind patterns in relation to kitchen use can help determine which section of the horizontal flue should be employed. In dense urban fabric or where there are obstructions in the wind path, ventilation efficiency may be reduced; thus, mechanical ventilation with a higher exhaust volume could be preferable. Because wind coefficients are much higher for high rise apartments, this system may not yet be practical in such structures, and further research is needed to optimize its performance.

In conclusion, this study highlights the impact of stack-induced airflow in vertically flued buildings on overall ventilation performance, while also demonstrating significant inter-floor imbalances in kitchen ventilation during cooking. Horizontally flued buildings were examined as a comparative parameter within the simulation limits, and the potential of horizontal flue ventilation systems as an alternative for apartment kitchen ventilation was explored. Furthermore, to prevent the kitchen's natural airflow path through the vertical flue when the kitchen is occupied, strategies such as installing an operable flue damper or hood damper to completely halt airflow may be considered. Given the varying dynamic performance of vertical flue airflow across different floors, it is also recommended that the efficiency of kitchen hood performance be evaluated on a per-floor basis.

As a final consideration, the recent fire at the Kartalkaya Hotel began in the kitchen and rapidly spread to the upper floors via the stack effect. This situation demonstrates that a natural ventilation system designed with a horizontal flue and isolated for each floor can be part of the solution for controlling kitchen-origin fires. Further investigation is required regarding fire safety in apartment buildings.

REFERENCES

Akgün, M. (2019). *Optimisation of ventilation grilles used in natural gas installations (Master's Thesis).* Muğla Sıtkı Koçman University, Muğla. Retrieved November 25, 2024, from https://tez.yok.gov.tr/UlusalTezMerkezi/tezSorguSonucYeni.jsp

AKSA Natural Gas Distribution Inc. (2014). *Technical specifications for natural gas in buildings.* Retrieved November 25, 2024, from http://www.bandirmagaz.com.tr/utility/Binalar-Icin-Dogalgaz-Teknik-Esaslari-Nisan-2015.pdf

Aktaş, A., & Özdemir, B. (2007). *Otel işletmelerinde mutfak yönetimi.* Ankara: Detay Yayıncılık

Allocca, C., Chen, Q., & Glicksman, L. R. (2003). Design Analysis of Single-Sided Natural Ventilation. *Energy and Buildings,* 35(8), 785–795. https://doi.org/10.1016/s0378-7788(02)00239-6

Ankara Valiliği Mahalli Çevre Kurulu. (2009, 27 Ağustos). Isınmadan kaynaklanan hava kirliliğinin kontrolü hakkında karar (Karar No: 2009/30). Ankara, Türkiye. Retrieved from http://www.ankara.gov.tr/arama/ara/karar

Arıoğlu, N., & Hatipoğlu, D. D. (2005). Çatı Cephe Fuarı . In *Çok Katlı Konut Yapılarında Şönt Baca Uygulama Sorunları ve Deprem Etkisi*. ÇATIDER. Retrieved January 9, 2024, from https://catider.org.tr/index.php?action=page&id=259.

ASHRAE & White Box Technologies. (2008). International Weather for Energy Calculation (IWEC). Retrieved from http://ashrae.whiteboxtechnologies.com/home

ASHRAE Board of Directors. (2025). (rep.). *ASHRAE Position Document on INDOOR CARBON DIOXIDE*. ASHRAE. Retrieved April 9, 2025, from https://www.ashrae.org/file%20library/about/position%20documents/pd_indoorcarbondioxide_2025.pdf.

Avcı Hosanlı, D. (2021). Housing in transition: The first apartments of the new capital city, Ankara. *Journal of Housing and the Built Environment, 36*, 1141–1163. https://doi.org/10.1007/s10901-020-09799-5

Beamish, J., Parrott, K. R., Emmel, J., & Peterson, M. J. (2013). *Kitchen planning: Guidelines, codes, standards*. Wiley. November 5, 2024, https://books.google.com.tr/books?id=dz5NyLDon-AC&printsec=frontcover&source=gbs_ge_summary_r&cad=0#v=onepage&q&f=false

Brager, G., Alspach, P., & Nall, D. H. (2011). Natural vs. Mechanical Ventilation and Cooling. *RSES Journal*, 18–22. Retrieved 2023.

Buckley, L. (2021). CFD: Hospital Operating Room (On-demand online training presentation). Integrated Environmental Solutions (IES) North America. Retrieved from https://distance-learning.iesve.com/courses/139263/lectures/48216959

Buonanno, G., Morawska, L., & Stabile, L. (2009). Particle Emission Factors During Cooking Activities. *Atmospheric Environment, 43*(20), 3235–3242. https://doi.org/10.1016/j.atmosenv.2009.03.044

Çalışkan, O., Parlak Temizel, N., Akay, M., & Mashhoodi, B. (2023). Typological diversity and morphological continuity in the modern residential fabric: The case of ankara, Turkey. *Habitat International, 142*, 102950. https://doi.org/10.1016/j.habitatint.2023.102950

Cengizkan, A.(2000), *Discursive formations in Turkish residential architecture: Ankara, 1948 – 1962* (Doctoral dissertation). Retrieved from https://tez.yok.gov.tr/UlusalTezMerkezi/tezDetay.jsp?id=EchITYfkrMTAZ3tO6hVrwA&no=EchITYfkrMTAZ3tO6hVrwA

Chartered Institution of Building Services Engineers (CIBSE). (2006). *CIBSE Guide A: Environmental design* (7th ed.). Retrieved from https://teg.com.vn/Pic/files/CIBSE%20Guide%20A%20-%20Environmental%20Design%202006.pdf

Chartered Institution of Building Services Engineers (CIBSE). (2015). *CIBSE Guide A: Environmental design*. Retrieved from https://teg.com.vn/Pic/files/CIBSE%20Guide%20A%20-%20Environmental%20Design%202006.pdf

Chartered Institution of Building Services Engineers. (2005). CIBSE Guide B: Ventilation and air conditioning (Requirements and systems equipment and control). London: CIBSE.

Chen, C., Zhao, Y., & Zhao, B. (2018). Emission Rates of Multiple Air Pollutants Generated from Chinese Residential Cooking. *Environmental Science & Technology*, *52*(3), 1081–1087. https://doi.org/10.1021/acs.est.7b05600

Chen, Z., Xin, J., & Liu, P. (2020). Air Quality and Thermal Comfort Analysis of Kitchen Environment with CFD Simulation and Experimental Calibration. *Building and Environment*, *172*, 106691. https://doi.org/10.1016/j.buildenv.2020.106691

Çiftçi, M. (2020). Türkiye'de Konut Üretim Özelliklerinin 1964-2019 Arasında Uzun Dönemli Dönüşümü. *Kırklareli Üniversitesi Sosyal Bilimler Dergisi*, *4*(1), 83–99.

Costanzo, V., Yao, R., Xu, T., Xiong, J., Zhang, Q., & Li, B. (2019). Natural Ventilation Potential for Residential Buildings in a Densely Built-Up and Highly Polluted Environment. A Case Study. *Renewable Energy*, *138*, 340–353. https://doi.org/10.1016/j.renene.2019.01.111

Davidsson, H., Bernardo, R., & Hellström, B. (2013). Theoretical and Experimental Investigation of a Heat Exchanger Suitable for a Hybrid Ventilation System. *Buildings*, *3*(1), 18–38. https://doi.org/10.3390/buildings3010018

Daxom. (n.d.). *Termomex*. Retrieved December 17, 2024, from https://www.daxom.com/product/termomex

Don, F., & Rich, S. (2014). 90.1 and Designing High Performance Commercial Kitchen Ventilation Systems. *ASHRAE Journal*, *52*(11), 12–24. Retrieved 2023, from https://www.proquest.com/docview/1628222531?pq-origsite=gscholar&fromopenview=true.

Dönmez Karagözler, D. (2022). Konut Mutfağının Tarihsel Gelişimi ve Modern Mutfak Kavramının Doğuşu. *Pearson Journal*, *7*(20), 63–79. https://doi.org/10.46872/pj.564

Elmaghraby, H. A., Chiang, Y. W., & Aliabadi, A. A. (2017). Ventilation Strategies and Air Quality Management in Passenger Aircraft Cabins: A Review of Experimental Approaches and Numerical Simulations. *Science and Technology for the Built Environment*, *24*(2), 160–175. https://doi.org/10.1080/23744731.2017.1387463

Environmental Design - *CIBSE Guide A* (2006) *(8th Edition), Section 4: Ventilation and Air Infiltration.* London: Chartered Institution of Building Services Engineers. Retrieved November 29, 2024, from app.knovel.com

Erçin, Ç., & Karaderi-Özsoy, Ş. (2013, April). *Mutfak mekânlarının endüstrileşme süreci* [The industrialization process of kitchen spaces]. Paper presented at the 3rd National Interior Architecture Symposium, Mimar Sinan Güzel Sanatlar Üniversitesi, Istanbul, Turkey. Retrieved from https://www.researchgate.net/publication/283709490_Mutfak_Mekanlarinin_Endustrilesme_Sureci

Erdaş, G., & Özmen, E. F. (2019). The Effects of Gender Concept on Housing Advertisements and Residential Organization. *MEGARON / Yıldız Technical University, Faculty of Architecture E-Journal*, *14*(1), 11–28. https://doi.org/10.5505/megaron.2018.01488

Flaga-Maryanczyk, A., Schnotale, J., Radon, J., & Was, K. (2014). Experimental Measurements and C.F.D. Simulation of a Ground Source Heat Exchanger Operating at a Cold Climate for a Passive House Ventilation System. *Energy and Buildings*, *68*, 562–570. https://doi.org/10.1016/j.enbuild.2013.09.008

Fu, N., Kim, M. K., Chen, B., & Sharples, S. (2021). Investigation of Outdoor Air Pollutant, PM2.5 Affecting the Indoor Air Quality in a High-Rise Building. *Indoor and Built Environment*, *31*(4), 895–912. https://doi.org/10.1177/1420326x211038279

Guney, Y. I., & Wineman, J. (2008). The Evolving Design of 20th-Century Apartments in Ankara. *Environment and Planning B: Planning and Design*, *35*(4), 627–646. https://doi.org/10.1068/b3401

Google. (n.d.). *[*Google Earth location 39°50'48"N 32°50'03"E for the years 2004 and 2024*]*. Retrieved November 15, 2024, from https://earth.google.com/web/@39.84668429,32.83444389,1169.90665974a,1000d,30y,0h,0t,0r/data=CgRCAggBMikKJwolCiExMUVRNU42dFZWSGZHaWwzRGk1RjQ3Z0tZOXFWYmhWLUwgAToDCgEwQgIIAEoICKbY9ZkGEAE

He, L., Gao, J., Chen, J., Zeng, L., Zhang, C., Zhang, M., Xu, Y., & Guo, H. (2021). Experimental Studies of Natural Makeup Air Distribution in Residential Kitchen. *Journal of Building Engineering*, *44*, 102911. https://doi.org/10.1016/j.jobe.2021.102911

Heiselberg, P. (2004). Natural Ventilation Design. *International Journal of Ventilation*, *2*(4), 295–312. https://doi.org/10.1080/14733315.2004.11683674

Hu, Y., Liu, Z., Ai, Z., & Zhang, G. (2023). Performance evaluation of ventilative cooling systems for buildings under different control parameters and strategies. *Journal of Building Engineering*, *65*, 105627. https://doi.org/10.1016/j.jobe.2022.105627

Huang, R. F., Peng, K.-L., Chen, J.-K., & Nian, Y.-C. (2010). Improving flow and spillage characteristics of range hoods by using an inclined air-curtain technique. *The Annals of Occupational Hygiene*, *55*(2), 164–179. https://doi.org/10.1093/annhyg/meq070

IES VE MicroFlo User Guide (n.d.). Retrieved January 3, 2025, from https://www.iesve.com/downloads/help/CFD/MicroFlo.pdf

Izadpanahi, P., Farahani, L. M., & Nikpey, R. (2021). Lessons from Sustainable and Vernacular Passive Cooling Strategies Used in Traditional Iranian Houses. *Journal of Sustainability Research*, *3*(3). https://doi.org/10.20900/jsr20210014

Kale, E. Ö. (2008). *Density as a transformative power of urbanization: Milletvekili lojmanları/Park Oran konutları / Kentselleşmenin dönüştürücü bir aracı olarak yoğunluk: Milletvekili lojmanları/Park Oran konutları* [Master's thesis, Middle East Technical University]. National Thesis Center. Retrieved from https://tez.yok.gov.tr/UlusalTezMerkezi/tezDetay.jsp?id=ldAjPnZL3qR3Mn26BZarAQ&no=6L5yHiN1c9Av8mhJvrgGvw

Kang, K., Kim, H., Kim, D. D., Lee, Y. G., & Kim, T. (2019). Characteristics of Cooking-Generated PM10 and PM2.5 in Residential Buildings with Different Cooking and Ventilation Types. *Science of The Total Environment*, *668*, 56–66. https://doi.org/10.1016/j.scitotenv.2019.02.316

Khan, N., Su, Y., & Riffat, S. B. (2008). A Review on Wind Driven Ventilation Techniques. *Energy and Buildings*, *40*(8), 1586–1604. https://doi.org/10.1016/j.enbuild.2008.02.015

Khankari, K. (2018). Computational Fluid Dynamics (CFD) Analysis of Hospital Operating Room Ventilation Systems. *ASHRAE Journal*, *60*(5)

Kim, O., & Yang, J.-H. (2016). On the Design to Improve the Bathroom Exhaust Performance in Multi-Unit Residential Buildings. *Journal of Asian Architecture and Building Engineering*, *15*(2), 349–356. https://doi.org/10.3130/jaabe.15.349

Kizildemir, Ö., Öztürk, E., & Sarıışık, M. (2014). Changes of Turkish Cuisine Culture in the Historical Development. *AİBÜ Sosyal Bilimler Enstitüsü Dergisi*, *14*(3), 191–210. https://www.researchgate.net/publication/320323435_TURK_MUTFAK_KULTURUNUN_TARIHSEL_GELISIMINDE_YASANAN_DEGISIMLER_CHANGES_OF_TURKISH_CUISINE_CULTUR_IN_THE_HISTORICAL_DEVELOPMENT

Lee, H., Lee, Y. J., Park, S. Y., Kim, Y. W., & Lee, Y. (2011). The Improvement of Ventilation Behaviours in Kitchens of Residential Buildings. *Indoor and Built Environment*, *21*(1), 48–61. https://doi.org/10.1177/1420326x11419360

Liddament, M. W. (1996). *A guide to energy efficient ventilation*. Oscar Faber. 2025, https://www.aivc.org/sites/default/files/members_area/medias/pdf/Guides/GU03%20GUIDE%20TO%20ENERGY%20EFFICIENT%20VENTILATION.pdf

Livchak, Andrey & Schrock, Derek & Sun, Zeqiang. (2005). The Effect of Supply Air Systems on Kitchen Thermal Environment. 111

Manshoor, B., Zaman, I., Asmuin, N., Ramlan, F., & Khalid, A. (2014). Optimizing of Make Up Air Performance for Commercial Kitchen Ventilation Improvement. *MATEC Web of Conferences*, *13*, 03002. https://doi.org/10.1051/matecconf/20141303002

Mata, T. M., Martins, A. A., Calheiros, C. S., Villanueva, F., Alonso-Cuevilla, N. P., Gabriel, M. F., & Silva, G. V. (2022). Indoor Air Quality: A Review of Cleaning Technologies. *Environments*, *9*(9), 118. https://doi.org/10.3390/environments9090118

Maviş, F. (2003). *Endüstriyel yiyecek üretimi.* Ankara: Detay Yayıncılık.

Mijorski, S., & Cammelli, S. (2016). Stack effect in high-rise buildings: A Review. *International Journal of High-Rise Buildings*, *5*(4), 327–338. https://doi.org/10.21022/ijhrb.2016.5.4.327

Ministry of Environment and Urbanization. (2017). Planned Areas Zoning Regulation. Resmî Gazete, 30113. Retrieved from https://www.resmigazete.gov.tr/eskiler/2017/07/20170703-8.htm

Ministry of Housing, Communities & Local Government, and Department for Levelling Up, Housing and Communities. (2021). *Approved Document F:* CIBSE. (2015). *Volume 1 - Dwellings (2021 edition).* Retrieved November 29, 2024, from https://assets.publishing.service.gov.uk/media/61deba42d3bf7f054fcc243d/ADF1.pdf

Nagda, N. L., Koontz, M. D., Fortmann, R. C., & Billick, I. H. (1989). Prevalence, use, and effectiveness of range-exhaust fans. *Environment International*, *15*(1-6), 615–620. https://doi.org/10.1016/0160-4120(89)90083-4

NIOSH. 1976. Criteria for a recommended standard: Occupational exposure to carbon dioxide. DHHS (NIOSH) Publication Number 76-194. National Institute for Occupational Safety and Health. www.cdc.gov/niosh/docs/76-194.

OSHA. 2017. Limits for air contaminants. Washington, DC: Occupational Safety & Health Administration,U.S. Department of Labor.www.osha.gov/lawsregs/regulations/standardnumber/1910/1910.1000 TABLEZ1

Özkocak, F. Z. (2015). *Konutlarda mutfak tasarımı, geçirdiği değişim ve "Frankfurt mutfağı" üzerinden değerlendirilmesi* (Master's thesis). Retrieved from https://tez.yok.gov.tr/UlusalTezMerkezi/tezDetay.jsp?id=lITf8v5REHDWNoa3FRgeBQ&no=GAhzrDJc-5E4S95o6KewWw

Özözlü, H. (1999). Atatürk evleri. İstanbul: Dünya Yayıncılık.

Pak, Z. (1993). *Konut Mutfaklarının Analizi ve Minimum Mutfak Tasarımı*. Fen Bilimleri Enstitüsü, Institute of Science and Technology. Retrieved from https://polen.itu.edu.tr/items/bd3c87ca-c35e-4a7a-b13a-b289d3414d61

Park, J., Choi, J.-I., & Rhee, G. (2016). Enhanced Single-Sided Ventilation with Overhang in Buildings. *Energies*, *9*(3), 122. https://doi.org/10.3390/en9030122

Qian, H., & Zheng, X. (2018). Ventilation Control for Airborne Transmission of Human Exhaled Bio-aerosols in Buildings. *Journal of Thoracic Disease*, *10*(S9). https://doi.org/10.21037/jtd.2018.01.24

Raji, B., Tenpierik, M. J., & van den Dobbelsteen, A. (2016). A Comparative Study: Design Strategies for Energy-Efficiency of High-Rise Office Buildings. *Journal of Green Building*, *11*(1), 134–158. https://doi.org/10.3992/jgb.11.1.134.1

Russell, M., Sherman, M., & Rudd, A. (2007). Review of Residential Ventilation Technologies. *HVAC&R Research*, *13*(2), 325–348. https://doi.org/10.1080/10789669.2007.10390957

Schütte, W. (1944). *Bugünkü Kültür ve İkametgah*. *Arkitekt*, XIV(3-4), 67-68. In

Secretary of State, *The Building Regulations* 2010, Ventilation, Approved Document, Volume 1: Dwellings, Requirement F1: Means of Ventilation Regulations: 39, 42 and 44. (2021). England.

Seo, J., Yoon, S., Lee, J., Song, D., & Kato, S. (2010). Influence of Stack Effect on Ventilation in a High-Rise Residential Building. *International Conference on Sustainable Building Asia*, 479–486. Retrieved 2023, from https://www.irbnet.de/daten/iconda/CIB17224.pdf.

Singer, B. C., Pass, R. Z., Delp, W. W., Lorenzetti, D. M., & Maddalena, R. L. (2017). Pollutant concentrations and emission rates from natural gas cooking burners without and with range hood exhaust in nine California homes. *Building and Environment*, *122*, 215–229. https://doi.org/10.1016/j.buildenv.2017.06.021

Soebiyan, V. (2021). Hybrid Ventilation Systems on Different Climate. *I.O.P. Conference Series: Earth and Environmental Science*, *794*(1), 012174. https://doi.org/10.1088/1755-1315/794/1/012174

Song, D., Yoon, S., Jeong, C., Kim, J., & Lim, H. (2019). Heat, vapor, and CO2 transportation caused by airflow in high-rise residential buildings. *Building and Environment*, *160*, 106176. https://doi.org/10.1016/j.buildenv.2019.106176

Stevens, A. (2010) Introduction to the Basic Drivers of Climate. *Nature Education Knowledge* 3(10):10

Sui, X., Tian, Z., Liu, H., Chen, H., & Wang, D. (2021). Field Measurements on Indoor Air Quality of a Residential Building in Xi'an Under Different Ventilation Modes in Winter. *Journal of Building Engineering*, *42*, 103040. https://doi.org/10.1016/j.jobe.2021.103040

Sun, L., & Wallace, L. A. (2021). Residential Cooking and Use of Kitchen Ventilation: The Impact on Exposure. *Journal of the Air & Waste Management Association*, *71*(7), 830–843. https://doi.org/10.1080/10962247.2020.1823525

Sundell, J. (2004). On the History of Indoor Air Quality and Health. *Indoor Air*, *14*(s7), 51–58. https://doi.org/10.1111/j.1600-0668.2004.00273.x

TS 7363: Natural gas building interior installation design and application rules. (2008).Türk Standartları Enstitüsü. Ankara. Retrieved from https://www.scribd.com/document/558285848/ts7363

Turkish Statistical Institute, Building and Housing Characteristics Survey, 2021 (2022). Retrieved January 9, 2024, from https://data.tuik.gov.tr/Bulten/Index?p=Bina-ve-Konut-Nitelikleri-Arastirmasi-2021-45870.

Turkish Statistical Institute. (n.d.). Average Household Size. Retrieved (15.11.2024), from https://nip.tuik.gov.tr/?value=OrtalamaHanehalkiBuyuklugu

U.S. Department of Energy. (2015). *Guidance on Demand Controlled Kitchen Ventilation*. Retrieved from https://betterbuildingssolutioncenter.energy.gov/sites/default/files/attachments/Guidance-on-Demand-Controlled-Kitchen-Ventilation.pdf.

Ulusoy, M., & Özkaynak, M. (2016). The Emergence of Studio Apartments. *ICONARP International Journal of Architecture and Planning*, *4*(2), 130–141. https://doi.org/10.15320/ICONARP.2016.11

Ural, T., Akgün, M., & Ertürk, M. (2020). Türkiye'de doğalgazın tüketildiği mahallerde kullanılan havalandırma menfezlerin optimizasyonu. *International Journal of Pure and Applied Sciences, 6*(2), 157–168. https://doi.org/10.29132/ijpas.814457

Uyar, P. (2014). Toplu Konutlarda Mutfak Mekanının 1950'lerden Günümüze Gelişimi. *ITU Sosyal Bilimler Enstitüsü Institute of Social Sciences*. http://hdl.handle.net/11527/12414

Ventilation Committee of The Inter-Agency Review Council. (2010). Make-Up Air. In *Ventilation Guidelines for Minnesota Commercial Kitchens* (4th ed., pp. 18–20). Book. Retrieved 2023, from https://www.co.nicollet.mn.us/DocumentCenter/View/93/Minnesota-Ventilation-Guidelines-PDF.

Wu, X., Xiu, G. L., Wang, L. N., & Xue, T. L. (2016). Impact of Oil Types on Emission Characteristics of Particles. Journal of East China University of Science and Technology, 42, 65–71.

Xia, T., Bian, Y., Shi, S., Zhang, L., & Chen, C. (2020). Influence of Nanofiber Window Screens on Indoor PM2.5 of Outdoor Origin and Ventilation Rate: An Experimental and Modeling Study. *Building Simulation, 13*(4), 873–886. https://doi.org/10.1007/s12273-020-0622-5

Yavuz, Y. (2000). 1923-1928 Ankara'sında Konut Sorunu ve Konut Gelişmesi (The Housing Problem and Development in Ankara in 1923–1928). In A. T. Yavuz (Ed.), Tarih İçinde Ankara (pp. 233–253). TBMM Basımevi: Ankara.

Yazgan Serinkaya, E. (2017). Mutfak Kültürünün Gaziantep'in Geleneksel Konutlarında İncelenmesi. Artium, 5(1), 27-41.

Yazgan-Serinkaya, E. (2017). Mutfak kültürünün Gaziantep'in geleneksel konutlarında incelenmesi. *Artium, 5*(1), 27-41. Retrieved from http://artium.hku.edu.tr/tr/download/article-file/279821

Yazgan-Serinkaya, E. (2022). Kültür – İç Mekân Etkileşiminin Konut Mutfak Tasarımına Etkileri. *Tasarım Mimarlık ve Mühendislik Dergisi, 2*(1), 10-19. Retrieved from https://dergipark.org.tr/tr/pub/dae/issue/68555/1073875

Yıldırım, K., Çağatay, K., & Özkan, A. (2009). Farklı Sosyo-Ekonomik Düzeye (SED) Sahip Kullanıcıların Mutfaklarındaki Havalandırma Sistemleri Üzerine Bir Araştırma. *Politeknik Dergisi*, *12*(4), 2779–289.

Yin, H., Liu, C., Zhang, L., Li, A., & Ma, Z. (2019). Measurement and Evaluation of Indoor Air Quality in Naturally Ventilated Residential Buildings. *Indoor and Built Environment*, *28*(10), 1307–1323. https://doi.org/10.1177/1420326x19833118

Yusoff, W. F., Sapian, A. R., Salleh, E., Adam, N. M., & Hamzah, Z. (2014). Mass Flow Rate Induced by Combined Roof Solar Collector and Vertical Stack in A Hot Humid Climate. *Journal of Green Building*, *9*(1), 166–177. https://doi.org/10.3992/1943-4618-9.1.166

Zhang, Q., Gangupomu, R. H., Ramirez, D., & Zhu, Y. (2010). Measurement of Ultrafine Particles and Other Air Pollutants Emitted by Cooking Activities. *International Journal of Environmental Research and Public Health*, *7*(4), 1744–1759. https://doi.org/10.3390/ijerph7041744

Zhang, X., Weerasuriya, A. U., Wang, J., Li, C. Y., Chen, Z., Tse, K. T., & Hang, J. (2022). Cross-Ventilation of A Generic Building with Various Configurations of External and Internal Openings. *Building and Environment*, *207*, 108447. https://doi.org/10.1016/j.buildenv.2021.108447

Zhao, B., & Chen, J. J. (2006). Numerical Analysis of Particle Deposition in Ventilation Duct. *Building and Environment*, *41*(6), 710–718. https://doi.org/10.1016/j.buildenv.2005.02.030

Zhao, H., Chan, W. R., Delp, W. W., Tang, H., Walker, I. S., & Singer, B. C. (2020). Factors impacting range hood use in California houses and low-income apartments. *International Journal of Environmental Research and Public Health*, *17*(23), 8870. https://doi.org/10.3390/ijerp

Zugmann, G. (n.d.). *Mak-Sammlung artikel*. MAK Museum Vienna. https://www.mak.at/en/collection/collection/mak-sammlung_artikel?article_id=1339957568483

URL

1. Hepsiemlak. (n.d.). *Konya Selçuklu Parsana Satılık Daire*. Retrieved November 19, 2024, from https://www.hepsiemlak.com/konya-selcuklu-parsana-s atilik/daire/144463-160
2. Hepsiburada.(n.d). *Window vent covers.* Retrieved February 25, 2025, from https://www.hepsiburada.com/menfezmatik-soguk-hava-onleyici-dogalgaz-kapagi-menfezmatik-pm-HB00001AL6WM
3. https://www.lenntech.com/calculators/ppm/converter-parts-per-million.htm#Documentation
4. https://en.air-q.com/einheiten-umrechner
5. https://planetcalc.com/9431/

APPENDIX

6.1 Results of Apache Dynamic Simulation

Table 13 shows the net flow volume (l/s) at the flue opening during cooking hours for V2 - F1. Positive values represent flow-out, while negative values indicate flow-in. Max flow volumes reach 44 l/s, and maximum flow-in volume reaches 12 l/s. As shown in Table 8 (Section 4.1.1), the flow-out rate is 98%.

Table 13.Annual net flow volume graphics for V2 - F1

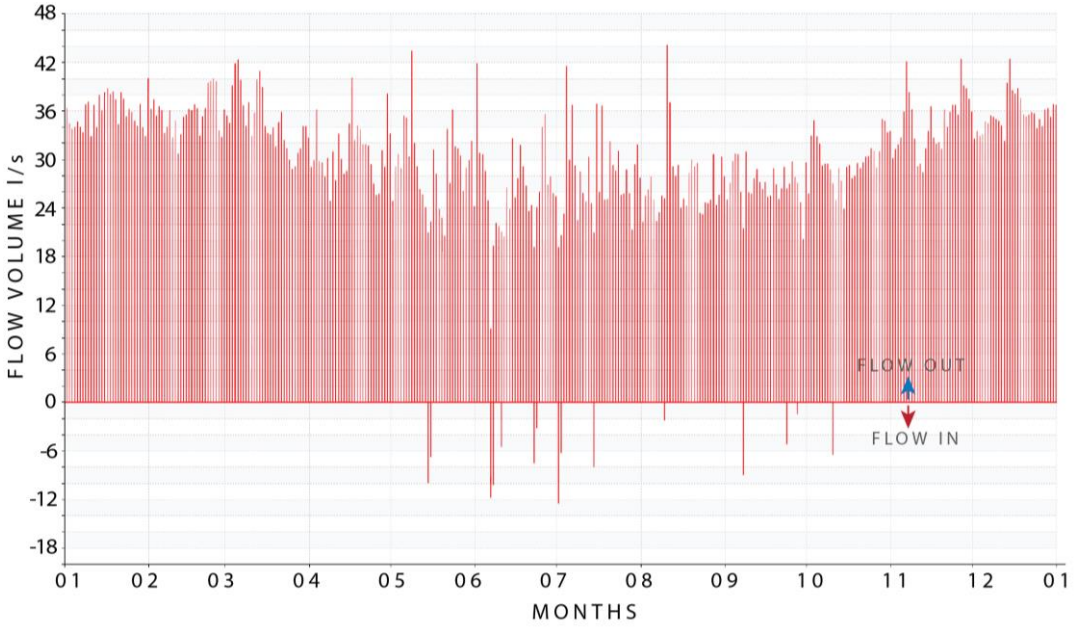

Table 14 shows the net flow volume (l/s) at the flue opening during cooking hours for V2 - F10. Max flow volumes reach 37 l/s, and maximum flow-in volume reaches 25 l/s. Flow-out is more prevalent, especially in autumn, while flow-in occurs more

frequently in winter and spring, indicating an irregular flow pattern. As shown in Table 8 (Section 4.1.1), the flow-out rate is 24%.

Table 14.Annual net flow volume graphics for V2 - F10

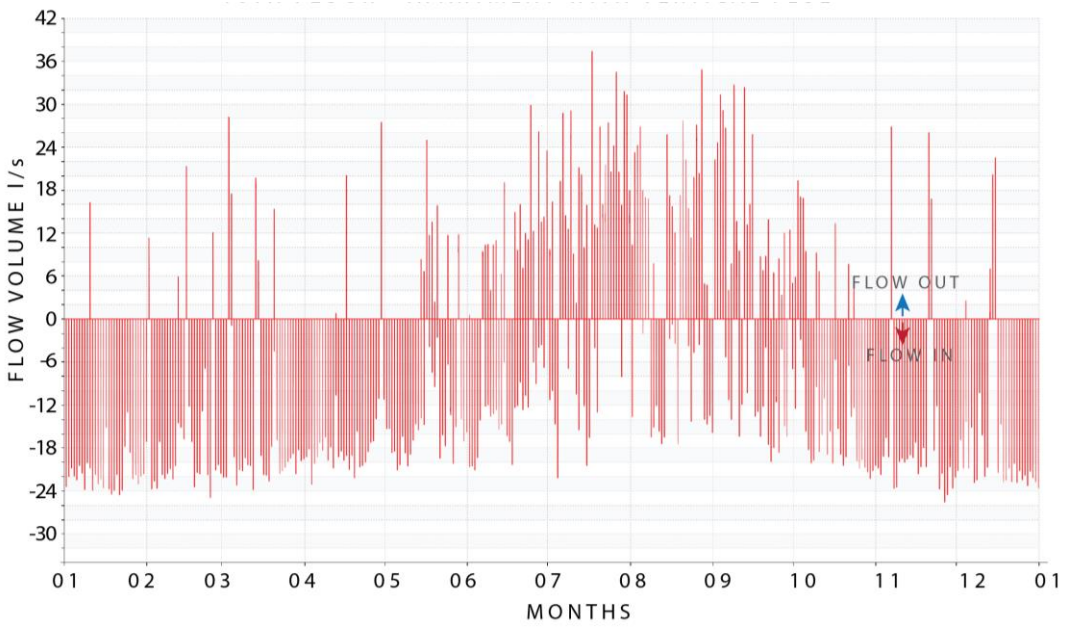

Table 15 shows the net flow volume (l/s) at the flue opening during cooking hours for H2 - S - F1. Max flow volumes reach 75 l/s, and maximum flow-in volume reaches 0.7 l/s. As shown in Table 9 (Section 4.1.2), the flow-out rate is 100%.

Table 15.Annual net flow volume graphics for H2 – S - F1

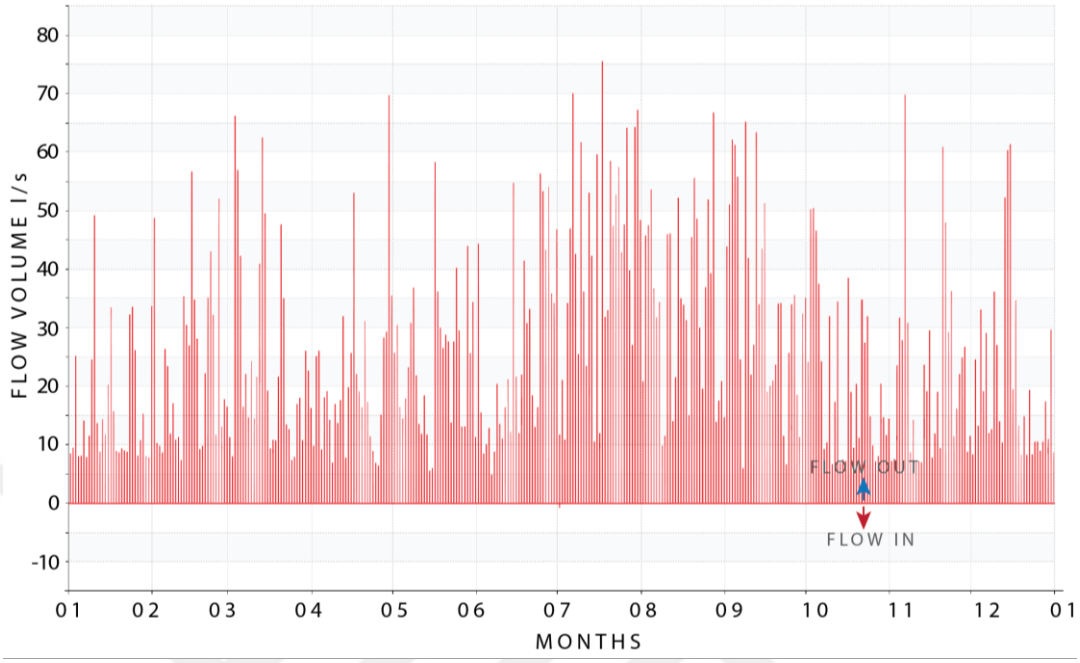

Table 16 shows the net flow volume (l/s) at the flue opening during cooking hours for H2 - S - F1. Max flow volumes reach 88 l/s, and maximum flow-in volume reaches 0.4 l/s. As shown in Table 9 (Section 4.1.2), the flow-out rate is 100%.

Table 16.Annual net flow volume graphics for H2 – S –F10

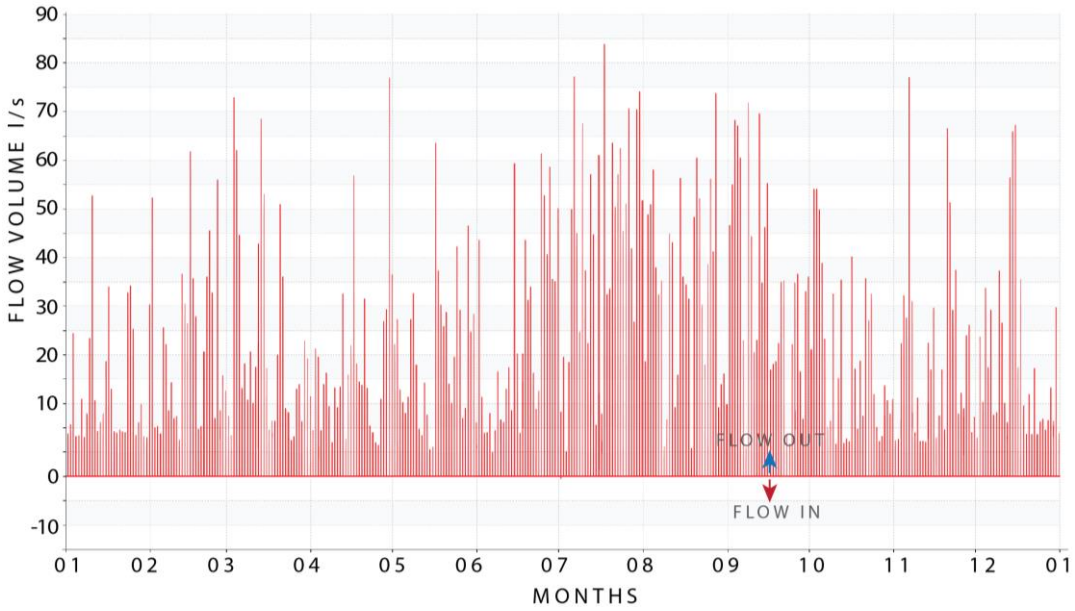

6.2 Carbon Dioxide Concentration Calculation Using a Conversion Calculator

In order to estimate the indoor CO_2 concentration from a given emission rate, the following data were used: a continuous CO_2 generation rate of 0.870 kg h^{-1} and a room volume of 30 m^3. The reference calculator I (URL-1) converts values expressed in [ppm] to [mg m^{-3}] and vice versa. Consequently, the procedure begins by expressing the mass flow rate in milligrams per hour:

0.870 kg h^{-1} = 0.870 × 10^3 g h^{-1} = 870 g h^{-1} = 870 × 10^3 mg h^{-1} = 870 000 mg h^{-1}.

Dividing this figure by the room volume results in the hourly increase in mass concentration: 870 000 mg h^{-1} / 30 m^3 ≈ 29 000 mg m^{-3} h^{-1}.
When this value (29 000 mg m^{-3}) is entered into the converter, with the output set to "parts per million in the proportion of volume," the calculated result is 1.497 e+4. Because 1.497 e+4 represents 1.497 × 10^4, the corresponding volumetric concentration is approximately 14 970 ppm (Figure 77).

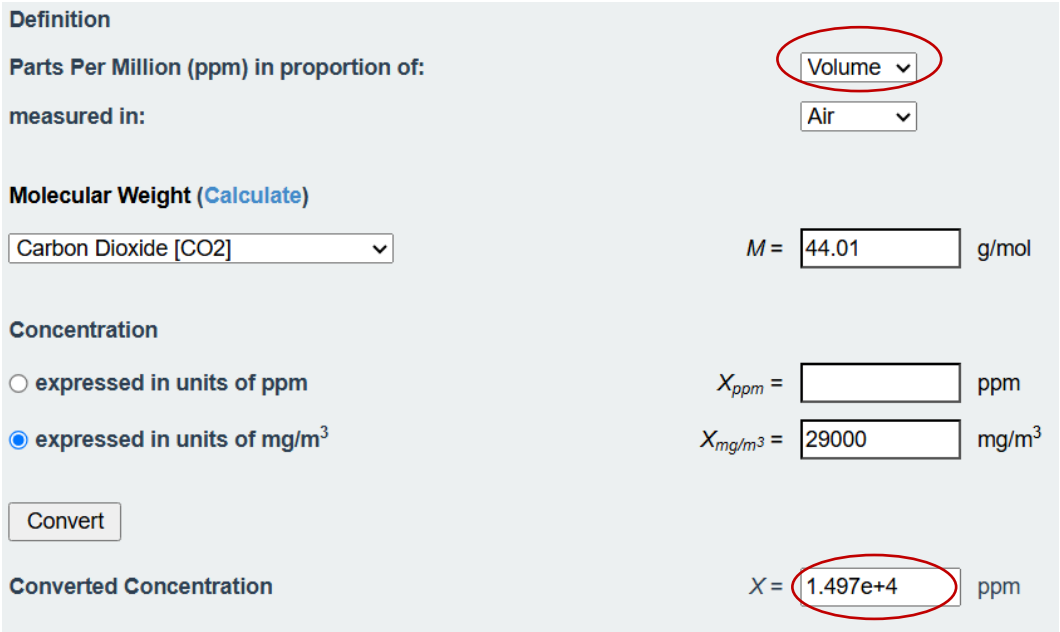

Figure 77. The CO_2 concentration in parts per million by volume is calculated from the input value expressed in mg m^{-3} by reference calculator I (URL-3)

When the calculator setting “parts per million in proportion by weight” was selected (Figure 78) and the input value of 29 000 mg m^{-3} was entered, the output was calculated as 22 420 ppm.

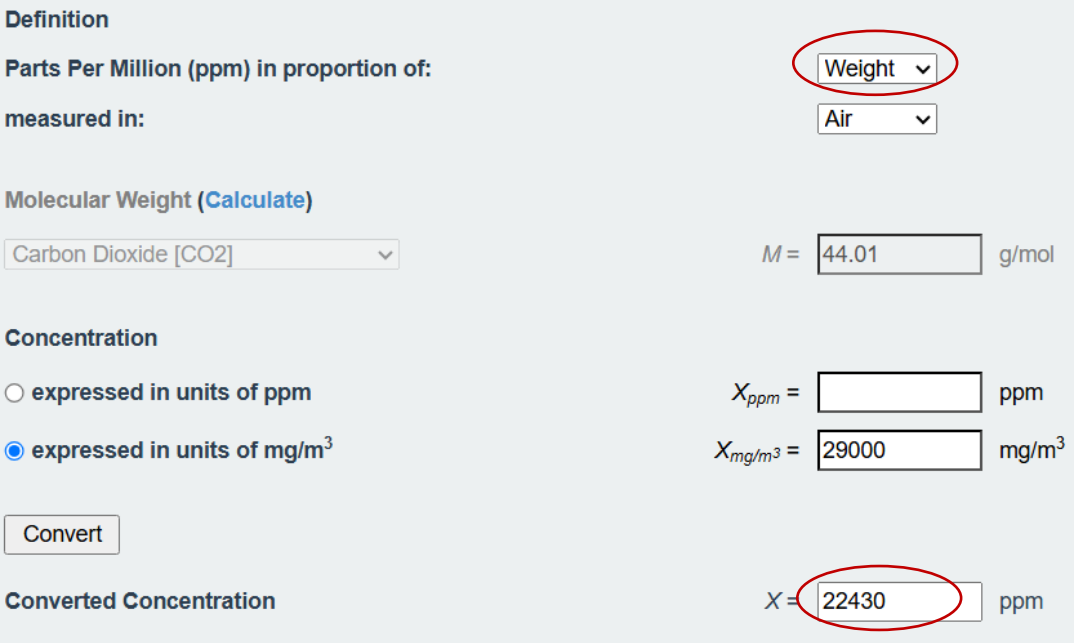

Figure 78. The CO_2 concentration in parts per million by weight is calculated from the input value expressed in mg m^{-3} by reference calculator I (URL-3)

The reference calculator II (URL -2) utilises temperature and pressure as additional input parameters. An average temperature of 30 degrees Celsius was considered for all scenarios (Figure 80 and Figure 81). When examining the pressure data for the tested kitchen scenarios, an average value of 90,909 Pa is observed across all cases. The CFD simulations show values close to absolute pressure rather than gauge (relative) pressure(Figure 79). Specifically, for Ankara, located at an altitude of 938 m above sea level, the atmospheric pressure is approximately 90,553 Pa. Comparing this to the CFD's average pressure of 90,909 Pa reveals a difference of 356 Pa and higher in the kitchen.

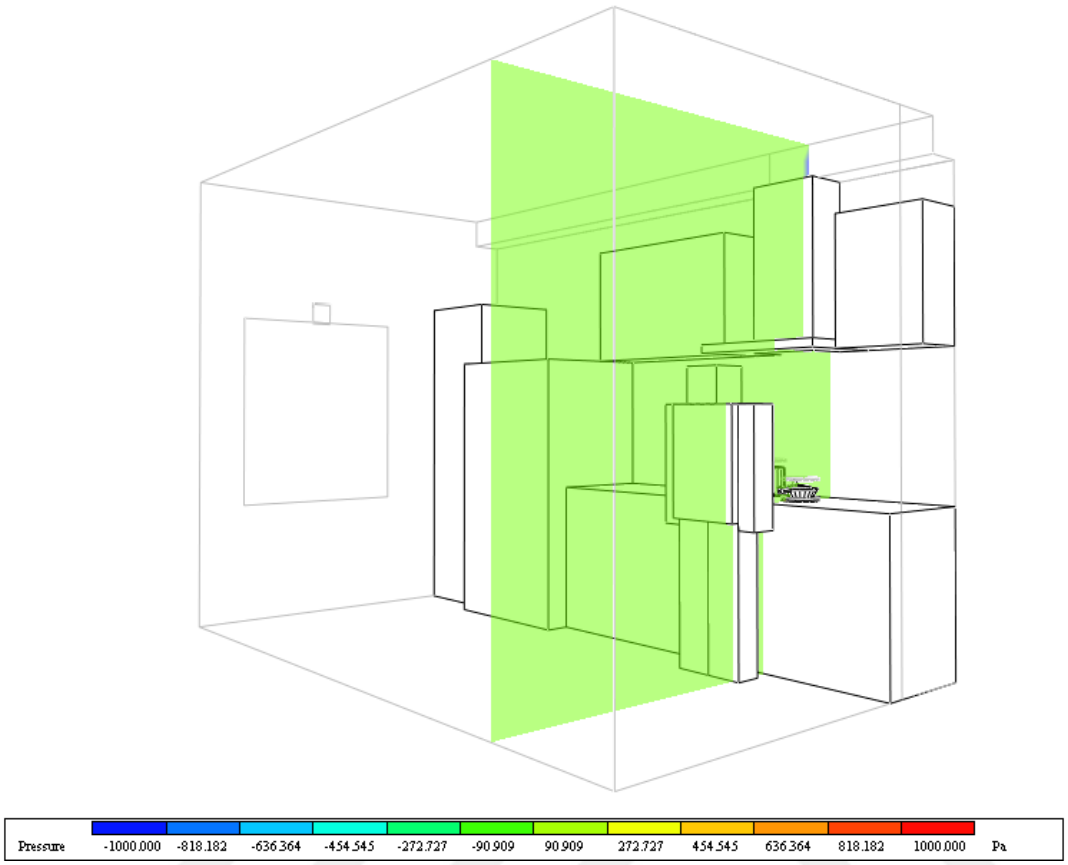

Figure 79. Axonometric view of the pressure boundary for all test kitchens

Since the calculator requires the pressure value in hPa, the 90,909 Pa value was divided by 100 to convert it into hPa (hectopascal): 90,909Pa÷100=909,09 hPa.

As a result, the calculator converted the CO_2 concentration to 18 281 ppm(Figure 80).

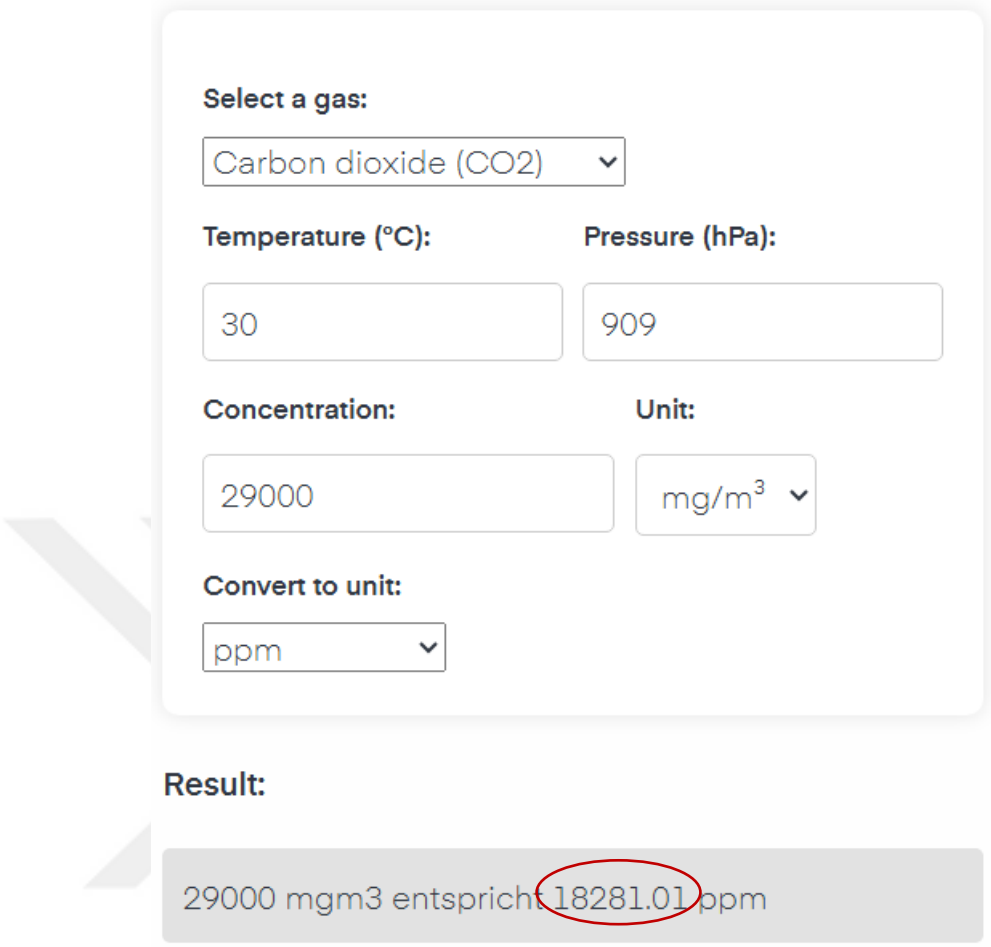

Figure 80. CO_2 ppm calculation accounting for temperature and pressure by reference calculator II (URL-4)

In reference calculator III(URL-3), the pressure value was used as 90,909 Pa, and the calculator converted the CO_2 concentration to 18 270 ppm (Figure 81).

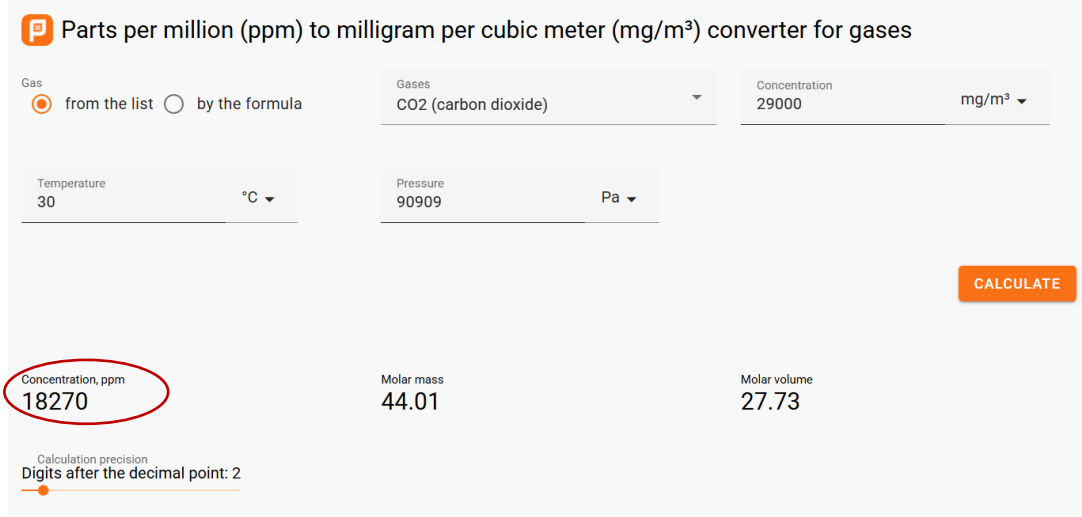

Figure 81. CO_2 ppm calculation accounting for temperature and pressure(URL-5)

As a result, for reference calculator I, assuming normal conditions, the CO_2 concentration was converted to 14 970 ppm (by volume) and 22 430 ppm (by weight). In reference calculators II and III, the CO_2 concentration was converted to 18 281 ppm and 18 270 ppm, respectively. These calculations represent the CO_2 concentration in a kitchen without any ventilation. While interpreting these results, it should be taken into account that CO_2 infiltration and exfiltration through the building envelope, as well as the spread of CO_2 to other rooms through the kitchen door, were disregarded.